Universität Rostock

Traditio et Innovatio

Synthesis of Heterocyclazines by Buchwald-Hartwig reaction and C-H activation

Cumulative Dissertation

by

Jan Radolko

born 07.10.1991 in Parchim, Deutschland

A Dissertation

Submitted to the Faculty of Mathematics and Natural Sciences

University of Rostock

To obtain the academic degree

Doctor rerum naturalium (Dr. rer. nat.)

https://doi.org/10.18453/rosdok_id00005827

The present work was completed between 01.10.2021 and 30.10.2025 at the Institute of Chemistry of the University of Rostock, at the Chair of Organic Chemistry, within the working group of Prof. Dr. Dr. h.c. mult. Peter Langer.

Die vorliegende Arbeit wurde zwischen 01.10.2021 und 30.10.2025 am Institut für Chemie der Universität Rostock am Lehrstuhl für Organische Chemie im Arbeitskreis von Prof. Dr. Dr. h.c. mult. Peter Langer angefertigt.

Reviewer:

I. Prof. Dr. Dr. h.c. mult. Peter Langer, Universität Rostock, Institut für Chemie

II. Prof. Dr. Thomas J.J. Müller, Heinrich-Heine-Universität Düsseldorf, Institut für Organische Chemie

- Date the dissertation was submitted: 30.10.2025
- Date of the thesis defense: 28.04.2026

Declaration

1. I hereby declare that I wrote this thesis independently and without outside help. I did not use any aids or sources other than those I specified. I marked the passages taken from the works I used in terms of content and wording.

2. The opportunity for this doctoral project has not been arranged for me commercially. Specifically, I have not hired any organization that seeks supervisors for the preparation of dissertations for a fee or that performs all or part of the duties delegated to me with regard to examinations.

Erklärung

1. Hiermit erkläre ich, dass ich die vorliegende Arbeit selbstständig angefertigt und ohne fremde Hilfe verfasst habe, keine außer den von mir angegebenen Hilfsmittel und Quellen dazu verwendet habe und die den benutzten Werken inhaltlich und wörtlich entnommenen Stellen als solche kenntlich gemacht habe.

2. Die Gelegenheit zum vorliegenden Promotionsvorhaben ist mir nicht kommerziell vermittelt worden. Insbesondere habe ich keine Organisation eingeschaltet, die gegen Entgelt Betreuerinnen/Betreuer für die Anfertigung von Dissertationen sucht oder die mir obliegenden Pflichten hinsichtlich der Prüfungsleistungen für mich ganz oder teilweise erledigt.

Rostock
30.10.2025



.....
Jan Radolko

Acknowledgment:

First, I wish to extend my sincere appreciation to Prof. Dr. Dr. h.c. mult. Peter Langer for granting me the opportunity to be part of his research group. Furthermore, I would like to express my gratitude for his support and guidance during my research at the University of Rostock. I am also grateful to Dr. Peter Ehlers for his support during my PhD. Without his guidance, support, and encouragement, I would never have been able to complete the work on my dissertation.

I want to seize this opportunity to extend my heartfelt thanks to several individuals who generously contributed their time and valuable insights. It is with great pleasure that I express my gratitude to Dr. Feist and Dr. Hein for their invaluable suggestions and precise assistance, as well as to Dr. Villinger for his work on single-crystal structures and to Dr. Michalik for the measurements of numerous Nuclear Magnetic Resonance (NMR) spectra. My heartfelt thanks also go to Jana Unger, Maximilian Quasdorf, and Alexander Klotzek for their support during our work in the laboratory.

Additionally, I would like to express my heartfelt appreciation to my colleagues who supported me during this time: Jonas, Rúben, Maryam, Franziska, Aleksandra, Karyna, Tuan, Elina, and Arpine.

Ultimately, I attribute my success to the steadfast love, encouragement, and support, especially from my brother and parents. Without their incredible backing, pursuing my goals wouldn't have been possible. Thank you, my dear family!

Summary of the Project

Within this dissertation, I develop efficient methodologies for the design of several new heteroaromatic polycycles, such as nitrogen and oxygen doped aceanthrylenes and nitrogen doped azulenofluorenes. The primary synthetic strategy is to perform Buchwald-Hartwig reaction and/or C-H activation to enable cyclization reactions on distinct starting materials such as imidazo[1,2-*a*]pyridine and 5*H*-dibenzo[*b,f*]azepine. In this regard, efficient and unique C-C and C-N bonds are formed to develop previously unknown heterocycl[3.3.2]azines and heterocycl[4.2.2]azines. Moreover, computational studies on aromaticity and energy levels, as well as experimental studies on electronic and optical properties, are performed on the newly designed molecules.

Zusammenfassung des Projekts

In dieser Dissertation entwickle ich effizienter Methoden für den Aufbau verschiedener neuer heteroaromatischer Polyzyklen, wie zum Beispiel Stickstoff und Sauerstoff dotierte Aceanthrylene und Stickstoff dotierte Azulenfluorene. Die primäre Synthesestrategie ist es, Buchwald-Hartwig-Reaktionen und/oder C-H-Aktivierungen durchzuführen um Zyklisierungsreaktionen an ausgewählten Startmaterialien wie zum Beispiel Imidazo[1,2-*a*]pyridin und 5*H*-Dibenz[*b,f*]azepin zu ermöglichen. In dieser Hinsicht werden effiziente und einzigartige C-C und C-N Bindungen für die Entwicklung unbekannter Heterocycl[3.3.2]azine und Heterocycl[4.2.2]azine aufgebaut. Darüber hinaus sind computergestützte Berechnungen zu der Aromatizität, den Energieniveaus sowie experimentelle Untersuchungen zu den elektronischen und optischen Eigenschaften an den neu entwickelten Molekülen durchgeführt worden.

Table of Contents

List of Schemes VIII
List of Figures X
List of Tables XI
List of Abbreviation XII
I. Introduction 1
1. Cyclazines: a unique class of heterocycles 1
2. Synthesis of Cyclazines 3
2.1. Synthesis of Cycl[3.2.2]azines 3
2.1.1. Cycloaddition on indolizine or pyridine scaffolds 3
2.1.2. Cycloaddition on 3*H*-pyrrolizin scaffolds 4
2.1.3. Synthesis of Heterocycl[3.2.2]azines 5
2.1.4. Synthesis of π-extended Cycl[3.2.2]azines 6
2.1.5. Alternative routes for synthesis of Cycl[3.2.2]azines 7
2.1.6. Synthesis of chemiluminescent or fluorescent Cycl[3.2.2]azines 8
2.2. Synthesis of Cycl[3.3.2]azines 9
2.3. Synthesis of Cycl[3.3.3]azines 13
2.4. Synthesis of Cycl[4.2.2]azines 17
2.5. Synthesis of Cycl[4.3.2]azines 18
2.6. Synthesis of Cycl[2.2.2]azine 20
3. Properties of Cyclazines 21
3.1. Aromatic properties of cyclazines 21
3.2. Electron Spin Resonance Studies 26
3.3. Investigations of excited states for cyclazines 29
4. Research on Cyclazines conducted by Prof. Langer's Group 34
5. Own Contributions to the Research of Cyclazines 34
5.1. Synthesis of 2,2a1,6-Triazaaceanthrylenes 35
5.2. N-Doped and Bowl-Shaped Azabenzo[3,4]azulenofluorene 36
5.3. Synthesis and Properties of N,O-doped Aceanthrylenes 38
Reference i
II. Contribution to Manuscripts 1
Publication I 2

Publication II 3
Publication III 4
Appendix 6

List of Schemes

Scheme 1. First synthesis of cycl[3.2.2]azine by Boekelheide and Windgassen 3

Scheme 2. [8+2] Cycloaddition reactions on indolizine and pyridine scaffolds to form cycl[3.2.2]azines 4

Scheme 3. Carbon annellation procedure on 3H-pyrrolizines 5

Scheme 4. Chiral cycl[3.2.2]azine derivatives due to organocatalytic cyclizations 5

Scheme 5. Formation of heterocycle[3.2.2]azines with n-Butyllithium 6

Scheme 6. Multi-component reaction for the formation of heterocycl[3.2.2]azines 6

Scheme 7. Examples for π-extended cycl[3.2.2]azines 7

Scheme 8. Alternative routes for the synthesis of cycl[3.2.2]azines 8

Scheme 9. Oxidative and palladium-catalyzed cyclization of an alkyne 8

Scheme 10. Synthesis of chemiluminescent and fluorescent Cycl[3.2.2]azines 9

Scheme 11. First advancements in the synthesis of heterocyclic cycl[3.2.2]azines 9

Scheme 12. Synthesis of the first ullazine, a derivative of a benzannulated cycl[3.3.2]azine 10

Scheme 13. Early examples for the synthesis of heterocycl[3.3.2]azines from pyridines 11

Scheme 14. Synthesis of ullazine via a chromium-mediated ring-closing 11

Scheme 15. Recent examples for the synthesis of cycl[3.3.2]azines 12

Scheme 16. Pathways for the synthesis of new ullazines as a derivative of cycl[3.3.2]azine. 13

Scheme 17. Early synthetic developments of cycl[3.3.3]azine 14

Scheme 18. Effective ring closure reactions on tri-aryl pyridines and quinolizine moieties .. 15

Scheme 20. Bridged triphenylamines and rylene chemistry as a waypoint to new cycl[3.3.3]azines 16

Scheme 21. Cyclization between phenyl and pyridinyl moiety through a rhodium(III)-catalyzed C-H annulation 17

Scheme 22. Stabilization of cycl[3.3.3]azinium salts and biradicals through bulky aryl substituents 17

Scheme 23. Synthesis of cycl[4.2.2]azine via 3H-pyrrolizine or pyrrolazepines under Vilsmeier reaction conditions 18

Scheme 24. Methods for the synthesis of cycl[4.3.2]azines by Wittig-olefination 19

Scheme 25. Methods for the synthesis of cycl[4.3.2]azines by rearrangement reaction 19
Scheme 26. Methods for the synthesis of cycl[4.3.2]azines by Pd-catalyzed aldol reaction .. 20
Scheme 27. Synthesis of rare cycl[2.2.2]azine framework 20
Scheme 28. Synthesis of benzo-fused cycl[3.3.2]azines by the group of Langer 33
Scheme 29. Synthesis of benzo-fused cycl[4.3.2]azine by acid-mediated cycloisomerization with Brønsted acid 34
Scheme 30. Cyclization by a twofold Buchwald-Hartwig reaction to form 6H-2,2a1,6-triazaaceanthrylenes 35
Scheme 31. Synthesis of 3a2,5-diazabenzo[3,4]azuleno[2,1,8,7-jklm]fluorene 37
Scheme 32. Synthesis of N,O-doped Aceanthrylenes 39

List of Figures

Figure 1. Nomenclature of cyclazines....1
Figure 2. Visualization of the π-conjugation for cyclazines....2
Figure 3. Examples for fluorescent (**IX**, **X**) and bioactive (**XI**, **XII**) cyclazines....2
Figure 4. Addressed aspects by comparison of cyclazines....23
Figure 5. Geometrically non-identical π-electron circuits, CRE (in β units), and circuit currents (CC, in I_0 units)....25
Figure 6. ^{1}H, ^{13}C, ^{15}N chemical shifts of cycl[3.2.2]azine and cycl[3.3.3]azine....26
Figure 7. Calculated geometry of cyclopenta[h]cycl[4.2.2]azine under the assumption of C_{2v} symmetry (distances in Å)....30
Figure 8. Stability of cycl[3.3.3]azine derivatives....32

List of Tables

Table 1. Aromaticity parameters for different cyclazine classes 24

Table 2. Coupling constants in gauss for the cyclazine negative ion…… 27

Table 3. Coupling constants of protons and ^{14N} nuclei (αH and αN in gauss), and calculated π-spin populatons (ϱ) in radical anions of 6-azacycl[3.2.2]azine, 6-nitrocycl[3.2.2]azine and cyclopenta[4.2.2]azine.....28

Table 4. Hyperfine Coupling Constants for the Radical Ions of cycl[3.3.3]azine.....29

List of Abbreviations

%TRE	Percentage of topological resonance energies
ΣNICS	Summation of nucleus-independent chemical shift
λ	wavelength
Ar	Aryl
BRE	Bond resonance energy
***n*-BuLi**	*n*-Butyllithium
CI	Conical intersection
CNDO	Complete neglect of differential overlap
CRE	Circuit resonance energy
DDQ	2,3-Dichloro-5,6-dicyano-1,4-benzoquinone
DEAD	Diethylacetylenedicarboxylate
DMAD	Dimethylacetylenedicarboxylate
DMF	*N,N*-Dimethylformamid
DNA	Deoxyribonucleic acid
ENDOR	Electron nuclear double resonance
ESIPT	excited state intramolecular proton transfer
ESR	Electron spin resonance
Et	Ethyl
HOMA	harmonic oscillator model of aromaticity
HOMO	Highest occupied molecular orbital
ICSS	Iso-Chemical-Shielding-Surface
INVEST	Inverted singlet-tripled
ISC	Intersystem crossing
LED	Light-emitting diode
LUMO	Lowest occupied molecular orbital
m	*meta*
MCPBA	*m*-chloroperbenzoic acid
Me	Methyl
Mes	Mesityl

MRE	Magnetic resonance energy
MREPE	Magnetic resonance energies per electron
MSE	Magnetic susceptibility exaltation
NICS	Nucleus-independent chemical shift
NMR	Nuclear magnetic resonance
o	*ortho*
p	*para*
PE	Photoemission spectroscopy
R	Organic moiety
REPE	Resonance energies per electron
rISC	Reversed intersystem crossing
rt.	Room temperature
S	Singlet state
T	Triplet state
Tf	Trifluoromethyl
THF	Tetrahydrofuran
TRE	Topological resonance energies
TREPE	Topological resonance energy per π-electron
TSNMR	Through-Space-Nuclear magnetic resonance
UV	ultraviolett

I. Introduction

1. Cyclazines: a unique class of heterocycles

Cyclazines refer to tricyclic compounds with an internal nitrogen atom. Initially, the term 'cyclazine' was proposed by Boekelheide in 1958 to characterize an overall group of compounds consisting of three conjugated unsaturated cycles connected to a mutual nitrogen atom.[1] Such compounds fall within the general category of bridged annulenes, characterized by different ring sizes. The rings attached to the central nitrogen can be distinguished by adding numbers in brackets to the name, which indicate the number of atoms on the ring between the bonds to nitrogen. Figure 1 shows the general principle, following from left to right: a cycl[2.2.2]azine (**I**), a cycl[3.2.2]azine (**II**), a cycl[3.3.3]azine (**III**), and a cycl[4.3.2]azine (**IV**).

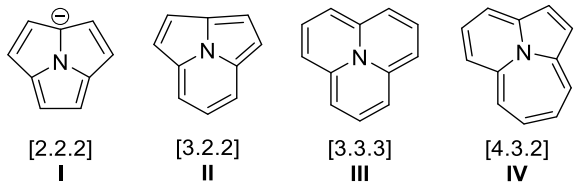


Figure 1. Nomenclature of cyclazines

Representations of cyclazines are shown in Figure 2. The common illustration of a 12π-electron system (Figure 1, **V**), can be misleading. Despite sp^2 hybridization, the centrally located nitrogen atom is not involved in the π-electron conjugation.[2] Hence, the peripheral delocalization of the aromatic π-electron system can be likened to a spinning toy (Figure 2, **VI**), where the handle (which is not moved) corresponds to the nitrogen lone pair. At the same time, the moving part resembles the ring current and displays a 10π-electron system. Consequently, these fused cyclic systems are intriguing regarding their aromaticity. From the perspective of their electronic properties, these compounds can be viewed as derivatives of their isoelectronic annulene family (Figure 2, **VII**).[3] The amount of π-electrons in the peripheral ring defines the nature of aromaticity or anti-aromaticity attributed to the characteristic of a paratropic or diatropic ring current (Figure 2, **VIII**).

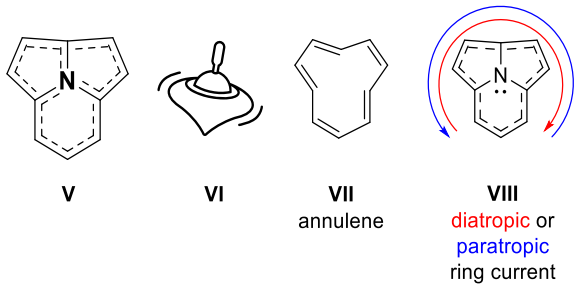


Figure 2. Visualization of the π-conjugation for cyclazines

Furthermore, cyclazines and their hetero- and benzo derivatives are valuable from a practical standpoint. They offer high potential as a fluorescent compound and have prospects in organic electronics.[4] For example, cyclazines (Figure 3, **IX**) can serve as a highly tunable scaffold that covers most of the visible spectrum in terms of emission. Moreover, it has been demonstrated to undergo excited-state intramolecular proton transfer (ESIPT) and act as yellow dyes with substantial bathochromic shifts. (Figure 3, **X**) Additionally, biological activity is observed in cyclazines.[5] On the one hand, it was shown to have high anti-inflammatory activity. (Figure 3, **XI**) It can bind with high affinity to the estrogen receptor (Figure 3, **XII**) and has demonstrated protection against bone loss in an ovariectomized mouse model of post-menopausal osteoporosis.

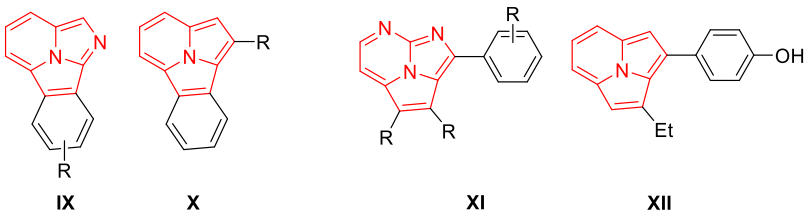
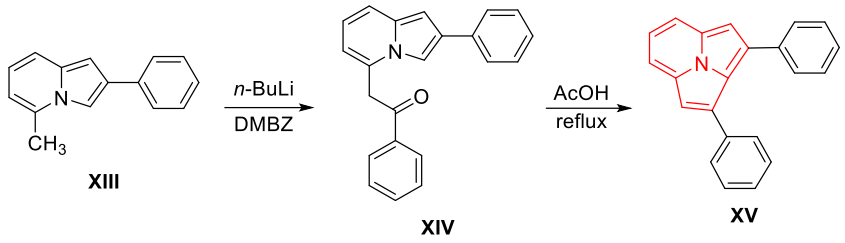


Figure 3. Examples for fluorescent (**IX**, **X**) and bioactive (**XI**, **XII**) cyclazines

First mentioned in 1958, cycl[3.2.2]azine was synthesized by V. Boekelheide and R. J. Windgassen[1] and studied by R. J. Windgassen through ultraviolet absorption measurements and molecular orbital calculations for some derivatives, marking the very first steps in the history of cyclazines.[6] The earliest synthesis method for this new class was described by starting from indolizine (Scheme 1, **XIII**), treating it with *n*-butyllithium, followed by *N,N*-dimethylbenzamide (DMBZ), producing the corresponding ketone (Scheme 1, **XIV**). Subsequently, heating the ketone in glacial acetic acid yielded the desired cycl[3.2.2]azine (Scheme 1, **XV**).



Scheme 1. First synthesis of cycl[3.2.2]azine by Boekelheide and Windgassen

2. Synthesis of Cyclazines

Having established cyclazines as a new class of molecules with potentially unique electronic properties, the next crucial step is to explore their synthetic accessibility.[7] The subsequent sections outline the history of synthetic strategies developments to obtain these compounds.

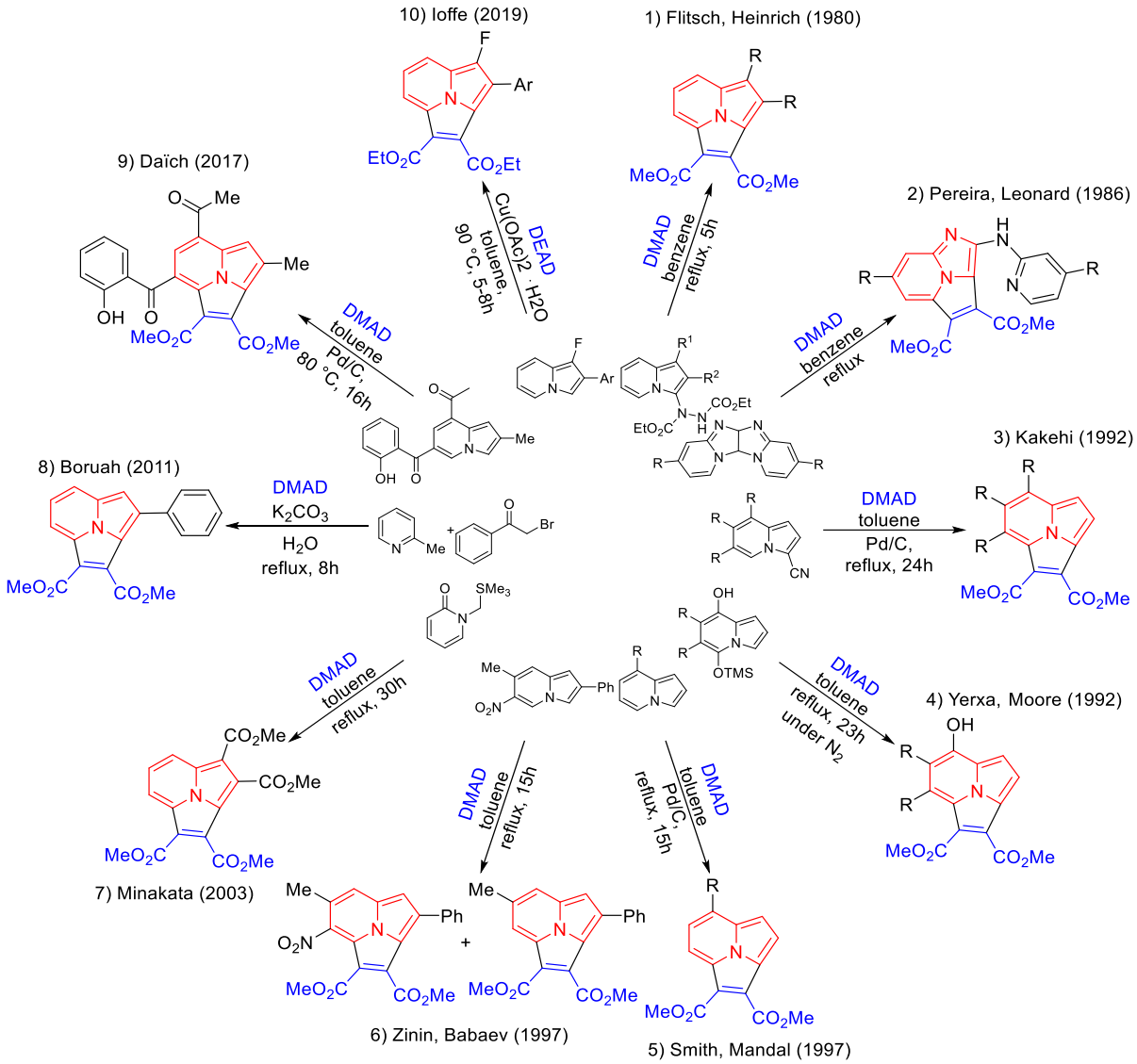
2.1.Synthesis of Cycl[3.2.2]azines

Among the various members of the cyclazine family, cycl[3.2.2]azine stands out as the first of its kind to be synthetically accessible. This can be explained by its high stability and easy access to starting materials, which facilitates the development of synthetic strategies.

2.1.1. Cycloaddition on indolizine or pyridine scaffolds

Continuous work on cyclazines eventually led to a key and practical synthetic strategy introduced by Boekelheide, Godfry, and colleagues.[8] An attack of dimethylacetylenedicarboxylate (DMAD) on the corresponding indolizine in toluene was demonstrated. Dehydrogenation, achieved by adding palladium on charcoal as a catalyst and heating the reaction mixture under reflux, provides the cycl[3.2.2]azine. This method also enabled the first studies on the reactivity of this class of compounds.[9] The key step of this procedure is a [8+2] cycloaddition on the indolizine scaffold. Throughout the following years and up to the present day, this methodology provides easy access to a wide range of cycl[3.2.2]azines. By using leaving groups, such as diethyl-1,2-hydrazinedicarboxylate[10] (Scheme 2, **1**) and trimethylsiloxy group[11] (Scheme 2, **4** and **7**), it allowed avoiding the use of a catalyst and could extend the scope further (Scheme 2, **2**).[12] However, unexpected side reactions were observed, such as a C-N bond cleavage[13] (Scheme 2, **3**) or elimination of a nitro group (Scheme 2, **6**).[14] More modern approaches include environmentally friendly solvents and multi-component reactions involving *in situ* generation of new indolizines

(Scheme 2, **8**), focused on more sophisticated starting materials (Scheme 2, **9**), and overcoming challenging groups (Scheme 2, **10**).[15]

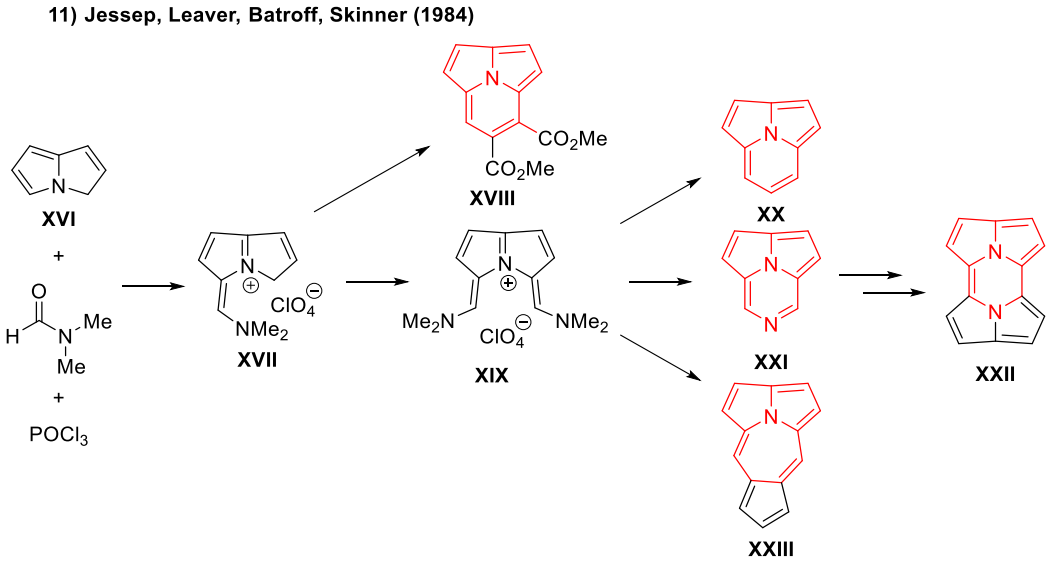


Scheme 2. [8+2] Cycloaddition reactions on indolizine and pyridine scaffolds to form cycl[3.2.2]azines

2.1.2. Cycloaddition on 3*H*-pyrrolizin scaffolds

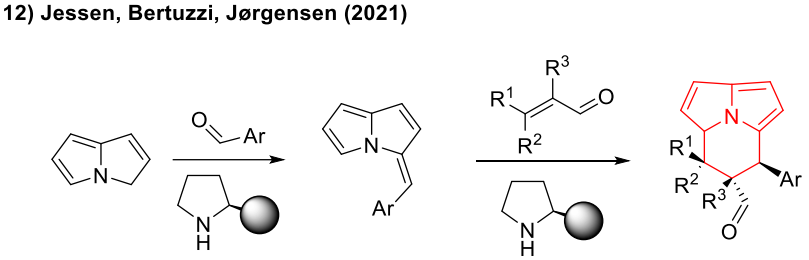
Further developments in the research on pyrrolizines enabled Jessep, Leaver, Batroff, and Skinner to utilize 3*H*-pyrrolizine as a starting material (Scheme 3, **11**). Beginning with a Vilsmeier-Haack reaction by treating the compound (Scheme 3, **XVI**) with *N*,*N*-dimethylformamide (DMF) and phosphoryl chloride at low temperature, implements an additional methylene group (Scheme 3, **XVII**). Further treatment with sodium hydride, in the presence of DMAD (Scheme 3, **XVIII**), yields a cycl[3.2.2]azine. Vinamidinium salts

(Scheme 3, **XIX**) allow for the diversification of subsequent steps (Scheme 3, **XX**, **XXI**).[16] A three-carbon annellation procedure, based on the work of Jutz and his coworkers, advanced the research,[17] and resulted in a doubly nitrogen-bridged annulene (Scheme 3, **XXII**) and a cycl[2.2.4]azines (Scheme 3, **XXIII**).[18]



Scheme 3. Carbon annellation procedure on 3*H*-pyrrolizines

Recent work by Jessen[19] expanded the research area to include chiral hydrogenated cycl[3.2.2]azines. Applying organocatalytic cycloadditions on a pyrrolizine scaffold was utilized to address chirality on the synthesis of new cycl[3.2.2]azine derivatives (Scheme 4, **12**).

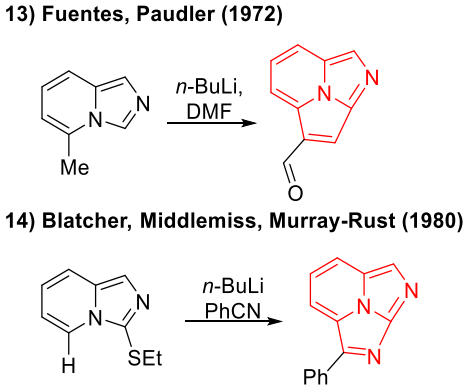


Scheme 4. Chiral cycl[3.2.2]azine derivatives due to organocatalytic cyclizations

2.1.3. Synthesis of Heterocycl[3.2.2]azines

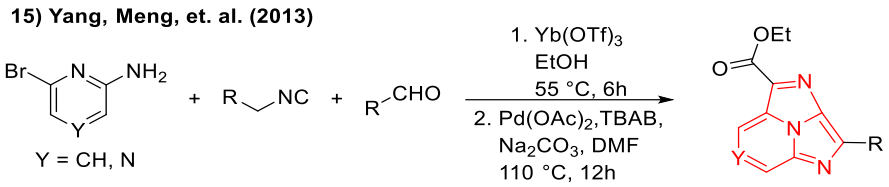
A common method to modify the electronic properties of polycyclic aromatic hydrocarbons is to dope the scaffold with heteroatoms.[20] Changing a carbon to a nitrogen, sulfur, or oxygen atom can influence both the electronic properties and the structural alignment in the solid state, thereby altering charge transport properties.[21] Modifying the periphery of a polycyclic

aromatic system has a significant influence on the aromatic properties of the molecule.[22] Early synthetic strategies include previously mentioned methods by using *n*-Butyllithium and DMF or DMAD in toluene with Pd/C on heteroatom-doped derivatives of indolizines (Scheme 5, **13**).[23] Later, direct insertion of a heteroatom into the scaffold became feasible by the attack of nitrile compounds (Scheme 5, **14**).[24]



Scheme 5. Formation of heterocycle[3.2.2]azines with *n*-Butyllithium

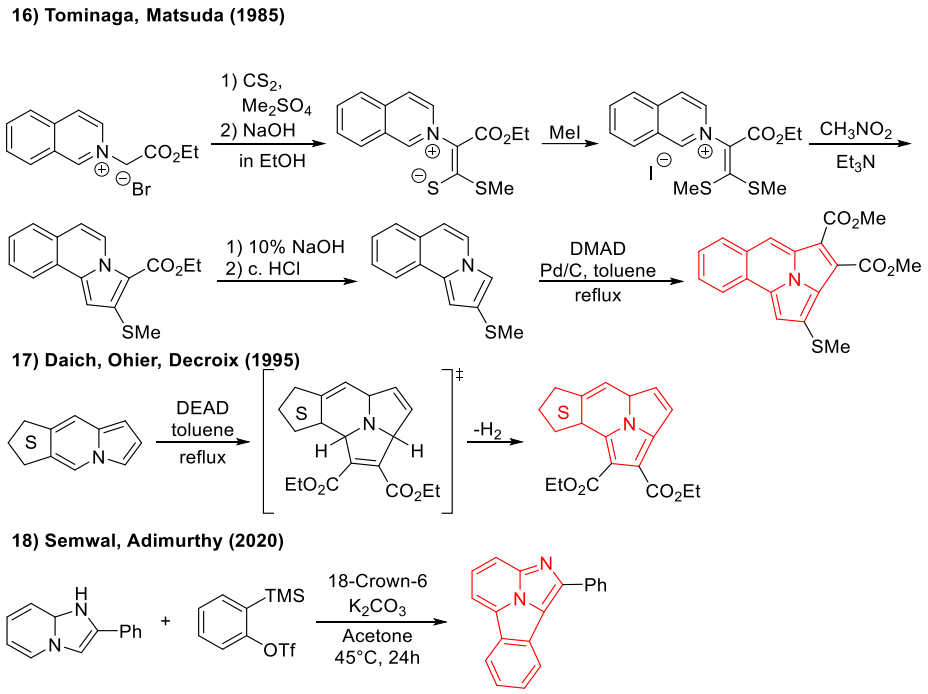
Continued development of synthesis strategies involved new approaches to palladium-catalyzed multi-component reactions, yielding N-doped cycl[3.2.2]azines from pyridine or pyrazine (Scheme 6, **15**).[25]



Scheme 6. Multi-component reaction for the formation of heterocycl[3.2.2]azines

2.1.4. Synthesis of π-extended Cycl[3.2.2]azines

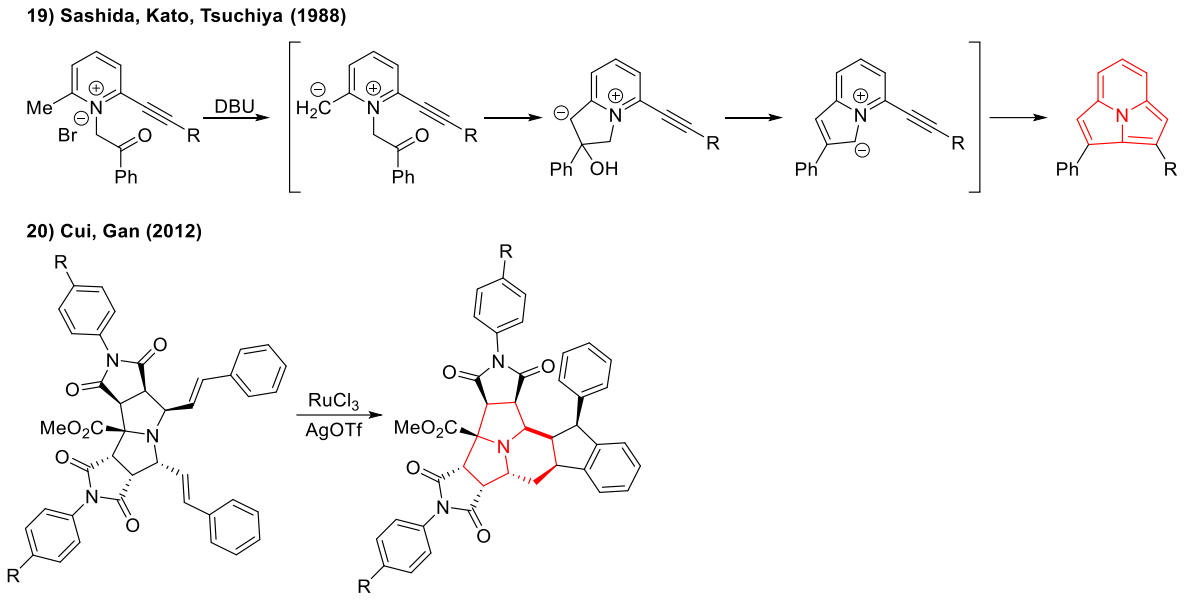
The expansion of the π-system can impact the aromaticity behavior of the scaffold. A wider π-system reduces the character of the electronic properties of a macrocyclic system due to a decreased bond localization in the macrocyclic ring.[26] A proactive design strategy to expand the ring system on the cycl[3.2.2]azine core is to carefully choose a suitable π-expanded quinoline,[27] pyridine,[28,29] indolizine[30] or thienoindolizines[31] derivative and perform a cycloaddition with DMAD (Scheme 7, **16** and **17**). More recent synthesis strategies could expand the work on cycloisomerization by gold catalysis[32] or avoid metal catalysis (Scheme 7, **18**).[33]



Scheme 7. Examples for π-extended cycl[3.2.2]azines

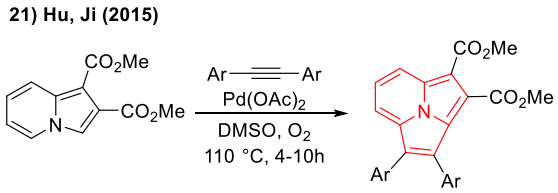
2.1.5. Alternative routes for synthesis of Cycl[3.2.2]azines

In the history of cyclazines, earlier synthesis routes to cycl[3.2.2]azines have included the use of DMAD or diethyl acetylenedicarboxylate (DEAD), which possess strong electrophilic character and are widely utilized as dienophiles in the cycloaddition reaction with indolizine or similar derivatives. Similar is the synthesis strategy of cyclazines involving *n*-Butyllithium, which deprotonates the methyl group on an indolizine scaffold. Subsequently, the deprotonated methyl group can react with an acetyl or nitrile group. The drawback of these examples, however, is the limited scope and/or practicability of both methods. Therefore, alternatives have been explored to overcome these limitations or to simplify reaction conditions. One of them is a thermal intramolecular cyclization, supported by a base, that facilitates a sigmatropic rearrangement (Scheme ***8***, **19**).[34] A rather unique example is an intramolecular Friedel-Crafts reaction followed by a 6-*exo*-trig cyclization. With the help of $RuCl_3$/AgOTf, a rare decahydrocycl[3.2.2]azine is obtained (Scheme 8, **20**).[35]



Scheme 8. Alternative routes for the synthesis of cycl[3.2.2]azines

More feasible and recent approaches include an oxidative and/or palladium-catalyzed cyclization of alkynes[36] or involve a visible-light-induced intermolecular [3+2] annulation (Scheme 9, **21**).[37]

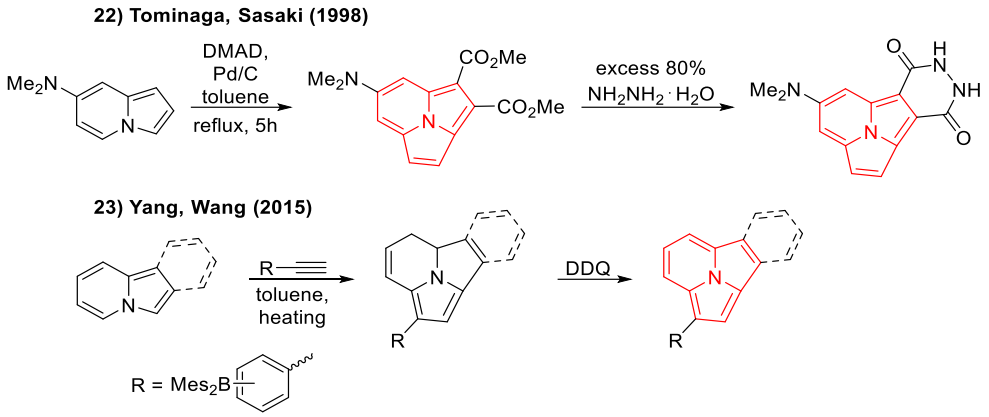


Scheme 9. Oxidative and palladium-catalyzed cyclization of an alkyne

2.1.6. Synthesis of chemiluminescent or fluorescent Cycl[3.2.2]azines

One final aspect of interest is the development of cycl[3.2.2]azines with high chemiluminescence or fluorescence. Their unique aromatic properties, combined with the introduction of strong acceptor or donor groups, enable further synthetic investigations for tuning and designing electronic and optical properties.[38] One approach involves the formation of cyclic hydrazide derivatives (Scheme 10, **22**).[39] Based on the work of Tominaga et al., a library of highly fluorescent cycl[3.2.2]azines with light intensity comparable to that of luminol has been synthesized, supporting advancements in the development of analytical methods for determining trace metals, diagnostic medicine, and biological science.[40] Additionally, the introduction of a $BMes_2$ group as a luminophore has been reported. This modification reduces intermolecular interactions in cycl[3.2.2]azine, leading to brightly blue or blue-green

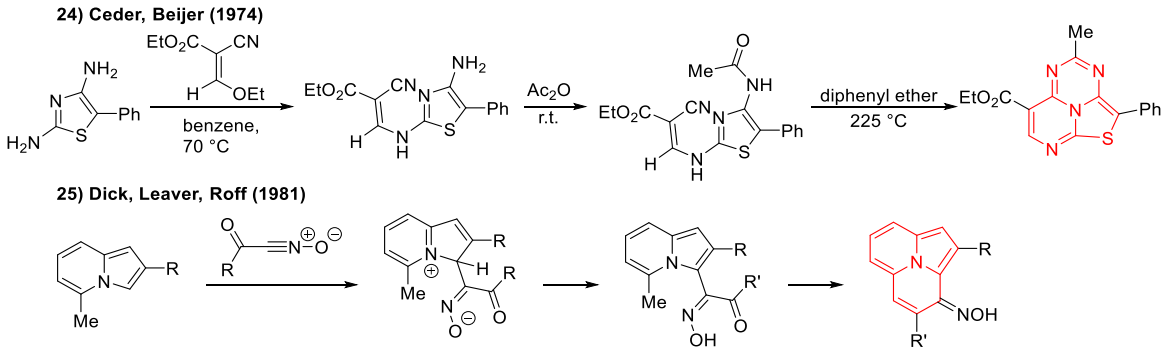
fluorescence with λ_{em} between 428 and 495 nm and a quantum yield ranging from 0.27 to 0.68 (Scheme 10, **23**).[41]



Scheme 10. Synthesis of chemiluminescent and fluorescent Cycl[3.2.2]azines

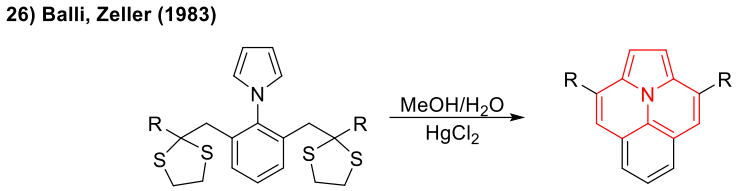
2.2.Synthesis of Cycl[3.3.2]azines

The first known report of a cycl[3.3.2]azin-related compound, cycl[3.3.2]azinium, was found in a footnote of the original publication on cyclazines by Boekelheide et al. in 1959.[6] Later, a base peak ($[M+1]^+$) in the electron-impact mass spectrum confirmed the presence of cycl[3.3.2]azinium, as reported in 1967 by R. M. Acheson and D. A. Robinson.[42] The molecule was possibly formed by a ring expansion of the cyclazine, resulting from the elimination of an electron and a hydrogen atom. Ongoing work focused on cycl[3.3.2]azines containing heteroatoms. The introduction of heteroatoms with their pronounced reactivity, such as nitrogen, oxygen, and sulfur,[43] enabled more practical synthetic routes and allowed for large-scale synthesis (Scheme 11, **24**).[44] Returning to the indolizine derivative as precursor, the known acidity of a 5-methyl group was exploited to initiate a base-induced condensation reaction with a *β*-carbonyl group (Scheme 11, **25**).[45]



Scheme 11. First advancements in the synthesis of heterocyclic cycl[3.2.2]azines

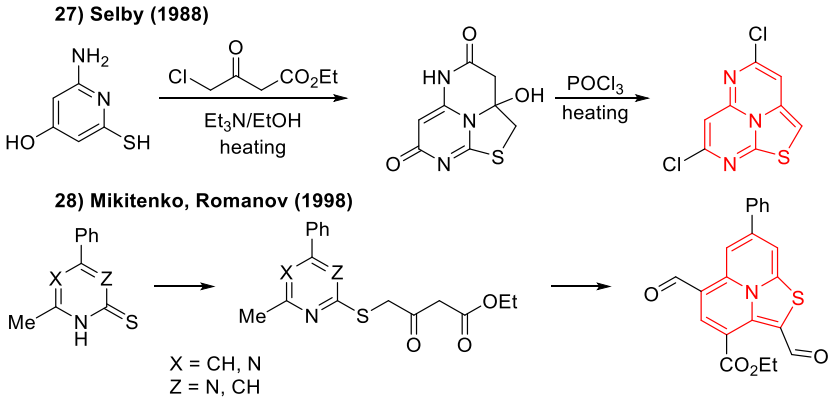
Within the framework of cycl[3.3.2]azines, ullazines can be seen as benzannulated derivatives, featuring an extra six-membered ring fused to the periphery of the two six-membered rings characteristic of the parent cyclazine structure. The initial synthesis of this class of molecules was reported by Balli and Zeller in 1983.[46] The described synthesis route begins with dimethyl 2-aminoisophthalate and involves an essential Clausen-Kaas reaction.[47] A phenylpyrrole resulting from this process was then substituted at the 2- and 6-position on the phenyl ring. Being prone to attack at the 2 and 5 positions on the pyrrole ring, further steps included side-chain elongation by one carbon atom, performed through reduction, conversion with thionyl bromide, and subsequent nucleophilic acylation. Lastly, hydrolysis in MeOH/H_2O with Hg_2Cl_2 led to ring closure, yielding ullazines as a benzannulated derivative of cycl[3.3.2]azine (Scheme 12**, 26**).



Scheme 12. Synthesis of the first ullazine, a derivative of a benzannulated cycl[3.3.2]azine

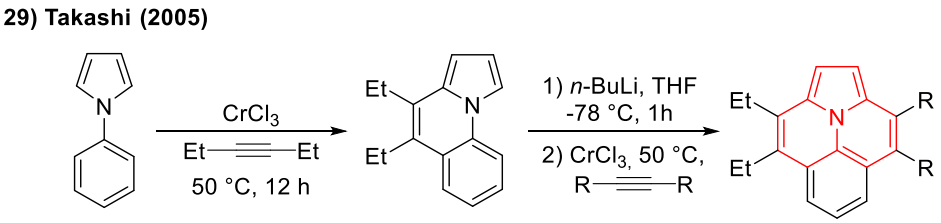
A cascade cyclization of an ester was reported and begins with a thiocarbamide unit, followed by a ring closure on an amine or hydroxy group[48] to yield partly saturated cycl[3.3.2]azines. Finally, a dehydrogenation of a tricyclic carbinolamine with phosphorus oxychloride completed the synthetic strategy (Scheme 13, **27**).[49]

Later, in 1998, it was reported that 2- and 4-mercaptopyrimidines with ethyl γ-bromoacetoacetate groups, a class of elaborated pyrimidines, were prepared and allowed to form new condensed cyclazine heterocycles. Present aldehyde groups on the scaffold have been further functionalized to obtain polymethine dyes and showed effects of the relative position of the methine group to the cycl[3.3.2]azines, as well as tendencies toward a reversed effect depending on the presence of a carboxyl or nitrogen group in the periphery (Scheme 13, **28**).[50] An intramolecular cyclization approach involving indolizine and an acyl group, catalyzed by Al_2O_3, which offers a unique method to access cyclazines. However, until now, no further investigation has been reported.[51]



Scheme 13. Early examples for the synthesis of heterocycl[3.3.2]azines from pyridines

Continued studies on ullazines have shown an alternative synthesis for cycl[3.3.2]azines via a chromium-mediated ring-closing of a phenylpyrrole. Lithiation, followed by the attack of alkylenes, catalyzed by the chromium salt, allowed for a broader range for the scope of ullazines (Scheme 14, **29**).[52]



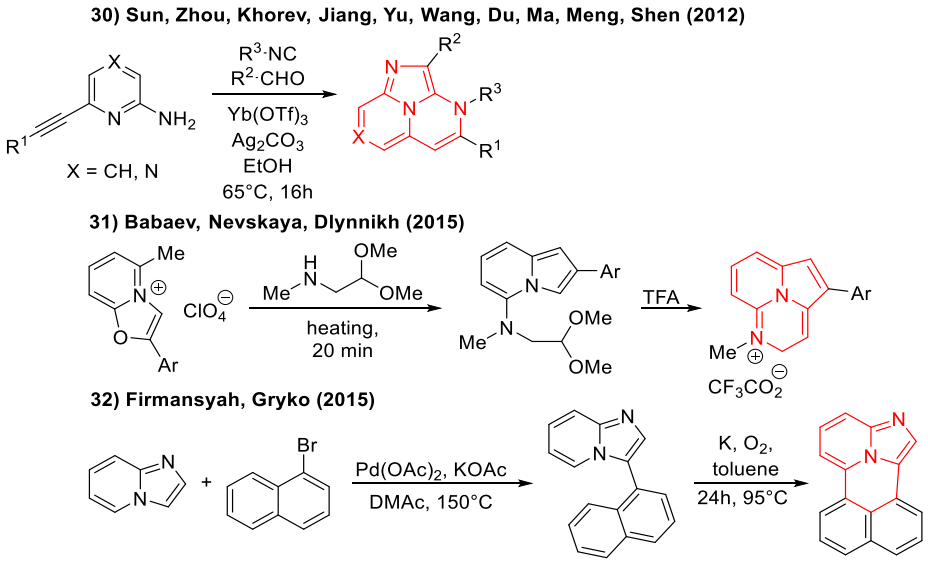
Scheme 14. Synthesis of ullazine via a chromium-mediated ring-closing

A novel approach was reported using the Groebke-Blackburn-Bienaymé reaction,[53] which is a multi-component reaction. It was applied in the development of cycl[3.3.2]azine, involving a condensation step followed by a transition metal-catalyzed intramolecular cyclization sequence (Scheme 15, **30**).[54]

It should be noted that Babaev's group reported nonstable cycl[3.3.2]azines.[55] When treating an indolizine derivative with CF_3COOH, it formed the salt pyrimidoindolizinium trifluoroacetate. However, attempts to form the corresponding base by treatment with an alkali metal or triethylamine resulted in decomposition (Scheme 15, **31**).

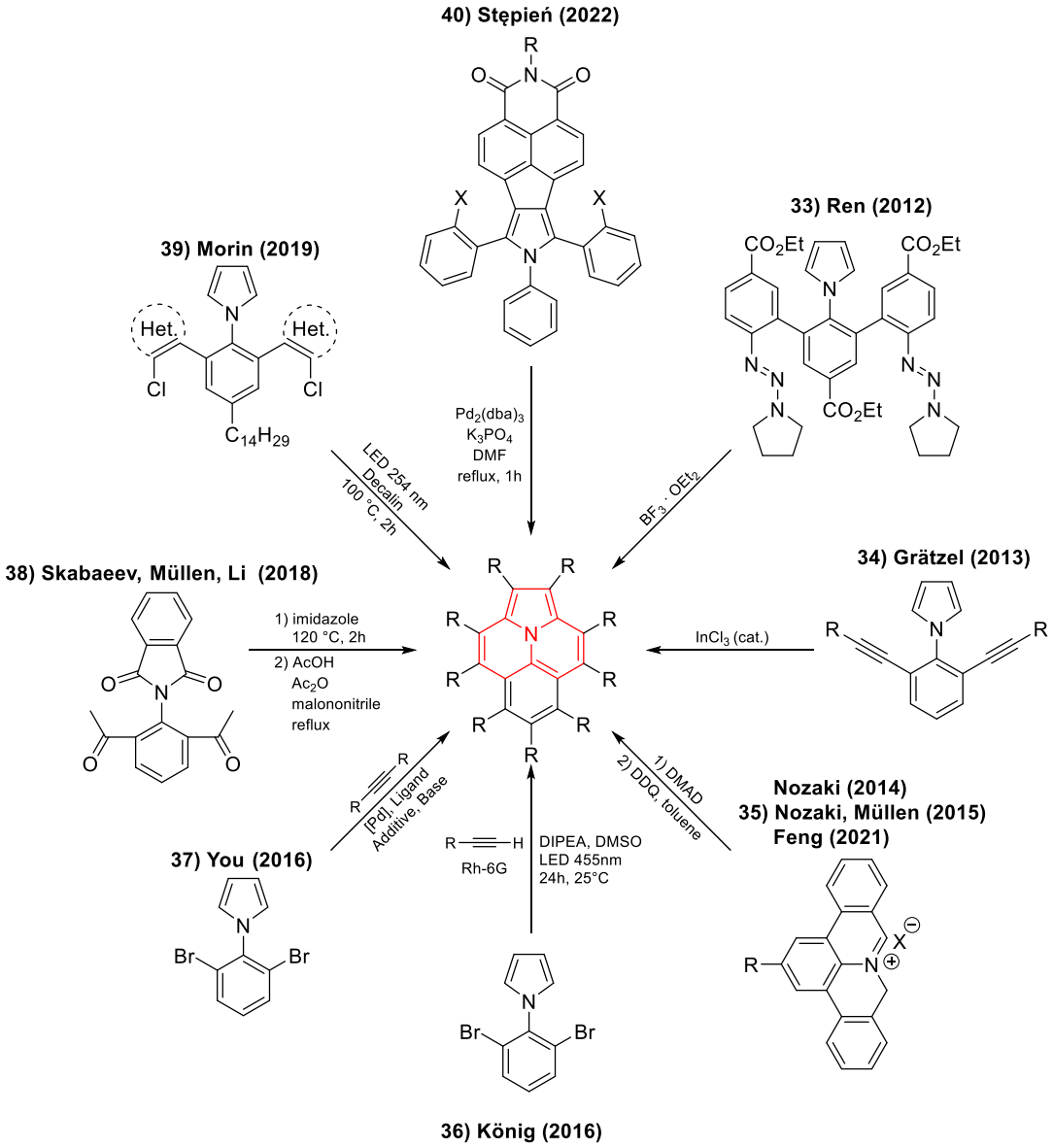
Meanwhile, a new method for vertical π-expansion on the scaffold of imidazo[1,2-*a*]pyridine with naphthalene has been discovered.[56] The route involves a dehydrogenative coupling enabled by the presence of potassium. Hereby, an anion-radical coupling reaction is applied to afford the new type cycl[3.3.2]azine and may describe a general application for two non-

electron-rich units which are not linked in the 1,1' positions. Moreover, the T_2 triplet state of the found compound was located close in energy to the S_1 state. Hence, efficient $S_1 \rightarrow T_2$ intersystem crossing, followed by $T_2 \rightarrow T_1$ internal conversion, allowed for the depopulation of the S_1 state and may be a reason for the low fluorescence quantum yield in the field of cycl[3.3.2]azines (Scheme 15, **32**).



Scheme 15. Recent examples for the synthesis of cycl[3.3.2]azines

Briefly summarized, significant progress in the field of ullazine synthesis has been reported from 2012 to 2022. New approaches in the synthesis involve the use of dipolarophiles, forming a ring closure around the central nitrogen through various methods, including Friedel-Crafts arylation (Scheme 16, **33**).[57] $InCl_3$-mediated cyclization (Scheme 16, **34**),[58] 1,3-dipolar cycloadditions (Scheme 16, **35**),[59] photo-catalyzed cyclization (Scheme 16, **36**),[60] palladium catalyzed cyclization (Scheme 16, **37** and **40**),[61] aldol condensation (Scheme 16, **38**),[62] and metathesis reactions (Scheme 16, **39**).[63]



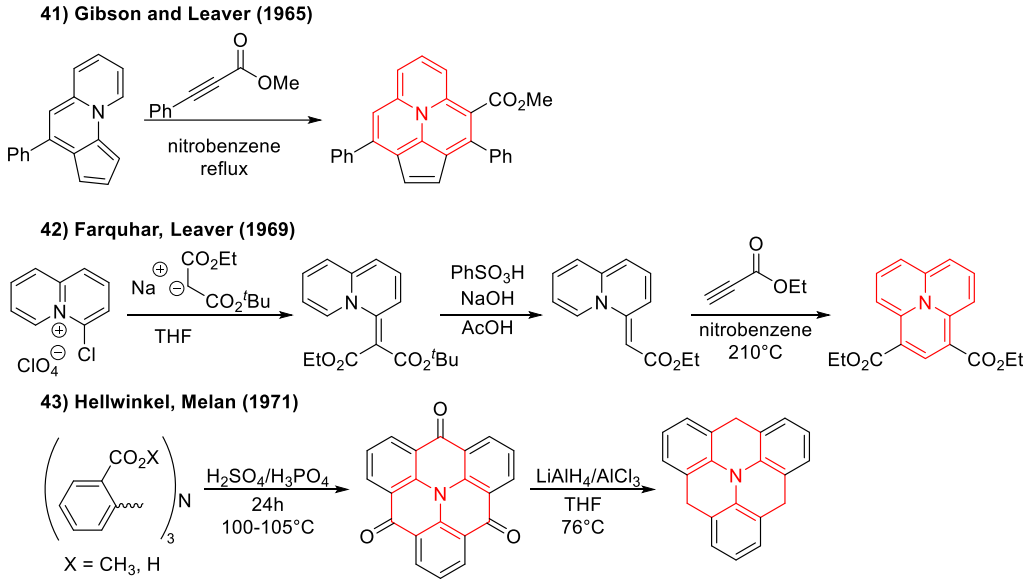
Scheme 16. Pathways for the synthesis of new ullazines as a derivative of cycl[3.3.2]azine

2.3.Synthesis of Cycl[3.3.3]azines

Also known as azaphenalene, cycl[3.3.3]azines have long been a challenging area in synthesis. Pioneering work was done by Leaver's group.[64] In 1965, a synthetic route to access a derivative of cycl[3.3.3]azine was reported by reacting cyclopenta[*c*]quinolizine with methyl phenylpropiolate in boiling nitrobenzene (Scheme 17, **41**). The work, using nitrobenzene as a dehydrogenating agent, proved effective, while no other media were found to be successful. Hereby, investigations centered on a cyclopenta[*c*]quinolizine system, which forms a maleic ester side chain.[65]

The core ring structure of cycl[3.3.3]azine was successfully synthesized by Farquhar in 1969, starting from 4-chloroquinolizinium perchlorate (Scheme 17, **42**).[66] It was found to be stable in a nitrogen atmosphere, but decomposed within minutes when exposed to air or when dissolved in chloroform or hydroxylic solvents.

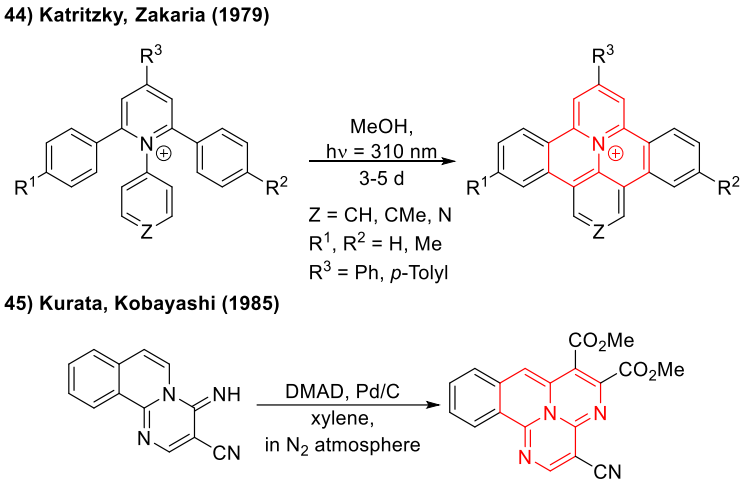
Starting from nitrilotribenzoic acid and treating with concentrated sulfuric acid or polyphosphoric acid allowed for cyclization to a triketone derivative of cycl[3.3.3]azine.[67] Further studies with UV-measurements indicated a non-planar structure. This route involved the reduction of ketone moieties to a methylene bridge, and a wider range of starting materials enabled functionalization of the methylene bridges (Scheme 17, **43**).



Scheme 17. Early synthetic developments of cycl[3.3.3]azine

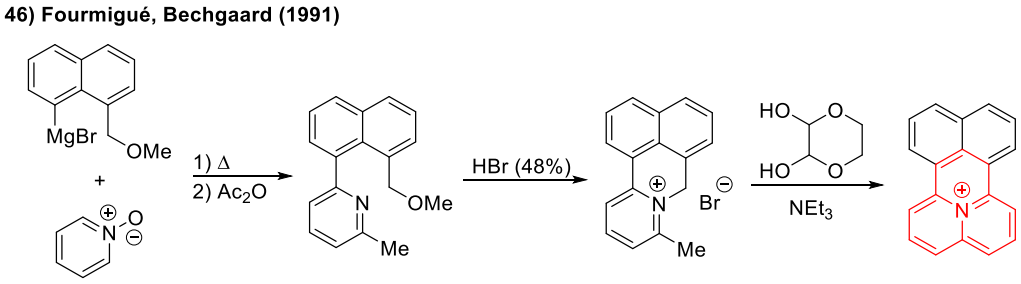
Katritzky and Zakaria reported a photobicyclization of a 1,2,6-triarylpyridinium cation.[68] The pyridinium salt was irradiated in a Rayonet photochemical reactor with 350 nm lamps. Conversion to the product was indicated by a decrease in absorption at 310 nm. Yields of up to 85% were achieved, and a broad scope of the bis-cyclization was demonstrated (Scheme 18, **44**). This method enabled applications in materials science[69] and the development of DNA intercalators.[70] Furthermore, its behavior of pseudo-base formation was observed and investigated through NMR and UV experiments during the synthesis of benzannulated cycl[3.3.3]azines via bis-photocyclization. The addition of D_2O shifted the ^{1}H and ^{13}C NMR spectra upfield by the amount of water used.[71]

Later, it was reported that *N,N*-dimethylformamide (DMF) induced a ring closure to an imine group to yield cycl[3.3.3]azines, making use of an effective ring-closing procedure on a quinolizine moiety (Scheme 18, **45**).[72]



Scheme 18. Effective ring closure reactions on tri-aryl pyridines and quinolizine moieties

Fourmigué, Eggert, and Bechgaard demonstrated an ambitious method by connecting naphthalene and quinolizin-5-ium to form the perylenic analogue in three steps.[73] The synthesized intermediate salt offers two potentially nucleophilic sites for a reaction with α-dioxo compounds. In the last step, reaction in the presence of a base with glyoxal equivalent, 2,3-dihydroxy-1,4-dioxane, yields the desired cycl[3.3.3]azine. Additional NMR studies revealed that the 10 π-electron fragments of quinolizinium and the naphthalene moiety interact only slightly **(**Scheme 19**, 46).**

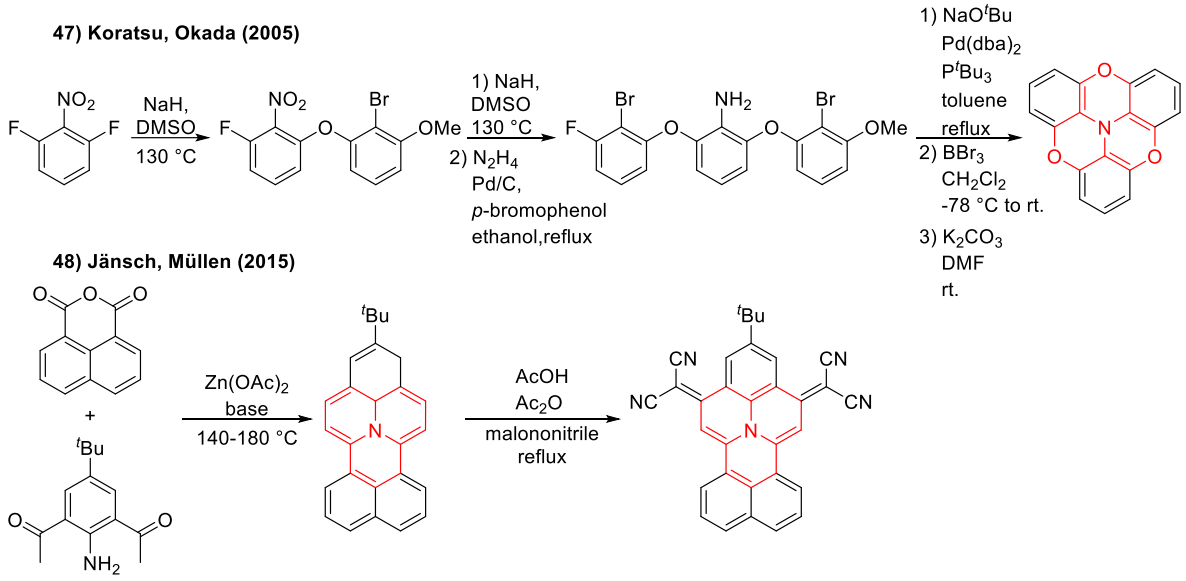


Scheme 19. Formation of a cycl[3.3.3]azine out of a naphthalene quinolizinium moiety

Work on triphenylamines by Hellwinkel, including bridges via oxygen atoms, resulted in the formation of a trioxycycl[3.3.3]azine derivative. The synthesis route began with a sequential aromatic nucleophilic substitution of 2,6-difluoro-nitrobenzene with 2-bromo-3-methoxyphenolate and 2-bromo-3-fluorophenolate. Followed by a selective reduction in the

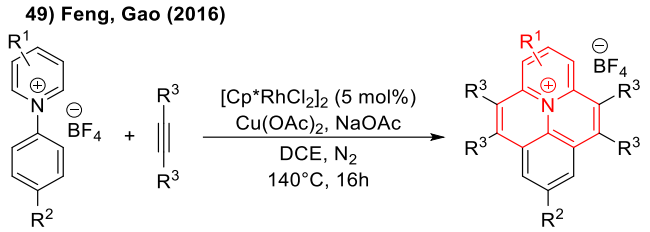
presence of *p*-bromophenol and an intramolecular palladium-catalyzed cyclization. Treatment with BBr_3 converted the remaining methoxy group into a hydroxy group, allowing it to substitute for the fluorine group and yielding the desired product (Scheme 20, **47**). Further theoretical studies confirmed that the structure resembles a good electron donor, characterized by a shallow bowl structure. It can form charge transfer complexes, and the radical cation of trioxycycl[3.3.3]azine is found to be a highly stable and planar compound.[74]

In the context of rylene chemistry, a transformation of the scaffold into new types of chromophores was achieved by using 2,6-diacetyl aniline, resulting in 3*a*-aza-1,6-phenalenedione-extended rylene skeletons. By enclosing the central nitrogen with two cyclizations, a new synthetic approach for cycl[3.3.3]azine was developed. The same synthetic approach was demonstrated for the tetra-*tert*-octylphenoxyperylenemonoanhydride and tetra-*tert*-octylphenoxypyrelenedianhydride (Scheme 20, **48**).[75]



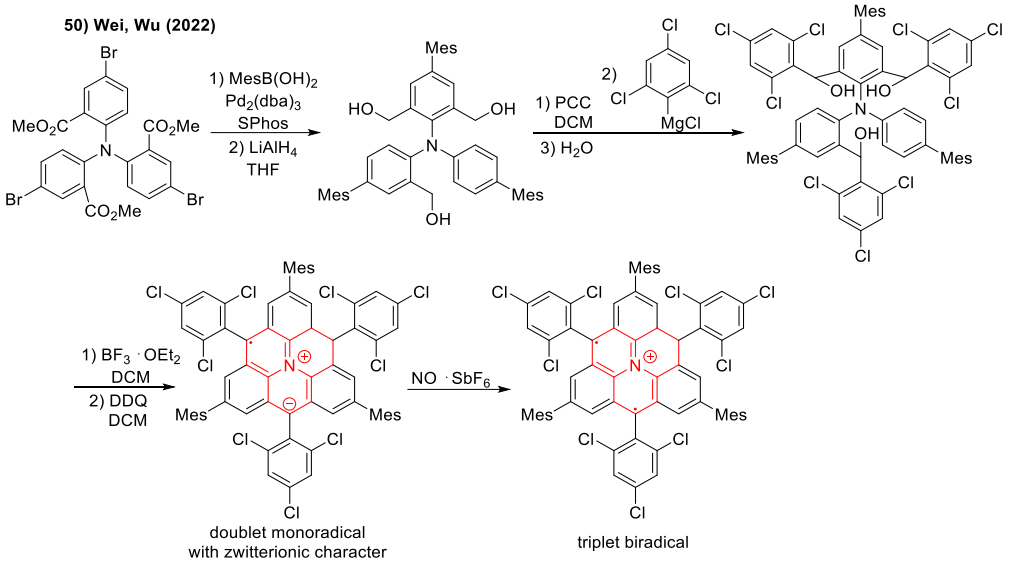
Scheme 20. Bridged triphenylamines and rylene chemistry as a waypoint to new cycl[3.3.3]azines

A transition metal-catalyzed synthetic method was reported based on a rhodium(III)-catalyzed C-H annulation of *N*-arylpyridinium salts with alkynes. This approach provides access to 12-azapyrene salts with tunable fluorescent emission in both solution and solid state. Additionally, the reaction mechanism was investigated through H/D exchange experiments. The work was extended by the conversion of quinolizinium salts with rhodium and cobalt catalysis. This procedure may allow for a general cyclization between a phenyl and pyridinyl moiety (Scheme 21, **49**).[76]



Scheme 21. Cyclization between phenyl and pyridinyl moiety through a rhodium(III)-catalyzed C-H annulation

Recently, a nitrogen-doped triangulene derivative and its cation were synthesized, which are electronically equivalent to a triangulene radical anion and a triangulene biradical. The required stability was achieved through the kinetic blocking of reactive sites by bulky and electron-withdrawing aryl substituents, as well as through intramolecular donor-acceptor interactions. The neutral derivative was shown to be a doublet monoradical with zwitterionic character. The corresponding cation is shown to be a triplet biradical with a significant triplet energy gap (Scheme 22, **50**).[77]



Scheme 22. Stabilization of cycl[3.3.3]azinium salts and biradicals through bulky aryl substituents

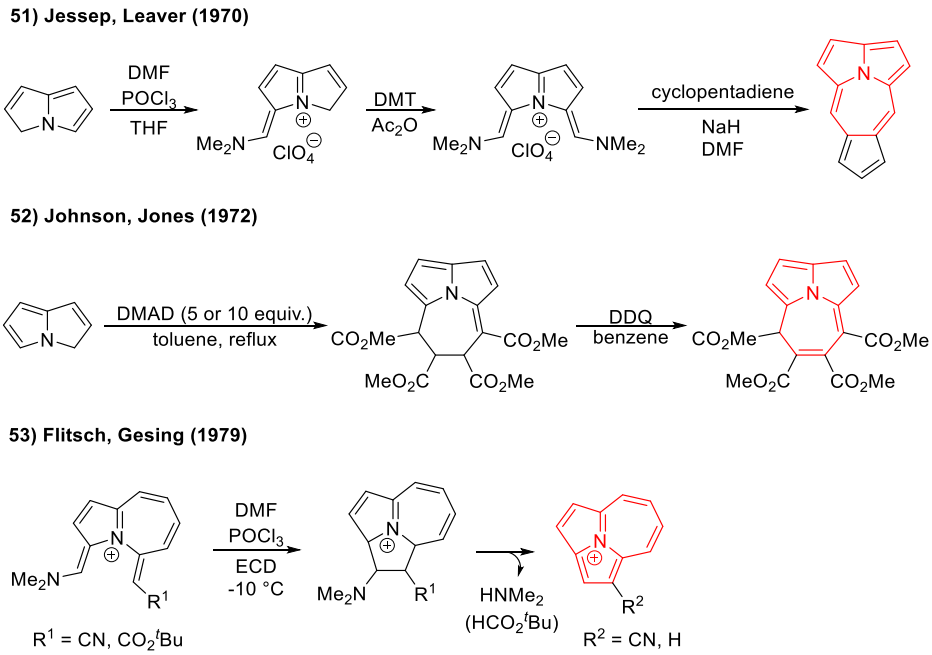
2.4.Synthesis of Cycl[4.2.2]azines

The first cycl[4.2.2]azine was synthesized by Jessep and Leaver in 1970,[16] during studies on the development of synthetic routes for cycl[3.2.2]azines with 3*H*-pyrrolizines. As mentioned earlier, the reaction with *N,N*-dimethylformamide and phosphoryl chloride produced a salt, which could be converted to 3,5-bis(dimethylaminomethylene)pyrrolizinium salt using *N,N*-dimethylthioformamide in acetic anhydride. Cycl[4.2.2]azine was obtained by reacting 3,5-bis(dimethylaminomethylene)pyrrolizinium salt with sodium hydride and cyclopentadiene

in DMF. The compound appears as green plates, containing 14 peripheral π-electrons, and can be viewed as an analogue of azulene (Scheme 23, **51**). Additionally, the same group reported a route starting from a fulvene derivative and pyrrolizine. However, it provided only traces of cyclopenta[*h*]cycl[4.2.2]azine.[78]

3*H*-pyrrolizine can be converted with DMAD in boiling toluene. To prevent the formation of the discussed 1:1 adduct and promote the 1:2 adduct, DMAD must be used in larger amounts (1:5 or 1:10). Reduction and oxidation reactions were successfully performed. However, the initial studies on the mechanism using deuterated [3^2*H*]-pyrrolizine could not provide conclusive insights (Scheme 23, **52**).[79]

Pyrroloazepine has been reported as a useful building block. The formation of the corresponding salt was found to stabilize cycl[4.2.2]azinium salt and its derivatives. Development of 3,5-disubstituded pyrrolo[1,2-*a*]azepines[80] would further enable the elimination of the dimethylamine and *tert*-butyl group to form the first parent cycl[4.2.2]azinium salt (Scheme 23, **53**).[81]

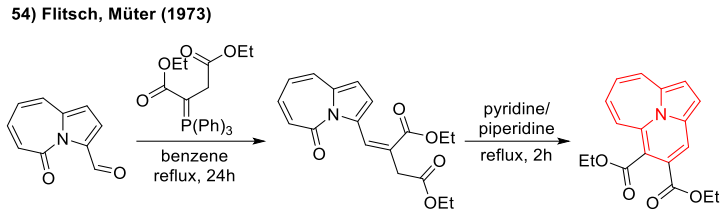


Scheme 23. Synthesis of cycl[4.2.2]azine via 3*H*-pyrrolizine or pyrrolazepines under Vilsmeier reaction conditions

2.5. Synthesis of Cycl[4.3.2]azines

In addition to cycl[3.3.3]azine, which possesses paratropic properties, a 12 π-system can also be formed by a cycl[4.3.2]azine. When comparing different tricyclic heterocycles, exploring

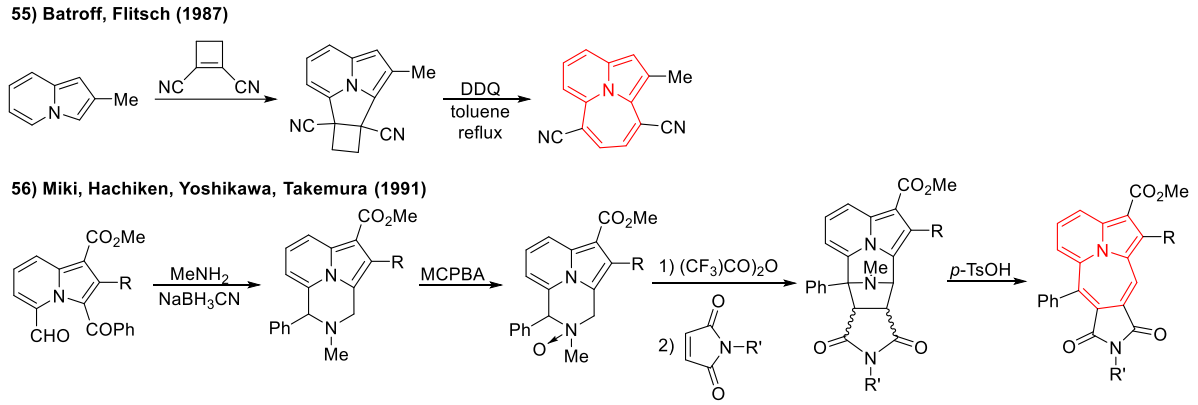
alternative derivatives of a 12π-system can be of great value in understanding aromatic and electronic properties. In 1973, the first cycl[4.3.2]azine was reported by Flitsch and Müter, initiated from a 3*a*-azaazulene-4-one.[82] The synthetic strategy involves a Wittig-Olefination followed by a base-catalyzed cyclization (Scheme 24, **54**).



Scheme 24. Methods for the synthesis of cycl[4.3.2]azines by Wittig-olefination

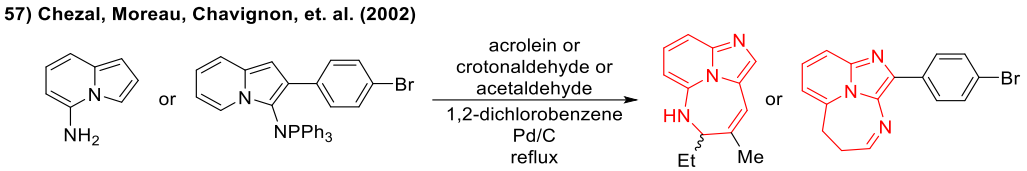
A synthetic strategy was reported by Batroff and Flitsch in 1987, using 1-cyclobuten-1,2-dicarbonitrile[83] to form a tetracycle on the framework.[84] Subsequently, a dehydrogenation with DDQ in boiling toluene was performed to break the 5- and 4-membered rings, establishing a new seven-membered ring and generating cycl[4.3.2]azine-6,9-dicarbonitrile (Scheme 25, **55**).

Miki and coworkers reported a similar route, using pyridinium bromide with DMAD or methyl propiolate to yield a new type of indolizines. The route further involves a cyclization through reductive amination and oxidation by *m*-chloroperbenzoic acid (MCPBA). Subsequent treatment with trifluoroacetic anhydride formed a betaine, which then rearranges with *N*-methyl- or *N*-phenylmaleimide to produce a mixture of *exo* and *endo* isomers. Finally, treatment with *p*-toluenesulfonic acid in boiling acetic acid yields the desired product (Scheme 25, **56**).[85]



Scheme 25. Methods for the synthesis of cycl[4.3.2]azines by rearrangement reaction

Aminoimidazopyridines or phosphoranylideneindolizinamine have been reported as suitable building blocks for the preparation of new cycl[4.3.2]azines via a Pd/C-catalyzed aldol reaction resulting in the formation of a *peri* annulated structure (Scheme 26, **57**).[86]

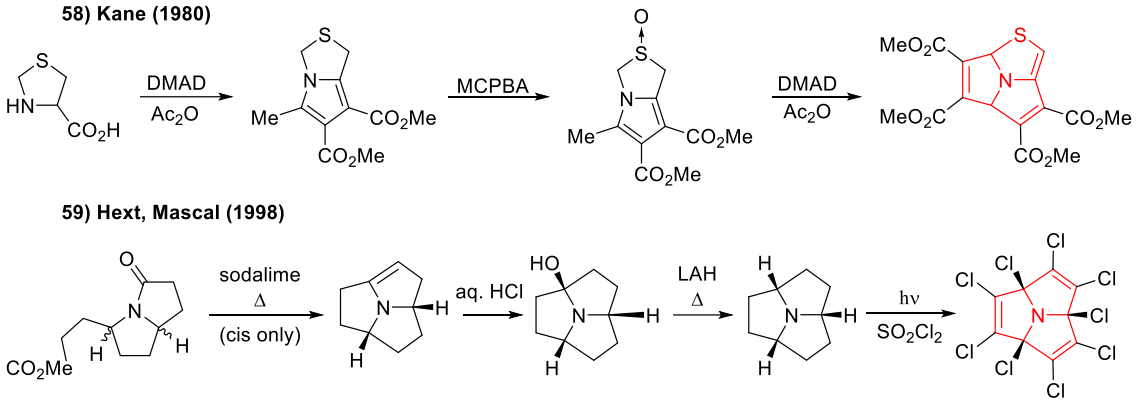


Scheme 26. Methods for the synthesis of cycl[4.3.2]azines by Pd-catalyzed aldol reaction

2.6.Synthesis of Cycl[2.2.2]azine

Throughout the history of synthesizing cyclazines, a significant challenge has been accessing cycl[2.2.2]azine. Early work was reported by John M. Kane in 1980,[87] starting from thiazolidine-4-carboxylic acid and acetic anhydride in the presence of DMAD, which afforded 1*H*,3*H*-pyrrolo[1,2-*c*]thiazole. Subsequent conversion was carried out to its corresponding sulfoxide using MCPBA, and dehydration in refluxing acetic anhydride led to the azomethine ylide. An unexpected result enabled a cycloaddition across an azomethine ylide with DMAD, ultimately yielding the rare heterocycle[2.2.2]azine (Scheme 27, **58**).

Eighteen years later, Hext and colleagues developed a dedicated synthesis strategy for azatriquinane through sequential cyclization,[88] starting from a 2,5-pyrrole-dipropanoic acid dimethyl ester (Scheme 27, **59**). Hydrogenation over rhodium on alumina resulted in a mixture of pyrrolidine. A second cyclization was carried out by prolonged heating at reflux in toluene, yielding a separable mixture of two isomers.



Scheme 27. Synthesis of rare cycl[2.2.2]azine framework

The *cis* compound was cyclized by dry distillation in a mixture with sodalime, followed by treatment with aqueous acid to yield the hemiaminal. Reduction with lithium aluminum hydride produced the triquinane. Finally, the oxidation-partial reduction protocol by Jacobson[89] allowed for the conversion to the anticipated azatriquinacene derivative. Attempts for subsequent dichlorination were not successful.

3. Properties of Cyclazines

Cyclazines are a distinct class of nitrogen-centered, π-conjugated tricyclic systems with intriguing electronic and structural features. Their frameworks and electron distribution patterns have attracted significant interest, especially regarding their aromaticity, magnetic properties, and their behavior in excited states.

3.1. Aromatic properties of Cyclazines

The concept of aromaticity is of great importance[90] and discussed from the standpoint of geometric,[91] energetic,[92] and magnetic criteria, including proton chemical shifts,[93] exaltation of magnetic susceptibilities,[94] ring current density plots,[95] harmonic oscillator model of aromaticity (HOMA),[91] HOMO-LUMO gaps and nucleus-independent chemical shifts (NICS).[96] Furthermore, a summation of NICS values (ΣNICS) as a global aromaticity index,[97] called "total NICS", produces a single quantity that can be compared with other global indicators of aromaticity, such as magnetic susceptibility exaltation (MSE) or global-HOMA.[98] The Hückel aromaticity rule states that planar, monocyclic conjugated systems with 4n + 2 π-electrons are aromatic.[99] However, the applicability of this rule to *peri*-fused conjugated systems, such as cyclazines, has been a matter of question.[100]

With the introduction of cyclazines, research into their properties has been actively pursued.[101] Their tricyclic system features a conjugated perimeter of sp^2-hybridized carbon or heteroatoms and is bridged by a centrally located N atom.[2] It was soon noted that the central nitrogen atom does not participate in the π-electron conjugation despite its sp^2-hybridization. This suggests that the molecular framework exhibits unexpected electronic behavior and warrants further investigation to enhance the current understanding of the concept of aromaticity. So far, the focus has mainly been on their physicochemical[102] and magnetic[103] properties. Considerable effort has also been devoted to computational analysis.[104,105] It is also worth noting that a

symmetrical cyclazine model could aid in predicting electronic spectra of aromatic scaffolds.[106]

Conjugated ring systems, when placed in a magnetic field, generally generate an induced ring current, allowing for the study of diamagnetic anisotropy and chemical shift of the structure. However, comparing calculated ring currents with experimental results can only be valid when considering the influence of various factors contributing to diamagnetic anisotropy and chemical shift. Early computational studies focused on the ring current, and a hypothetical cycl[3.2.2]azine was envisioned to examine how the electronegativity of the central nitrogen atom affects the ring current. It was concluded that increasing the electronegativity would also increase the chemical shift and decrease the range of values for the different protons. The conclusion was that the higher electronegativity would lead to a closer 10-electron ring formed only by peripheral carbon atoms, with the two electrons on the central nitrogen becoming localized.[107]

To study the electronic properties, cyclazines were often compared across different aspects, such as the central atom, ring size, or the periphery of the cyclazine.[108] Changing the ring sizes significantly affected the stability of the molecule, revealing challenges in the synthesis. Another focus was to examine the periphery of cyclazines by comparing parent cyclazines to heteroatom-doped peripheries and both symmetrically and unsymmetrically π-extended cyclazines. Comparing these structural features can provide insights into the general behavior of aromaticity in cyclazines and polyaromatic systems (Figure 4).[109–111]

As the first synthetically established example, the cycl[3.2.2]azine has been the most studied derivative due to its stability. It can be seen as the prototypical tricycle of the family, featuring a C_{2v} spatial symmetry and a 10π-peripheral diatropic conjugation.[108] Furthermore, due to its accessibility, reactivity on this scaffold could be examined very early.[9] It was also observed that the central nitrogen showed no basic character, indicating a weak interaction between the nitrogen lone pair and the peripheral conjugated system.[112]

Compared to the cycl[3.2.2]azine, the derivative with three six-membered rings remained synthetically challenging. Early interpretations of MO calculations for the cycl[3.3.3]azine

predicted an anti-aromatic character, which drew particular interest in this scaffold. It was Leaver and coworkers who firstly reported access to the cycl[3.3.3]azine in 1965.[64]

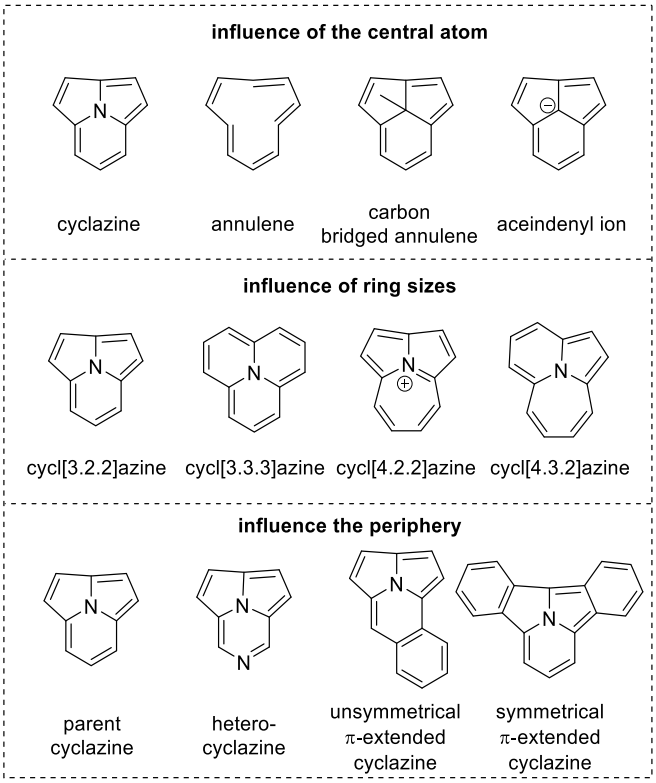


Figure 4. Studies of cyclazines comparing different aspects

Placing nitrogen atoms on the periphery of a cycl[3.3.3]azine allows for protonation. A sequential protonation of three peripheral nitrogen atoms in aqueous sulfuric acid was shown, and a color change was noticeable, reaching from purple red to orange ($pK_1 = 3.46$, $H \leftrightarrows H^+$), to yellow orange ($pK_2 \cong -2.2$, $H^+ \leftrightarrows H^{2+}$), to yellow ($pK_3 \cong -7.2$, $H^{2+} \leftrightarrows H^{3+}$). However, the central nitrogen atom is completely non-basic, as previously reported.[113]

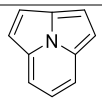
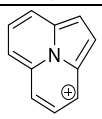
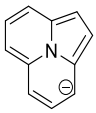
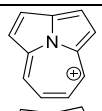
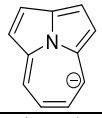
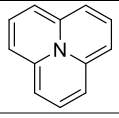
As a representative for the class of cycl[4.2.2]azines, mainly the cyclopenta[*h*]cycl[4.2.2]azine was first synthetically established. Its properties and characteristics were studied, and early investigations suggested a planar [14]annulene cross-linked with single bonds.

Furthermore, parent cycl[4.3.2]azine can be regarded as a mixed indolizine-cyclobutadiene structure. It combines known aromaticity from the indolizine with observed anti-aromatic behavior of a seven-membered ring.

The aromaticity of cyclazines has been studied computationally in a work by Fallah-Bagher-Shaidaei, Farkhonde, and Navideh.[111] Comparatively, the values of the magnetic criteria Λ, (magnetic susceptibility exaltations, MSE), ΣNICS, ^{1}H NMR chemical shifts, geometry-based HOMA index, and HOMO-LUMO gaps were evaluated to elucidate the aromaticity of various cyclazine classes and to predict aromatic or anti-aromatic behavior. Each parameter of aromaticity was consistent in its indication, offering a view of the aromatic behavior of cyclazines that could be provided (Table 1).

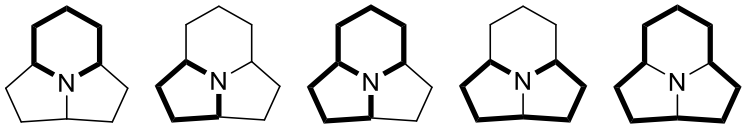
Furthermore, the influence of aromaticity on benzene ring fusion in cyclazines has been examined by topological resonance energy,[114] (TRE) bond resonance energy,[115] (BRE) circuit resonance energy,[116] (CRE) resonance energy per electron (REPE) and magnetic resonance energy (MRE). The values of TRE, BRE, CRE, and REPE are given in units of |β|, where β is the standard resonance integral in Hückel theory.[99] To understand the effect of the central nitrogen atom, the same values were calculated for the corresponding annulenes as reference compounds. Results indicate that the central nitrogen atom significantly influences global and local aromaticity, contributing to the aromaticity of the entire compound.

Table 1. Aromaticity parameters for different cyclazine classes

system	**structure**	**π-electron count**	**ΣNICS(1)** (ppm)	**MSE (Λ)** cgs ppm	**HOMA** (global)	**Δ_{HL}**[a] (eV)	**aromaticity**
[3.2.2]		10	-35.4	-30.4	0.809	4.08	aromatic
[3.3.2]		10	-32.8	-30.3	0.812	4.24	aromatic
[3.3.2]		12	37.8	55.6	0.722	2.31	antiaromatic
[4.2.2]		10	-36.4	-34.2	0.863	3.59	aromatic
[4.2.2]		12	107.0	159.8	0.563	1.77	antiaromatic
[3.3.3]		12	51.3	103.7	0.935	2.20	antiaromatic

[a] Δ_{HL} = HOMO-LUMO gap

However, it is essential to note that in the studies of Mattursun and Kerim, none of the examined compounds support a peripheral π-system, which contradicts earlier results in the literature.[6,29,102,117] Additionally, fused benzene rings on the cyclazine show a relatively larger local aromaticity and decrease the local aromaticity of the central cyclazine. In this context, Clar's π-sextet rule aligns with the results,[118] and compounds with three double bonds in their six-membered rings indicate a relatively larger local aromaticity, as reflected by an increased value of CRE. Calculated circuit current (CC) and CRE results for cycl[3.2.2]azines and their derivatives conclude that the ring current that passes through a six-membered ring or a single five-membered ring contributes to a diatropic effect. In contrast, the ring current of a pyrrolizidine moiety contributes to a paratropic effect (Figure 5).[110]



CRE:	0.0308	0.0718	0.0365	-0.0134	0.0630
CC:	0.1386	0.2140	0.2733	-0.0796	0.6584

Figure 5. Geometrically non-identical π-electron circuits, CRE (in β units), and circuit currents (CC, in I_0 units)

Kleinpeter and Koch continued their investigation of aromaticity in cyclazines, exploring compounds from cycl[2.2.2]azine to cycl[4.4.4]azines, including hetero-analogues and corresponding hydrocarbon derivatives. Their research involved analysis of ^{1}H, ^{13}C, and ^{15}N chemical shifts, NICS values, and Trough-Space NMR Shielding Surfaces (TSNMRSSs) using Iso-Chemical-Shielding-Surfaces (ICSSs). While ^{13}C chemical shifts are less helpful in characterizing aromaticity, aromatic compounds tend to cause more noticeable deshielding or shielding effects on ^{1}H chemical shifts. The ^{15}N chemical shift of the nitrogen atom in the cyclazines nodal position is particularly significant. For example, the ^{15}N chemical shifts of cycl[3.2.2]azine ($\delta(^{15}N)$ = -192 ppm) and cycl[3.3.3]azine ($\delta(^{15}N)$ = -151 ppm) differ by 43 ppm, reflecting the expected high field shift in a paratropic ring current and a low field shift in a diatropic ring current. The chemical shift of the ^{15}N at the center of the molecule is highly dependent on the size of the ring systems involved. Additionally, the lone pair on nitrogen generally does not participate in the peripheral ring current that influences aromatic behavior (Figure 6). The study also examined NICS values and visualized TSNMRS. It was observed that larger rings attached to the central nitrogen or more heteroatoms on the periphery can compromise planarity and ring current, making NICS less reliable and potentially leading to

incorrect conclusions about aromatic or antiaromatic characteristics.[111] However, NICS values on a grid around the structure[119] (spatial NICS) can be computed as TSNMRSs and were visualized as ICSSs. Besides peripheral ring currents on planar or slightly bowl-shaped cyclazines, certain ring currents within specific ring structures were observed in negatively charged cycl[3.3.2]azine, neutral cycl[4.3.2]azine, and positively charged cycl[4.3.3]azine and cycl[4.4.2]azine, indicating the presence of two ring currents with different directions within the same molecule. Furthermore, cyclazines with larger rings, such as cycl[4.4.3]azine, and negatively or positively charged cycl[4.4.4]azine, tend to be heavily twisted and do not exhibit a peripheral ring current.[109]

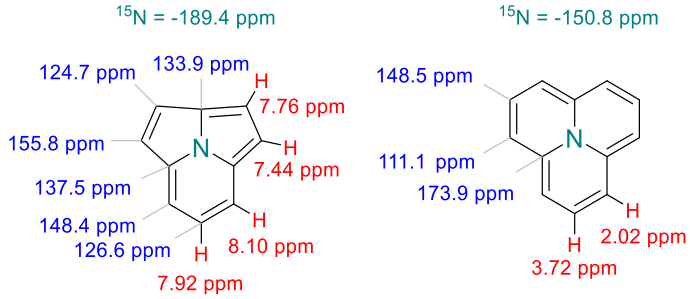


Figure 6. ^{1}H, ^{13}C, ^{15}N chemical shifts of cycl[3.2.2]azine and cycl[3.3.3]azine

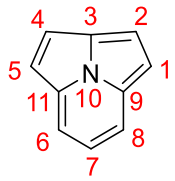
3.2. Electron Spin Resonance Studies

Electron Spin Resonance (ESR) spectroscopy, also known as Electron Paramagnetic Resonance (EPR), is used to study molecules with unpaired electrons, such as radicals or radical ions. In π-conjugated systems, it can provide insights into the distribution of unpaired electron density. Cyclazines often form stable radical anions and cations, making them interesting targets for investigating the π-spin population and unpaired electron density in such structures. For instance, the obtained coupling constants can indicate higher or lower local spin density and, overall, aid in interpreting the unique electronic properties of cyclazines.

Early experimental investigations of electron spin distribution on a cycl[3.2.2]azine anion were performed by Atherton, Gerson, and Murrel in 1962.[120] It was the first spectrum of a radical containing a conjugated nitrogen atom having no σ-lone-pair electrons. The work compared the anion derived from sodium and potassium. Differences in the spectrum were initially attributed to metal splitting effects but were ultimately attributed to variation in proton or nitrogen coupling within the cyclazine anion itself. Absolute values of the splitting were

obtained by comparing with the spectrum of peroxylamine disulphonate (Table 2).[121] Additionally, theoretical calculations of the spin densities were performed and compared with those of the aceindylenyl ion, the parent hydrocarbon of cycl[3.2.2]azine. The radical ion contains thirteen π-electrons in the parent hydrocarbon, and the unpaired electron is antisymmetric, causing the two-fold symmetric axis. Replacing carbon with nitrogen provides a first-order stabilization of symmetric orbitals. However, it was assumed that this effect would not change the lowest vacant orbital of cycl[3.2.2]azine, which is antisymmetric. Molecular Orbital (MO) theory predicts four protons in positions 2, 4, 6, and 8 to be equivalent, matching the experimental results ($\alpha_2 \simeq \alpha_3$). Yet, experimentally, non-zero spin densities are observed on the protons at the positions 1, 5, and 7 (α_3), contradicting the Hückel theory. Semi-empirical methods for the Hückel theory were used to refine the model, bringing it into agreement with experimental results and additionally confirming the cation dependence for positions 2 and 4 in their coupling constant.

Table 2. Coupling constants in gauss for the cyclazine negative ion



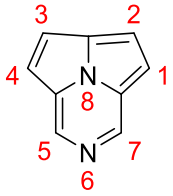
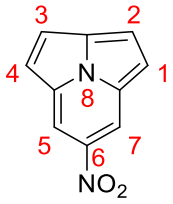
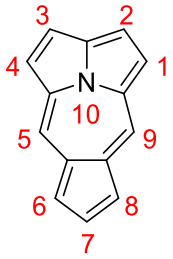
Coupling constant	Cation	
	Na	K
α_N	0.59±0.02	0.59±0.02
α_1	1.18±0.04	1.18±0.04
α_2	5.42±0.17	5.59±0.17
α_3	6.02±0.18	6.02±0.18

Furthermore, the structure of cycl[3.2.2]azine provided an interesting case for the further development of semi-empirical models to calculate coupling constants of the ^{14}N nucleus (α_N) in azaaromatic radical anions.[122]

Following progress in the synthesis of cyclazines by Jessep and Leaver, research on radical anions was continued for three new molecules: 6-azacycl[3.2.2]azine, 6-nitrocycl[3.2.2]azine, and cyclopenta[4.2.2]azine. The formation of the radical anions was achieved through electrolysis of the compound in DMF with tetraethylammonium perchlorate as the supporting salt, in addition to the previous chemical method using alkali metals. The 6-azacycl[3.2.2]azine exhibited coupling constants similar to those of the parent cycl[3.3.2]azine. It showed nearly identical π-spin distribution, which aligns with theoretical considerations, as the nitrogen on the periphery resides on a nodal plane of the lowest antibonding π-orbital and does not significantly influence this orbital to a first approximation. Substituting a nitro group significantly alters the π-spin distribution. The electron-affine group maintains the bulk of the

π-spin population. The cyclopenta[*h*]cycl[4.2.2]azine displays comparable π-charges, π-bond orders, and atom localization energies to those of azulene. Additionally, the π-spin population is primarily localized on the azulene-like moiety, and its distribution closely follows the pattern of an azulene (Table 3). This prediction is further supported by experimental proton coupling constants, which are comparable to those for azulene.[123]

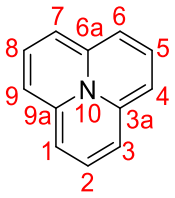
Table 3. Coupling constants of protons and ^{14}N nuclei (α_H and α_N in gauss), and calculated π-spin populatons (ϱ) in radical anions of 6-azacycl[3.2.2]azine, 6-nitrocycl[3.2.2]azine and cyclopenta[4.2.2]azine

	Coupling constant	**π-spin populations (ϱ)**
	$\alpha_{H(1,4)} = 1.07 \pm 0.01$	$\varrho_{1,4} = 0.045$
	$\alpha_{H(2,3)} = 5.92 \pm 0.04$	$\varrho_{2,3} = 0.233$
	$\alpha_{H(5,7)} = 6.22 \pm 0.04$	$\varrho_{5,7} = 0.237$
	$\alpha_{N6} = 2.03 \pm 0.02$	$\varrho_{6} = -0.066$
	$\alpha_{N8} = 0.55 \pm 0.01$	$\varrho_{8} = -0.013$
	$\alpha_{H(1,4)} = 1.28 \pm 0.01$	$\varrho_{1,4} = 0.053$
	$\alpha_{H(2,3)} = 0.47 \pm 0.01$	$\varrho_{2,3} = -0.031$
	$\alpha_{H(5,7)} = 3.42 \pm 0.02$	$\varrho_{5,7} = 0.153$
	$\alpha_{N8} = 0.82 \pm 0.01$	$\varrho_{8} = 0.023$
	$\alpha_{N}^{NO_2} = 9.75 \pm 0.05$	$\varrho_{N} = 0.239$ $\varrho_{O} = 0.199$
	$\alpha_{H(1,4)} = 2.91 \pm 0.02$	$\varrho_{1,4} = 0.115$
	$\alpha_{H(2,3)} = 0.53 \pm 0.01$	$\varrho_{2,3} = -0.057$
	$\alpha_{H(5,9)} = 6.11 \pm 0.04$	$\varrho_{5,9} = 0.318$
	$\alpha_{H(6,8)} = 0.12 \pm 0.01$	$\varrho_{6,8} = -0.017$
	$\alpha_{H(7)} = 3.60 \pm 0.02$	$\varrho_{7} = 0.116$
	$\alpha_{N10} = 1.55 \pm 0.01$	$\varrho_{10} = 0.047$

Lastly, ESR studies on cycl[3.3.3]azine radical anions were conducted, and for the first time, the corresponding cation was investigated (Table 4). The electron distribution in the singly occupied MO of the cation is reflected by the fact that the six equivalent protons in positions 1,3,4,6,7, and 9 have a larger coupling constant (6.45 G) than the three equivalent 2,5, and 8 protons (1,78 G), as well as the ^{14}N nucleus (1,29 G). For the anion, the pattern is reversed, with the coupling constants for the three equivalent protons at positions 2,5, and 8 being larger (4.84 G), as well as for the ^{14}N nucleus (6.54 G). In contrast, the protons on positions 1,3,4,6,7, and 9 exhibit small coupling constants (0.05 G). The effects of substitution were further investigated through the study of 1,3-dicyano and 1,3-di-*tert*-butyl ester derivatives. Results show that the radical cation of cycl[3.3.3]azine and the isoelectronic, carbon-bridged radical anion, the phenalenyl radical, display nearly identical π-spin populations. It is proposed that

the central nitrogen in both, the radical cation and anion is coplanar with the 12-membered ring. Additionally, both radicals are considered not to show bond length alternation on the periphery. A redistribution of the π-spin population was observed due to the substitution effect.[124]

Table 4. Hyperfine Coupling Constants for the Radical Ions of cycl[3.3.3]azine

	No. of nuclei	Coupling constant		Assignment to positions
		Cation	Anion	
	6 ^{1}H	6.45 ± 0.03	0.05 ± 0.01[a,b]	1,3,4,6,7,9
	3 ^{1}H	1.78 ± 0.01	4.84 ± 0.03	2,5,8
	1 ^{14}N	1.29 ± 0.01	6.54 ± 0.03	10
	6 ^{13}C	9.69 ± 0.08	4.47 ± 0.05	1,3,4,6,7,9
	3 ^{13}C	8.71 ± 0.08[c]	6.56 ± 0.05	2,5,8
	3 ^{13}C	7.73 ± 0.08[c]	1.62 ± 0.05	3a, 6a, 9a

[a] Splitting unresolved,
[b] Value obtained by computer simulation of the spectrum,
[c] A reverse assignment of these two coupling constants cannot be excluded[124]

Additionally, electron-nuclear double resonance (ENDOR) spectroscopy on the radical anions of 2-phenylcycl[3.2.2]azine and 6-methyl-2-phenyl-5-azacycl[3.2.2]azine was performed. Hereby, the assignments of couplings were made based on four different aspects:

- radio frequency coherence effects,
- calculations of relative ENDOR intensities
- computer simulation of the ESR spectra
- MO calculations of π-spin distribution

Finally, with the help of ENDOR spectroscopy, it enabled the analysis of more complex ESR hyperfine structures and the interpretation of molecules with lower symmetry, such as asymmetrically substituted cyclazines.[125]

3.3. Investigations of excited states for Cyclazines

Research on the excited electronic states of conjugated heterocycles helps in understanding chemical reactivity, photophysical properties, and leads to applications such as OLED/TDAF materials,[126] n-type semiconductors,[62,127] and photocatalysts.[128] Cyclazines show high potential in organic electronics due to their rich electronic behavior and extended π-system. It

is essential to gain insight into charge transfer processes, the nature of the lowest singlet and triplet states, their energies, and their transition characteristics to interpret their electronic structure.

One of the early examples is the cyclopenta[*h*]cycl[4.2.2]azine, which was studied using photoelectron spectroscopy (PE) and polarized electronic absorption spectroscopy. The structure of the chosen cyclazine resembles a planar, bridged [14]annulene, which is cross-linked by essential single bonds. Thus, calculations could interpret the molecule's geometry assuming C_{2v} symmetry (Figure 7). While previous spectra of alkyl-bridged [14]annulenes[81] had to account for their non-planarity, twisting perimeter, and hyperconjugative effects of saturated bridges, the cyclopenta[*h*]cycl[4.2.2]azine, with its transannular interactions, can be treated as a planar [14]annulene cross-linked system. Therefore, the bands in the PE and electronic absorption spectra can be explained by standard π-electron theory. The first few bands in the PE spectrum and the first four transitions involving orbitals similar to those of a planar [14]annulene. The remaining transitions involve orbitals, more influenced by transannular interactions.[129]

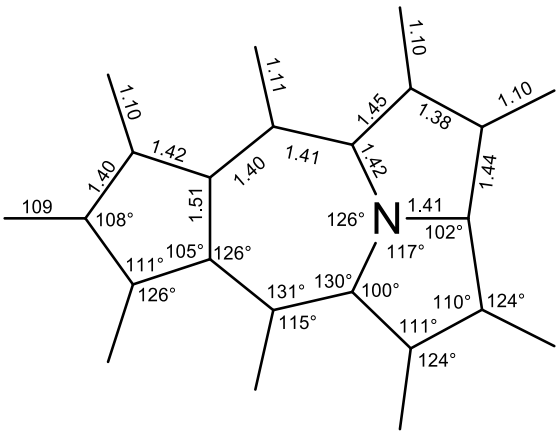


Figure 7. Calculated geometry of cyclopenta[*h*]cycl[4.2.2]azine under the assumption of C_{2v} symmetry (distances in Å)

With access to cycl[3.3.3]azine, the focus on understanding the behavior of energy transition states has increased. Leupin and Wirz studied a symmetry-forbidden transition to the lowest excited single state S_1 of cycl[3.3.3]azine, which occurs in the near-infrared range (7800 cm^{-1}). The position of this absorption band is sensitive to inductive effects. In a series of aza-substituted derivatives, it is observed that this band shifts gradually from the near-infrared to the ultraviolet region. A slight energy difference between the lowest excited singlet and triplet

states, S_1 and T_1, is found, and excitation of cycl[3.3.3]azine causes a significant redistribution of charge due to frontier orbitals localized on two different, alternate geometries. Moreover, more information about the triplet energy (T_1) for the parent cycl[3.3.3]azine was obtained indirectly through the measurement of energy transfer rates k_{et} from a series of triplet sensitizers (benzenoid hydrocarbons with varying excitation energies) to cycl[3.3.3]azines and their derivatives. The rate constant k_{et} was measured by tracking the sensitizers' decay rates after flash photolysis as a function of the added quencher concentration in a benzene solution. These rates are typically near the diffusion-controlled limit (approximately 10^{10} M^{-1} s^{-1}) when the energy-transfer process is exothermic. Assuming no other quenching process, they decrease rapidly (one decade per 5.7 kJ mol^{-1} $\simeq$ 500 cm^{-1}). The observed quenching rate constants depend on the E_T of the energy donors, supporting that the process corresponds to triplet energy transfers. An estimate of $E_T \simeq 7000 \pm 1000$ cm^{-1} indicates a slightly higher energy value than that of S_1, consistent with a small energy gap between S_1 and T_1. The possibility of a nearly isoenergetic decay path for T_1 (intersystem crossing to S_1) may explain its short lifetime of 100ns.[105] Additionally, the lifetime of the second excited singlet state S_2 was measured for both the parent cycl[3.3.3]azine and a derivative. Using a new method developed by the same group, the lifetimes of the $S_2 \rightarrow S_0$ and $S_2 \rightarrow S_1$ transitions were determined and agreed with calculated results[105] from a Strickler-Berg analysis.[130] Both predicted lifetimes for parent cyclazine, with 80 ± 25 ps for $S_2 \rightarrow S_0$ and 110 ± 30 ps for $S_2 \rightarrow S_1$, demonstrated anti-Kasha photophysics.[131]

Further studies on 1,4,7-Triazacycl[3.3.3]azine and the 2,5,8-trimethyl derivative examine their physical and chemical properties, which are intermediate between those of the antiaromatic or biradicaloid[105] parent cycl[3.3.3]azine and the essentially inert hexaaza derivative (Figure 8).[132] The first ionization potential and the first absorption band evidence this. The stabilizing effect of nitrogen in the periphery was observed as an example of the "topological charge stabilization" concept,[133] which favors atoms of greater electronegativity in positions where the structure's topology and electron-filling level tend to accumulate extra charge in the isoelectronic hydrocarbon. Moreover, the $S_0 \rightarrow S_1$ excitation (HOMO $\rightarrow$ LUMO) involves significant charge redistribution, making the position of the first absorption band sensitive to inductive effects. The addition of methyl substituents destabilizes only the LUMO. It causes a hypsochromic shift, which is unexpected since alkyl substitution on aromatic

structures usually results in a bathochromic shift in the absorption bands. Additionally, 1,4,7-triazacycl[3.3.3]azine is a borderline case between the parent cycl[3.3.3]azine, which emits only from S_2 in violating Kasha's rule,[105,131] and tri-*s*-aza-triazine, which exhibits typical S_1 fluorescence.[134] This trend may be due to a substantial shift of the S_1 band, which is accompanied by a decrease of the $S_2 \rightarrow S_1$ energy gap. Moreover, protonation of the molecule further decreases the $S_2 \rightarrow S_1$ energy gap. Lastly, a small singlet-triplet energy gap correlates with the separation of frontier orbitals in space and the short lifetime of the triplet T_1, which results from rapid radiationless deactivation through $T_1 \rightarrow S_1$ intersystem crossing after electronic excitation or triplet sensitization.[135]

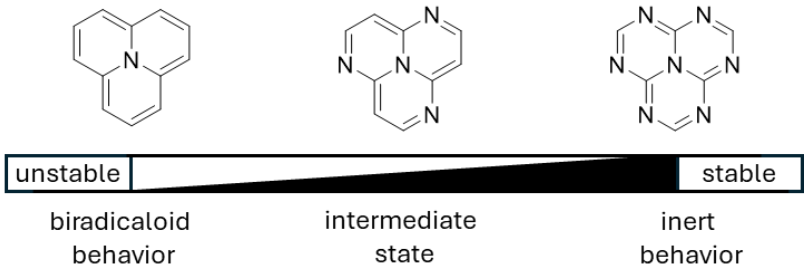


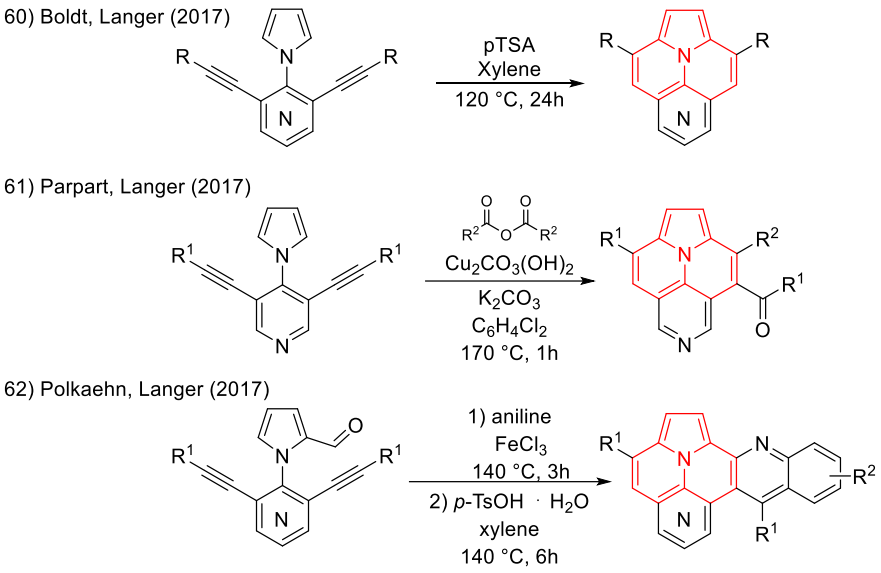
Figure 8. Stability of cycl[3.3.3]azine derivatives

The continued study of the triplet and singlet states of cyclazines focused on inverted singlet-triplet gap (INVEST) materials and effective triplet harvesting for applications in organic light-emitting diodes (OLEDs). Here, a reverse intersystem crossing (rISC) was observed between the lowest excited S_1 and T_1 states through the minimum-energy crossing point (MECP). Typical closed-shell organic molecules have T_1 states lower than S_1 states, as described by Hund's first rule, which makes S_1 to T_1 intersystem crossing (ISC) more likely than rISC. Experimental studies on cycl[3.3.3]azine[105] and 1,4,7-triazacycl[3.3.3]azine[135] revealed unusual optoelectronic behavior with nearly degenerate S_1 and T_1 states and short T_1 lifetime. Density plots between S_1 and the ground state (S_0), as well as between T_1 and S_0 states, support a short-range charge transfer pattern, confirming weak overlaps between hole and electron densities that correlate with a small exchange energy.[136] Additionally, 1,3,4,6,7,9,9b-heptaazaphenalene (heptazine) showed no evidence of a T_1 state below the S_1 state, which would be consistent with a rISC and would violate Hund's rule.[137] It was concluded that higher-lying states do not participate in the ISC/rISC process and that this is thermally activated with an energy barrier that increases with the number of nitrogen atoms per triangulene core (cyclazine → pentazine → heptazine). The crossing structure between the ground and the first

singlet states was found to be twisted by the central nitrogen atom, which distorts out of the molecular plane. This out-of-plane motion is energetically unfavorable because it disrupts the π-system, and the energetic barriers increase as the number of nitrogen atoms decreases. The high rigidity of these compounds supports the nonradiative decay mechanism of the ground states as a relatively slow process for the cycl[3.3.3]azine, pentazine, and heptazine since the conical intersections between S_0 and S_1 are located at high energy levels. (0.4 to 2.0 eV) Finally, experimentally observed Anti-Kasha emission in cycl[3.3.3]azine could be due to the energetically inaccessible conical intersections between the S_2 and S_1 states, which would permit emission from the S_2 state to the S_0 state. As proposed by Veys and Escudero[138] and Padula[139] et al., a rule for dominant anti-Kasha $S_2 \rightarrow S_0$ emission is a large S_2-S_1 energy gap, leading to a very slow internal conversion from S_2 to S_0.[126]

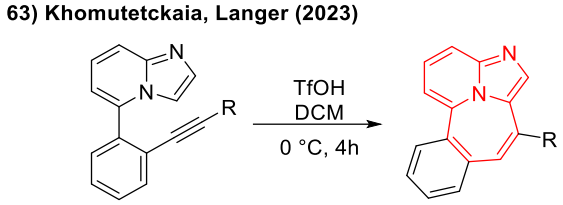
4. Research on Cyclazines conducted by Prof. Langer's Group

In 2017, Prof. Peter Langer's group began researching the synthesis of aza-ullazines, which can be viewed as a benzo-fused cycl[3.3.2]azine. Synthetic methods included a metal-free cyclization promoted by a Brønsted acid-mediated cycloisomerisation, such as *p*-toluenesulfonic acid (Scheme 28, **60**),[140] and intramolecular alkynyl carbonyl metathesis (Scheme 28, **61**).[141] Later publications further utilized cycloisomerisation,[142] and combined previous methods with a Povarov reaction (Scheme 28, **62**).[143]



Scheme 28. Synthesis of benzo-fused cycl[3.3.2]azines by the group of Langer

Furthermore, Langer's group conceptualized a Brønsted acid and acid-mediated cycloisomerization reaction, which provided further insight into the selectivity between the attack on the six-membered or five-membered ring of the imidazopyridine and an acetylene moiety. By choosing the appropriate conditions, it is possible to selectively control the formation of cycl[4.3.2]azines (Scheme 29, **63**).[144] Additionally, the optical and electrochemical properties of the compounds were studied using UV/vis, fluorescence, and cyclic voltammetry measurements. The experimental results were also supported by density functional theory calculations.



Scheme 29. Synthesis of benzo-fused cycl[4.3.2]azine by acid-mediated cycloisomerization with Brønsted acid

Building on previous studies, which explored synthetic methods and electronic properties in the field of cyclazines, this work introduces new synthetic techniques. These methods have been developed to create previously unknown derivatives of less-studied types of cyclazines, including heterocyclic and π-extended variants that were previously inaccessible. A systematic investigation of C-C and C-N bond formations, primarily through Buchwald-Hartwig coupling and C-H activation, has led to the synthesis of several new heteroaromatic frameworks for cycle[3.3.2]azines and cycl[4.2.2]azines. Moreover, detailed studies of their electronic structures and aromatic properties, using both experimental and computational approaches, have enhanced the understanding of aromaticity in ring-fused systems. These results offer valuable insights into designing nitrogen-centered polycyclic architectures and establish a foundation for future functional applications in material science. The following publications provide a more detailed perspective on these results and will expand on the findings in the chemistry of cyclazines.

5. Own Contributions to the Research of Cyclazines

Building on the research from Prof. Langer's group, this chapter briefly highlights my own contributions, with the help of my colleagues, to the field of cyclazines. These contributions are summarized in three publications, each addressing different aspects of cyclazine synthesis

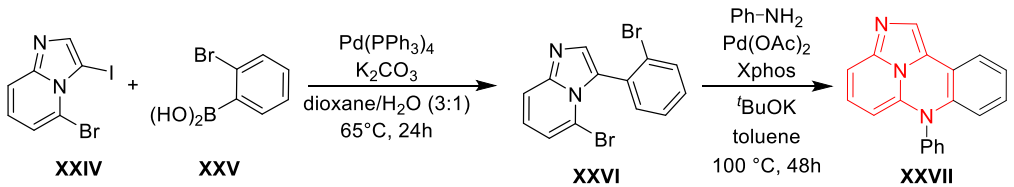
and properties. Together, they show the methodological advances and new molecular scaffolds developed in this thesis.

5.1 Synthesis of 2,2a1,6-Triazaaceanthrylenes

In this work, it was aimed to access a novel heterocyclic core structure, the 6*H*-2,2a1,6-triazaaceanthrylenes starting from 5-bromo-3-(2-bromophenyl)imidazo[1,2-*a*]pyridine (Scheme 30, **XXVI**). A chemoselective Suzuki-Miyaura reaction with 5-bromo-3-iodoimidazo[1,2-*a*]pyridine (Scheme 30, **XXIV**) and 2-bromophenylboronic acid (Scheme 31, **XXV**), provided the necessary building block. Hereby, a more reactive iodinated carbon atom ensured a chemoselective attack on the five-membered ring.

The synthesis was followed by a study of a twofold Buchwald-Hartwig reaction with aniline to form the final product, 6*H*-2,2a1,6-triazaaceanthrylene (Scheme 30, **XXVII**). Best results were achieved using palladium(II) acetate as the precatalyst, dicyclohexyl[2′,4′,6′-tris(propan-2-yl)[1,1′-biphenyl]-2-yl]phosphane (Xphos) as the ligand, potassium *tert*-butoxide as the base, and toluene as the solvent with a reaction time of 48 hours. The scope included both electron-rich and electron-poor anilines, but did exclude aliphatic amines such as *n*-hexylamine, cyclohexylamine, and benzylamine.

Further insights into the electronic properties of the products were pursued by comparing 6*H*-2,2a1,6-triazaaceanthrylenes with the corresponding hydrocarbon. DFT calculations revealed that HOMOs and LUMOs are equally distributed. However, an additional contribution from the attached phenyl ring to the LUMO is observed despite its orthogonal orientation. Both HOMO and LUMO are energetically more stabilized, resulting in a reduced band gap. Additionally, NICS(1.7) and NICS2BC ring current calculations have been performed for both compounds. The fused benzene and imidazole rings of the triazaanthrylene exhibit aromaticity, indicated by their negative NICS(1.7) values, while the “pyrimidine” reveals antiaromaticity.



Scheme 30. Cyclization by a twofold Buchwald-Hartwig reaction to form 6*H*-2,2a1,6-triazaaceanthrylenes

This paratropic ring current impacts the fused “pyridine” ring and results in only weak to non-aromaticity. Therefore, the NICS2BC ring current maps display local diatropic ring currents for the benzene and imidazole moieties. At the same time, the central “pyrimidine” displays a strong paratropic ring current, which further influences the current of the fused “pyridine” ring. These findings align well with the experimentally obtained NMR spectra, which show characteristic high-field shifts for the respective “pyridine-protons.” The chemical shifts of the “pyridine” are more similar to typical enamine or allylamine motifs rather than an aromatic pyridine ring.

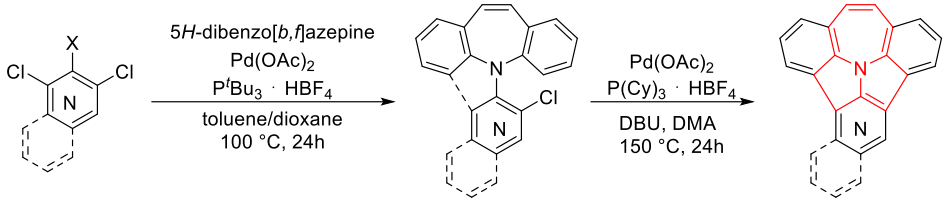
Furthermore, the photophysical properties of the compounds were studied using steady-state absorption and photoluminescence (PL) spectra. All compounds display distinct bands with vibrational progression in their absorption spectra. Two prominent and well-defined bands are observed at approximately 360 nm and 380 nm, along with three weaker absorption bands at higher wavelengths extending up to about 500 nm. The variation of substituents on the attached phenyl ring has little to no effect on the absorption spectra. All compounds exhibit very weak and complex emission behavior, characterized by five distinct emission bands and quantum yields of 2% or less.

The redox properties of 6*H*-2,2a1,6-triazaaceanthrylene were also studied using cyclic voltammetry and differential pulse voltammetry. For reduction, two peaks were observed at -1.55 V vs. Fc^{+}/Fc with an onset potential of -1.31 V, and at -2.93 V with an onset potential of -2.80 V vs. Fc^{+}/Fc. Therefore, aceanthrylene is easier to reduce than 6*H*-2,2a1,6-triazaaceanthrylene, due to its lower LUMO level. The oxidation occurred in a quasi-reversible manner, with one peak at 0.78 V vs. Fc^{+}/Fc and an onset potential of 0.64 V. This contrasts with aceanthrylene, which shows no oxidation behavior within the applied potential range.

5.2 N-Doped and Bowl-Shaped Azabenzo[3,4]azulenofluorene: Synthesis and Characterization of Bridged Aza-Triarylamines

In this work, it was aimed to further investigate the scaffold of fully bridged triphenylamines (TPA) by incorporating nitrogen into the system, in the presence of a seven-membered ring, and examining the effect of delocalization of the lone pair of electrons. As starting materials, different substituted pyridine and quinoline were used, and halogenation was performed over

one or two steps to establish the proper conditions for a subsequent Buchwald-Hartwig reaction. A subsequent, selective C-N coupling with 5*H*-dibenzo[*b*,*f*]azepine was investigated. However, instead of the desired single C-N coupling, the product was accompanied by a one-sided C-H activation during the Buchwald-Hartwig reaction, which was successfully isolated. A pure Buchwald-Hartwig reaction was isolated for one of three examples. Next, the focus moved to the final cyclization step to afford the desired compound (Scheme 31, **XXX**). Using the catalytic system consisting of $Pd(OAc)_2/P(Cy)_3 \cdot HBF_4$, the desired fully bridged azatriarylamine derivatives were obtained in excellent yields.



XXVIII
X = Br, I

XXIX

XXX

Scheme 31. Synthesis of 3a2,5-diazabenzo[3,4]azuleno[2,1,8,7-*jklm*]fluorene

For all three intermediates and final compounds, crystal structures were obtained. The final compounds exhibit a bowl-shaped structure, with depths ranging from 0.68 Å to 0.95 Å, and adopt slip-stacking arrangements. Bond lengths, angles, and bowl depths were compared to compounds of a similar structure.

These molecules were further analyzed using DFT calculations. All methods predict a bowl-shaped structure as the lowest energy minimum for all compounds. Varying the position of the pyridinic nitrogen results in a deeper bowl depth of approximately 0.25 Å. π-Extension at the pyridine moiety causes a slight increase in bowl depth. DFT calculations further elucidated the inversion dynamics of the bridged-TPA and show that, for all compounds, the inversion occurs via a planar transition state (TS). The inversion proceeds with inversion activation free energies ranging from 3.7 to 6.9 kJ · mol^{-1}. Further, the presence and extent of dispersion forces, i.e. π···π- and CH···π contacts in the crystal lattices of the bridged-TPAs was examined. Therefore, the predominance of CH···π interactions enables the stabilization of a planar TS-like structure. In contrast, strong π···π interactions or the simultaneous occurrence of both types of dispersion forces stabilizes a bowl-like conformation in the crystal state. The extent and ratio of the respective dispersion interactions therefore determine the degree of curvature.

The nucleus-independent chemical shifts (NICS) were calculated as a magnetic criterion of aromaticity, and the respective ring currents were visualized. All six- and five-membered rings in the analyzed molecules exhibit negative NICS values, indicating aromaticity. Positive NICS values are observed for the seven-membered azepine ring, indicating its antiaromatic character. Incorporating nitrogen results in less negative NICS values for the pyridine and its fused pyrrole rings, while the benzene rings in the dibenzoazepine moiety remain almost unaffected. The associated ring currents were visualized using anisotropy of the induced current density (ACID), NICS2BC bond current, and gauge-including magnetically induced current (GIMIC) methods.

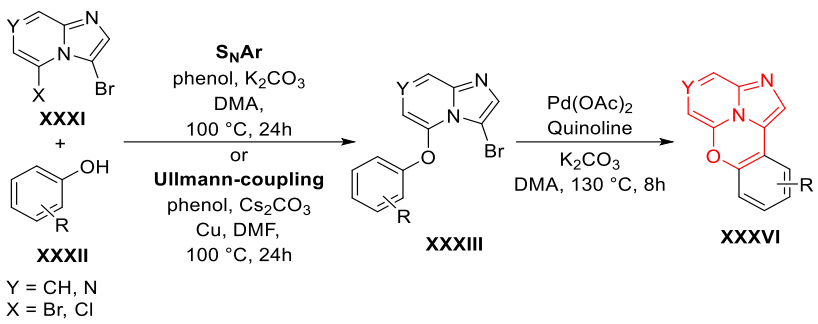
Furthermore, steady-state absorption and photoluminescence (PL) spectra of the compounds were studied. Incorporation of nitrogen causes a slight bathochromic shift in the absorption spectrum. This shift is more pronounced in non-symmetric compounds and is accompanied by a loss of fine structure. As expected, the most significant redshift occurs in the benzo-annulated derivative. The position of the emission bands is less affected, but their emission intensity is influenced by the nitrogen's location within the compound.

The redox properties were determined by cyclic voltammetry (CV) and differential pulse voltammetry (DPV) measurements. All three compounds exhibit two quasi-reversible reduction peaks and three irreversible oxidation peaks. Each compound showed slightly higher oxidation potentials compared to their carbon analogs. Notably, the compound with pyridinic nitrogen in *para*-position to the “TPA”-nitrogen is oxidized at a slightly higher potential than the non-symmetric compounds.

5.3 Synthesis and Properties of N,O-doped Aceanthrylenes

In this work, a methodology to synthesize 6-oxa-2,2a^1-diazaaceanthrylenes and 6-oxa-2,2a^1,4-triazaaceanthrylenes through an Ullmann-coupling or S_NAr reaction followed by an intramolecular direct arylation was developed (Scheme 32). It was essential to use more electron-rich and bulky ligands, such as Buchwald’s biaryl ligands and $PCy_3 \cdot HBF_4$. However, employing these ligands led to inseparable mixtures, which were caused by the cleavage of the bromine on the five-membered ring as the main side reaction. Therefore, instead of the

typically employed phosphine ligands, nitrogen-containing ligands were examined. The use of quinoline resulted in excellent yields.



Scheme 32. Synthesis of N,O-doped Aceanthrylenes

The structure of 6-oxa-2,2a[1],4-triazaaceanthrylenes was independently confirmed by X-ray crystallography. The polycyclic compound exhibits a planar arrangement across all four fused rings.

Additional DFT calculations were performed to gain further insight into the electronic structure of the as-prepared heterocyclic aceanthrylene analogs, and structural optimization by DFT accurately reproduced the crystallographic data. NICS calculations reveal different magnetic properties for individual rings of the scaffold. As expected, the benzene and imidazole moieties are strongly aromatic, while the pyrazine ring exhibits non-aromatic behavior. The central oxazine ring is strongly anti-aromatic. The additional nitrogen atom does not affect the aromatic properties of the entire molecule. NICS2BC calculations of both structures confirm these findings. However, a weak semi-global ring current is observed for the fused imidazopyrazine and -pyridine moieties, respectively.

Reference

[1] V. Boekelheide, R. J. Windgassen, *J. Am. Chem. Soc.* **1958**, *80*, 2020.

[2] O. Ceder, B. Beijer, *J. Heterocycl. Chem.* **1976**, *13*, 1029.

[3] a) H. J. Dewey, H. Deger, W. Froelich, B. Dick, K. A. Klingensmith, G. Hohlneicher, E. Vogel, J. Michl, *J. Am. Chem. Soc.* **1980**, *102*, 6412; b) K. A. Klingensmith, H. J. Dewey, E. Vogel, J. Michl, *J. Am. Chem. Soc.* **1989**, *111*, 1539; c) L. Catani, C. Gellini, P. R. Salvi, *J. Phys. Chem. A* **1998**, *102*, 1945.

[4] a) E. V. Babaev, I. A. Shadrin, *Molecules* **2021**, *26*; b) Y.-M. Shen, G. Grampp, N. Leesakul, H.-W. Hu, J.-H. Xu, *Eur. J. Org. Chem.* **2007**, *2007*, 3718; c) C. Zeng, K. Yuan, N. Wang, T. Peng, G. Wu, S. Wang, *Chem. Sci.* **2019**, *10*, 1724; d) A. J. Stasyuk, M. Banasiewicz, B. Ventura, M. K. Cyrański, D. T. Gryko, *New J. Chem.* **2014**, *38*, 189; e) R. Maitra, J.-H. Chen, C.-H. Hu, H. M. Lee, *Eur. J. Org. Chem.* **2017**, *40*, 5975; f) É. Lévesque, W. S. Bechara, L. Constantineau-Forget, G. Pelletier, N. M. Rachel, J. N. Pelletier, A. B. Charette, *J. Org. Chem.* **2017**, *82*, 5046.

[5] a) A. S. Jørgensen, P. Jacobsen, L. B. Christiansen, P. S. Bury, A. Kanstrup, S. M. Thorpe, L. Naerum, K. Wassermann, *Bioorg. Med. Chem. Lett.* **2000**, *10*, 2383; b) A. S. Jørgensen, P. Jacobsen, L. B. Christiansen, P. S. Bury, A. Kanstrup, S. M. Thorpe, S. Bain, L. Naerum, K. Wassermann, *Bioorg. Med. Chem. Lett.* **2000**, *10*, 399; c) S. Sanivarapu, N. Vaddiraju, L. Velide, *Med. Chem. Res.* **2019**, *28*, 1461.

[6] R. J. Windgassen, W. H. Saunders, V. Boekelheide, *J. Am. Chem. Soc.* **1959**, *81*, 1459.

[7] Y. Tominaga, Y. Shiroshita, A. Hosomi, *Heterocycles* **1988**, *27*, 2251.

[8] a) J. Godfry, *J. Org. Chem.* **1959**, *24*, 581; b) V. Boekelheide, K. Fahrenholtz, *J. Am. Chem. Soc.* **1961**, *83*, 458; c) V. Boekelheide, A. Miller, *J. Org. Chem.* **1961**, *26*, 431; d) A. Galbraith, T. Small, R. A. Barnes, V. Boekelheide, *J. Am. Chem. Soc.* **1961**, *83*, 453.

[9] V. Boekelheide, T. Small, *J. Am. Chem. Soc.* **1961**, *83*, 462.

[10] W. Flitsch, J. Heinrich, *Tetrahedron Lett.* **1980**, *21*, 3673.

[11] B. R. Yerxa, H. W. Moore, *Tetrahedron Lett.* **1992**, *33*, 7811.

[12] K. Matsumoto, T. Uchida, H. Yoshida, M. Toda, A. Kakehi, *J. Chem. Soc., Perkin Trans. 1* **1992**, *0*, 2437.

[13] D. E. Pereira, N. J. Leonard, *Tetrahedron Lett.* **1986**, *27*, 4129.

[14] A. I. Zinin, E. V. Babaev, *Russ. Chem. Bull.* **1997**, *46*, 609.

[15] a) J. O. Smith, B. K. Mandal, *J. Heterocycl. Chem.* **1997**, *34*, 1441; b) T. Lepitre, R. Le Biannic, M. Othman, A. M. Lawson, A. Daïch, *Org. Lett.* **2017**, *19*, 1978; c) M. Komatsu, Y. Kasano, S. Yamaoka, S. Minakata, *Synthesis* **2003**, *9*, 1398; d) S. Gogoi, M. Dutta, J. Gogoi, R. Boruah, *Tetrahedron Lett.*, **2011**, *52*, 813; e) V. A. Motornov, A. A. Tabolin, Y. V. Nelyubina, V. G. Nenajdenko, S. L. Ioffe, *Org. Biomol. Chem.* **2019**, *17*, 1442.

[16] M. A. Jessep, D. Leaver, *J. Chem. Soc. D* **1970**, 790.

[17] C. Jutz, R. Kirchlechner, H.-J. Seidel, *Chem. Ber.* **1969**, *102*, 2301.

[18] a) V. Batroff, W. Flitsch, D. Leaver, D. Skinner, *Chem. Ber.* **1984**, *117*, 1649; b) D. Leaver, D. Skinner, *J. Chem. Soc., Chem. Commun.* **1984**, 821; c) D. Farquhar, T. T. Gough, D. Leaver, *J. Chem. Soc., Perkin Trans. 1* **1976**, 341.

[19] a) N. I. Jessen, G. Bertuzzi, M. Bura, M. L. Skipper, K. A. Jørgensen, *J. Am. Chem. Soc.* **2021**, *143*, 6140; b) N. I. Jessen, M. Bura, G. Bertuzzi, K. A. Jørgensen, *Angew. Chem. Int. Ed. Engl.* **2021**, *60*, 18527.

[20] C. Cebrián, *J. Mater. Chem. C* **2018**, *6*, 11943.

[21] C. J. Boyle, M. Upadhyaya, P. Wang, L. A. Renna, M. Lu-Díaz, S. Pyo Jeong, N. Hight-Huf, L. Korugic-Karasz, M. D. Barnes, Z. Aksamija et al., *Nat. Commun.* **2019**, *10*, 2827.

[22] G.-B. Shen, T. Yu, Y.-L. Zhang, L.-P. Ma, L. Chen, J.-J. Lu, T. Meng, *J. Heterocycl. Chem.* **2018**, *55*, 814.

[23] O. Fuentes, W. W. Paudler, *J. Org. Chem.* **1975**, *40*, 1210.

[24] P. Blatcher, D. Middlemiss, P. Murray-Rust, J. Murray-Rust, *Tetrahedron Lett.* **1980**, *21*, 4193.

[25] a) A. Yang, R. Jiang, O. Khorev, T. Yu, Y. Zhang, L. Ma, G. Chen, J. Shen, T. Meng, *Adv. Synth. Catal.* **2013**, *355*, 1984.

[26] R. H. Mitchell, *Isr. J. Chem.* **1980**, *20*, 294.

[27] a) Y. Tominaga, H. Gotou, Y. Oniyama, Y. Nishimura, Y. Matsuda, *Chem. Pharm. Bull.* **1985**, *33*, 3038; b) Y. Tominaga, Y. Shiroshita, H. Gotou, Y. Matsuda, *Heterocycl.* **1986**, *24*, 3071; c) Y. Tominaga, Yoshihide Shiroshita, Y. Matsuda, A. Hosomi, *Heterocycl.* **1987**; d) Y. Tominaga, Y. Shiroshita, T. Kurokawa, H. Gotou, Y. Matsuda, A. Hosomi, *J. Heterocycl. Chem.* **1989**, *26*, 477.

[28] S. Kanemasa, S. Takenaka, H. Watanabe, O. Tsuge, *J. Org. Chem.* **1989**, *54*, 420.

[29] K. Matsumoto, H. Katsura, T. Uchida, K. Aoyama, T. Machiguchi, *J. Chem. Soc., Perkin Trans. 1* **1996**, *0*, 2599.

[30] a) *1, 3-Dipolar Cycloaddition of Pyrazolo (1, 2-a) indazoles with Dimethyl Acetylenedicarboxylate*, **1987**; b) M. Aginagalde, Y. Vara, A. Arrieta, R. Zangi, V. L. Cebolla, A. Delgado-Camón, F. P. Cossío, *J. Org. Chem.* **2010**, *75*, 2776.

[31] a) A. Daich, P. Ohier, B. Decroix, *Tetrahedron Lett.* **1995**, *36*, 83; b) P. Ohier, A. Daïch, B. Decroix, *Tetrahedron* **1996**, *52*, 13547.

[32] C. C. Chintawar, M. V. Mane, A. G. Tathe, S. Biswas, N. T. Patil, *Org. Lett.* **2019**, *21*, 7109.

[33] R. Semwal, A. Joshi, R. Kumar, S. Adimurthy, *New J. Chem.* **2020**, *44*, 20530.

[34] a) T. Tsuchiya, M. Kato, H. Sashida, *Chem. Pharm. Bull.* **1984**, *32*, 4666; b) H. Sashida, M. Kato, T. Tsuchiya, *Chem. Pharm. Bull.* **1988**, *36*, 3826.

[35] P. Cui, L. Xu, H. Cheng, L. Gan, *Tetrahedron* **2012**, *68*, 152.

[36] a) M. Ghosh, A. Naskar, S. Mishra, A. Hajra, *Tetrahedron Lett.* **2015**, *56*, 4101; b) H. Hu, G. Li, W. Hu, Y. Liu, X. Wang, Y. Kan, M. Ji, *Org. Lett.* **2015**, *17*, 1114; c) S. K. Ghosh, D. Ghosh, R. Maitra, Y.-T. Kuo, H. M. Lee, *Eur. J. Org. Chem.* **2016**, *2016*, 5722; d) E. V. Babaev, I. A. Shadrin, V. B. Rybakov, *Chem. Heterocycl. Comp.* **2018**, *54*, 339.

[37] a) Y. Liang, L. Teng, Y. Wang, Q. He, H. Cao, *Green Chem.* **2019**, *21*, 4025; b) Y. Zhang, Y. Yu, B.-B. Liang, Y.-Y. Pei, X. Liu, H.-G. Yao, H. Cao, *J. Org. Chem.* **2020**, *85*, 10719.

[38] a) T. G. Burdo, W. R. Seitz, *Anal. Chem.* **1975**, *47*, 1639; b) R. B. Brundrett, D. F. Roswell, E. H. White, *J. Am. Chem. Soc.* **1972**, *94*, 7536; c) C. C. Wei, E. H. White, *Tetrahedron Lett.* **1971**, *12*, 3559.

[39] a) Y. Tominaga, K. Komiya, S. Kataoka, Y. Shigemitsu, T. Hirota, K. Sasaki, *Heterocycles* **1998**, *48*, 1985; b) Y. Tominaga, K. Sasaki, R. N. Castle, *J. Heterocycl. Chem.* **1998**, *35*, 1219.

[40] a) D. C. Young, S. D. Kingsley, K. A. Ryan, F. J. Dutko, *Anal. Biochem.* **1993**, *215*, 24; b) J. A. Matthews, A. Batki, C. Hynds, L. J. Kricka, *Anal. Biochem.* **1985**, *151*, 205; c) M. P. Wymann, V. von Tscharner, D. A. Deranleau, M. Baggiolini, *Anal. Biochem.* **1987**, *165*, 371; d) R. Lock, A. Johansson, K. Orselius, C. Dahlgren, *Anal. Biochem.* **1988**, *173*, 450; e) H. P. Misra, P. M. Squatrito, *Arch. Biochem. Biophys.* **1982**, *215*, 59; f) J. Arnhold, S. Mueller, K. Arnold, E. Grimm, *J. Biolumin. Chemilumin.* **1991**, *6*, 189; g) G. Merényi, J. Lind, T. E. Eriksen, *J. Biolumin. Chemilumin.* **1990**, *5*, 53.

[41] D.-T. Yang, J. Radtke, S. K. Mellerup, K. Yuan, X. Wang, M. Wagner, S. Wang, *Org. Lett.* **2015**, *17*, 2486.

[42] R. M. Acheson, D. A. Robinson, *Chem. Commun.* **1967**, 175.

[43] O. Ceder, B. Beijer, *Tetrahedron* **1974**, *30*, 3657.

[44] T. Ikemoto, T. Kawamoto, H. Wada, T. Ishida, T. Ito, Y. Isogami, Y. Miyano, Y. Mizuno, K. Tomimatsu, K. Hamamura et al., *Tetrahedron* **2002**, *58*, 489.

[45] J. W. Dick, W. K. Gibson, D. Leaver, J. E. Roff, *J. Chem. Soc., Perkin Trans. 1* **1981**, 3150.

[46] H. Balli, M. Zeller, *Helv. Chim. Acta* **1983**, *66*, 2135.

[47] N. Clauson-Kaas, Z. Tyle, M. Rottenberg, E. Stenhagen, S. Östling, *Acta Chem. Scand.* **1952**, *6*, 667.

[48] E. Campaigne, J. C. Huffman, T. P. Selby, *J. Heterocycl. Chem.* **1979**, *16*, 725.

[49] T. P. Selby, *J. Org. Chem.* **1988**, *53*, 2386.

[50] E. K. Mikitenko, N. N. Romanov, *Chem. Heterocycl. Comp.* **1998**, *34*, 359.

[51] E. V. Babaev, K. Y. Pasichnichenko, V. B. Rybakov, S. G. Zhukov, *Chem. Heterocycl. Comp.* **2000**, *36*, 1192.

[52] K. Kanno, Y. Liu, A. Iesato, K. Nakajima, T. Takahashi, *Org. Lett.* **2005**, *7*, 5453.

[53] a) T. Meng, Z. Zhang, D. Hu, L. Lin, J. Ding, X. Wang, J. Shen, *J. Comb. Chem.* **2007**, *9*, 739; b) C. Martini, M. I. D. Mardjan, A. Basso, *Beilstein J. Org. Chem.* **2024**, *20*, 1839; c) A. Boltjes, A. Dömling, *Eur. J. Chem.* **2019**, *2019*, 7007.

[54] H. Sun, H. Zhou, O. Khorev, R. Jiang, T. Yu, X. Wang, Y. Du, Y. Ma, T. Meng, J. Shen, *J. Org. Chem.* **2012**, *77*, 10745.

[55] E. V. Babaev, A. A. Nevskaya, I. V. Dlynnikh, *Chem. Heterocycl. Comp.* **2015**, *51*, 269.

[56] D. Firmansyah, M. Banasiewicz, I. Deperasińska, A. Makarewicz, B. Kozankiewicz, D. T. Gryko, *Chem. - Asian J.* **2014**, *9*, 2483.

[57] J. Zhou, W. Yang, B. Wang, H. Ren, *Angew. Chem. Int. Ed.* **2012**, *51*, 12293.
[58] J. H. Delcamp, A. Yella, T. W. Holcombe, M. K. Nazeeruddin, M. Grätzel, *Angew. Chem. Int. Ed.* **2013**, *52*, 376.
[59] a) S. Ito, Y. Tokimaru, K. Nozaki, *Chem. Commun.* **2015**, *51*, 221; b) R. Berger, M. Wagner, X. Feng, K. Müllen, *Chem. Sci.* **2015**, *6*, 436; c) S. Ito, Y. Tokimaru, K. Nozaki, *Angew. Chem. Int. Ed.* **2015**, *54*, 7256.
[60] A. Das, I. Ghosh, B. König, *Chem. Commun.* **2016**, *52*, 8695.
[61] a) D. Wan, X. Li, R. Jiang, B. Feng, J. Lan, R. Wang, J. You, *Org. Lett.* **2016**, *18*, 2876; b) J. Hager, S. Kang, P. J. Chmielewski, T. Lis, D. Kim, M. Stępień, *Org. Chem. Front.* **2022**, *9*, 3179.
[62] A. Skabeev, U. Zschieschang, Y. Zagranyarski, H. Klauk, K. Müllen, C. Li, *Org. Lett.* **2018**, *20*, 1409.
[63] D. Miao, C. Aumaitre, J.-F. Morin, *J. Mater. Chem. C* **2019**, *7*, 3015.
[64] W. K. Gibson, D. Leaver, *Chem. Commun.* **1965**, 11.
[65] R. P. Cunningham, D. Farquhar, W. K. Gibson, D. Leaver, *J. Chem. Soc., C* **1969**, 239.
[66] D. Farquhar, D. Leaver, *J. Chem. Soc. D* **1969**, 24.
[67] D. Hellwinkel, M. Melan, *Chem. Ber.* **1971**, *104*, 1001.
[68] a) A. R. Katritzky, Z. Zakaria, E. Lunt, P. G. Jones, O. Kennard, *J. Chem. Soc., Chem. Commun.* **1979**, 268; b) A. R. Katritzky, G. de Ville, R. C. Patel, R. Harlow, *Tetrahedron Lett.* **1982**, *23*, 1241.
[69] D. Wu, L. Zhi, G. J. Bodwell, G. Cui, N. Tsao, K. Müllen, *Angew. Chem. Int. Ed. Engl.* **2007**, *46*, 5417.
[70] M. L. Di Pietro, F. Puntoriero, F. Tuyéras, P. Ochsenbein, P. P. Lainé, S. Campagna, *Chem. Commun.* **2010**, *46*, 5169.
[71] A. R. Katritzky, B. Agha, G. Z. de Ville, E. Lunt, M. L. Podmore, *Org. Magn. Reson.* **1983**, *21*, 649.
[72] K. Kurata, H. Awaya, H. Gotou, Y. Tominaga, Y. Matsuda, G. Kobayashi, *Chem. Pharm. Bull.* **1985**, *33*, 3034.
[73] M. Fourmigue, H. Eggert, K. Bechgaard, *J. Org. Chem.* **1991**, *56*, 4858.
[74] M. Kuratsu, M. Kozaki, K. Okada, *Angew. Chem. Int. Ed. Engl.* **2005**, *44*, 4056.
[75] D. Jänsch, C. Li, L. Chen, M. Wagner, K. Müllen, *Angew. Chem. Int. Ed. Engl.* **2015**, *54*, 2285.
[76] B. Feng, D. Wan, L. Yan, V. D. Kadam, J. You, G. Gao, *RSC Adv.* **2016**, *6*, 66407.
[77] H. Wei, X. Hou, T. Xu, Y. Zou, G. Li, S. Wu, Y. Geng, J. Wu, *Angew. Chem. Int. Ed. Engl.* **2022**, *61*, e202210386.
[78] M. A. Jessep, D. Leaver, *J. Chem. Soc., Perkin Trans. 1* **1980**, 1324.
[79] D. Johnson, G. Jones, *J. Chem. Soc., Perkin Trans. 1* **1972**, 844.
[80] W. Flitsch, F. Kappenberg, H. Schmitt, *Chem. Ber.* **1978**, *111*, 2407.
[81] W. Flitsch, E. R. Gesing, *Tetrahedron Lett.* **1979**, *20*, 3405.

[82] a) W. Flitsch, B. Müter, *Angew. Chem.* **1973**, *85*, 543; b) W. Flitsch, A. Gurke, B. Müter, *Chem. Ber.* **1975**, *108*, 2969.
[83] D. Bellus, H. Sauter, C. D. Weis, A. J. Arduengo, W. A. Sheppard, *Org. Synth.* **1978**, *58*, 67.
[84] V. Batroff, W. Flitsch, *Liebigs Ann. Chem.* **1987**, *7*, 621.
[85] Y. Miki, H. Hachiken, M. Yoshikawa, S. Takemura, *Heterocycles* **1991**, *32*, 655.
[86] J. M. Chezal, E. Moreau, O. Chavignon, V. Gaumet, J. Métin, Y. Blache, A. Diez, X. Fradera, J. Luque, J. C. Teulade, *Tetrahedron* **2002**, *58*, 295.
[87] J. M. Kane, *J. Org. Chem.* **1980**, *45*, 5396.
[88] a) N. M. Hext, J. Hansen, A. J. Blake, D. E. Hibbs, M. B. Hursthouse, O. V. Shishkin, M. Mascal, *J. Org. Chem.* **1998**, *63*, 6016; b) M. Mascal, N. M. Hext, O. V. Shishkin, *Tetrahedron Lett.* **1996**, *37*, 131.
[89] I. T. Jacobson*, Acta Chem. Scand., **1967**, 21, 2235.*
[90] a) D. Lloyd, *J. Chem. Inf. Comput. Sci.* **1996**, *36*, 442; b) T. M. Krygowski, M. K. Cyrañski, Z. Czarnocki, G. Häfelinger, A. R. Katritzky, *Tetrahedron* **2000**, *56*, 1783; c) P. Lazzeretti, *Prog. Nucl. Magn. Reson. Spectrosc.* **2000**, *36*, 1; d) P. Lazzeretti, *Phys. Chem. Chem. Phys.* **2004**, *6*, 217.
[91] J. Kruszewski, T. M. Krygowski, *Tetrahedron Lett.* **1972**, *13*, 3839.
[92] M. K. Cyrański, *Chem. Rev.* **2005**, *105*, 3773.
[93] F. Faglioni, A. Ligabue, S. Pelloni, A. Soncini, R. G. Viglione, M. B. Ferraro, R. Zanasi, P. Lazzeretti, *Org. Lett.* **2005**, *7*, 3457.
[94] W. H. Flygare, R. C. Benson, *J. Am. Chem. Soc.* **1970**, *92*, 7523.
[95] a) I. Cernusak, P. W. Fowler, E. Steiner, *Mol. Phys.* **2000**, *98*, 945; b) P. Fowler, E. Steiner, *Chem. Phys. Lett.* **2002**, *364*, 259; c) E. Steiner, P. W. Fowler, L. W. Jenneskens, *Angew. Chem. Int. Ed.* **2001**, *40*, 362.
[96] Z. Chen, C. S. Wannere, C. Corminboeuf, R. Puchta, P. v. R. Schleyer, *Chem. Rev.* **2005**, *105*, 3842.
[97] P. von Ragué Schleyer, M. Manoharan, H. Jiao, F. Stahl, *Org. Lett.* **2001**, *3*, 3643.
[98] M. K. Cyrañski, T. M. Krygowski, M. Wisiorowski, N. J. R. van Eikema Hommes, P. v. R. Schleyer, *Angew. Chem. Int. Ed.* **1998**, *37*, 177.
[99] E. Hückel, *Z. Physik* **1931**, *70*, 204.
[100] M. K. Cyrański, R. W. A. Havenith, M. A. Dobrowolski, B. R. Gray, T. M. Krygowski, P. W. Fowler, L. W. Jenneskens, *Chem. Eur. J.* **2007**, *13*, 2201.
[101] a) Alfred Taurins in *Chemistry of Heterocyclic Compounds*, John Wiley & Sons, Ltd, **2008**, pp. 245–270; b) W. Flitsch, U. Krämer in *Advances in Heterocyclic Chemistry* (Ed.: A. R. Katritzky), Academic Press, **1963**, pp. 321–365.
[102] Kiyoshi Matsumoto, Hideki Katsura, Jun Yamauchi, Takane Uchida, Kinuyo Aoyama, Takahisa Machiguchi, *Bull. Soc. Chim. Fr.* **1996**, *9*, 891.

[103] a) K. Matsumoto, J. Yamauchi, T. Uchida, *Heterocycles* **1985**, *23*, 2773; b) L. W. Castle, Y. Tominaga, R. N. Castle, *J. Heterocycl. Chem.* **1994**, *31*, 1209.
[104] a) M. H. Palmer, D. Leaver, J. D. Nisbet, R. W. Millar, R. Egdell, *J. Mol. Struct.* **1977**, *42*, 85; b) M. H. Palmer, R. H. Findlay, R. G. Egdell, *J. Mol. Struct.* **1977**, *40*, 191; c) Y. Shigemitsu, M. Uejima, T. Sato, K. Tanaka, Y. Tominaga, *J. Phys. Chem. A* **2012**, *116*, 9100.
[105] W. Leupin, J. Wirz, *J. Am. Chem. Soc.* **1980**, *102*, 6068.
[106] U. Howeler, P. S. Chatterjee, K. A. Klingensmith, J. Waluk, J. Michl, *Pure Appl. Chem.* **1989**, *61*, 2117.
[107] G. G. Hall, A. Hardisson, L. M. Jackman, *Discuss. Faraday Soc.* **1962**, *34*, 15.
[108] F. Gerson, *Pure Appl. Chem.* **1971**, *28*, 131.
[109] E. Kleinpeter, A. Koch, *Eur. J. Org. Chem.* **2022**, *8*.
[110] A. Mattursun, A. Kerim, *J. Heterocycl. Chem.* **2017**, *54*, 3265.
[111] H. Fallah-Bagher-Shaidaei, R. Farkhonde, L. G. Navideh, *Comp. Theor. Chem.* **2011**, *963*, 525.
[112] F. Gerson, E. Heilbronner, N. Joop, H. Zimmermann, *Helv. Chim. Acta* **1963**, *46*, 1940.
[113] M. DePompei, W. W. Paudler, *J. Org. Chem.* **1976**, *41*, 1661.
[114] a) J. Aihara, *J. Am. Chem. Soc.* **1976**, *98*, 2750; b) I. Gutman, M. Milun, N. Trinajstic, *J. Am. Chem. Soc.* **1977**, *99*, 1692; c) J. Aihara, *BCSJ* **2016**, *89*, 1425; d) R. Sekine, Y. Nakagami, J. Aihara, *J. Phys. Chem. A* **2011**, *115*, 6724.
[115] a) J. Aihara, *J. Am. Chem. Soc.*, **1995**, *117*, 4130; b) J. Aihara, T. Ishida, H. Kanno, *Bull. Chem. Soc. Jpn*., **2007**, *80*, 1518.
[116] a) J. Aihara, *J. Am. Soc.,* **2006**, *128*, 2873; b) J. Aihara, *Phys. Chem. Chem. Phys.,* **2016**, *18*, 11847.
[117] K. Matsumoto, H. Iida, S. Mimori, H. Hamana, T. Uchida, A. Kakehi, *Heterocycl.,* **2007**, *74*, 1019.
[118] M. Solà, *Front. Chem.,* **2013**, *1*, 22.
[119] S. Klod, E. Kleinpeter, *J. Chem. Soc.,* **2001**, 1893.
[120] N. M. Atherton, F. Gerson., J. N. Murrell, *Mol. Phys.*, **1963**, *6*, 265.
[121] G. E. Pake, S. I. Weissmann, J. Townsend, *Discuss. Faraday Soc.*, **1955**, *19*, 147.
[122] F. Gerson, *Mol. Phys.*, **1972**, *24*, 445.
[123] F. Gerson, J. Jachimowicz, B. Kowert, D. Leaver, *Helv. Chim. Acta*, **1973**, *56*, 258.
[124] F. Gerson, J. Jachimowicz, D. Leaver, *J. Am. Chem. Soc.*, **1973**, *95*, 6702.
[125] F. Gerson, J. Jachimowicz, K. Moebius, R. Biehl, J. Hyde, D. Leniart, *J. Magn. Reson.*, **1975**, *18*, 471.
[126] D. Valverde, C. T. Ser, G. Ricci, K. Jorner, R. Pollice, A. Aspuru-Guzik, Y. Olivier, *ACS Appl. Mater. Interfaces*, **2024**, *16*, 49, 66991.
[127] J. Li, L. Tao, Y. Wang, Y. Yao, Q. Guo, *Front. Chem.*, **2021**, *9*, 717569.
[128] J. Zhang, G. Ye, C. Zhang, Z. Pan, S. Wang, G. Zhang, X. Wang, *ChemSusChem*,

2022, *15*, e202201616.
[129] J. Spanget-Larsen, R. Gleiter, *Helv. Chim. Acta*, **1978**, *61*, 2999.
[130] S. J. Strickler, R. A. Berg, *J. Chem. Phys.*, **1962**, *37*, 814.
[131] W. Leupin, S. J. Berens, D. Magde, *J. Phys. Chem.*, **1984**, *88*, 1376.
[132] R. S. Hossmane, M. A. Rossman, N. J. Leonard, *J. Am. Chem. Soc.*, **1982**, *104*, 5497.
[133] B. M. Girmac, *J. Am. Chem. Soc.*, **1983**, *105*, 1979.
[134] A. M. Helpern, M. A. Rossman, R. S. Hosmane, N. J. Leonard, *J. Phys. Chem*, **1984**, *88*, 4324.
[135] W. Leupin, D. Magde, G. Persy, J. Wirz, *J. Am. Chem. Soc.*, **1986**, *108*, 17.
[136] A. Pershin, D. Hall, V. Lemaur, J., -C. Sancho-Garcia, L. Muccioli, E. Zysman-Colman, D. Beljonne, Y. Olivier, *Nat. Commun*., **2019**, *10*, 597.
[137] a) J. Ehrmaier, E. J. Rabe, S. R. Pristash, K. L. Corp, C. W. Schlenker, A. L. Sobolewski, W. Domcke, *J. Phys. Chem. A*, **2019**, *123*, 8099; b) P. -F. Loos, F. Lipparini, D. Jacquemin, *J. Phys. Chem. Lett.*, **2023**, *14*, 11069.
[138] K. Veys, D. Escudero, *Acc. Chem. Res*., **2022**, *55*, 2698.
[139] Ö. H. Omar, T. Nematiaram, A. Troisi, D. Padula, *Sci. Data*, **2022**, *9*, 54.
[140] a) S. Boldt, S. Parpart, A. Villinger, P. Ehlers, P. Langer, *Angew. Chem. Int. Ed. Engl*., **2017**, *56*, 4575; b) S. Janke, S. Boldt, P. Nakielski, A. Villinger, P. Ehlers, P. Langer, *J. Org. Chem.*, **2023**, *88*, 10470.
[141] S. Parpart, S. Boldt, P. Ehlers, P. Langer, *Org. Lett.*, **2018**, *20*, 122.
[142] J. Polkaehn, R. Molenda, M. A. Cordero, S. Lochbrunner, S. Boldt, P. Ehlers, A. Villinger, P. Langer, *J. Org. Chem.*, **2024**, *89*, 2169.
[143] a) Polkaehn, P. Ehlers, A. Villinger, P. Langer, *Molecules*, **2024**, *29*, 2159; b) Polkaehn, R. Thom, P. Ehlers, A. Villinger, P. Langer, *Org. Biomol. Chem.*, **2024**, 22, 2027.
[144] A. Khomutetckaia, P. Ehlers, A. Villinger, P. Langer*, J. Org. Chem.*, **2023**, 88, 7929.

II. Contribution to Manuscripts

Original publications are presented in the next chapter. A summary of my contributions to each publication is given in the subchapter.

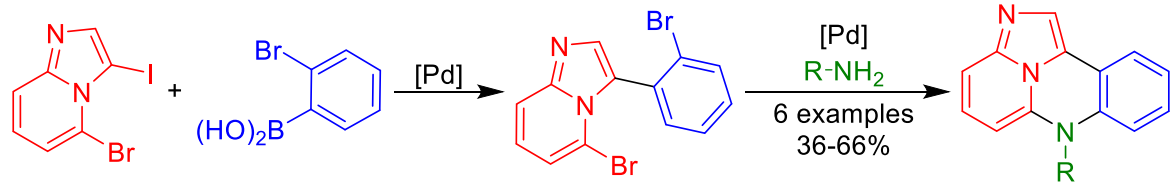
Publication I

Synthesis of 2,2a1,6-Triazaaceanthrylenes

Jan Radolko,[a] Karyna Kulyk,[a,b] Peter Ehlers,[a] Peter Langer[a,c]*

[a] *Institut für Chemie, Universität Rostock, Albert-Einstein-Str. 3a, 18059 Rostock,Germany.*
[b] *Department of Organic and Bioorganic Chemistry, State Scientific Institution "Institute for Single Crystals" NAS of Ukraine, 60 Nauky ave., Kharkiv, Ukraine 61072*
[c] *Leibniz-Institute of Catalysis e. V. at the University of Rostock, Albert-Einstein-Str. 29a, 18059 Rostock, Germany*

DOI: https://doi.org/10.1016/j.tetlet.2023.154834
Full paper*: Tetrahedron Letters* 134 (2024) 154834



Abstract: Hitherto unknown 6-aryl-6*H*-2,2*a*1,6-triazaaceanthrylenes were prepared from readily available 5-bromo-3-iodoimidazo[1,2-*a*]pyridine by chemoselective Suzuki-Miyaura reaction with 2-bromophenylboronic acid and subsequent two-fold Buchwald-Hartwig reaction.

Keywords: Catalysis; cyclizations; heterocycles; palladium; regioselectivity

Contribution to this work: 65%

In this paper, two series of 2,2*a*1,6-triazaaceanthrylenes were synthesized. The first 4 examples were investigated by me and the remaining two by Karyna Kulyk.
I optimized the reaction condition of the Buchwald Hartwig reaction. The substrate scope as well the isolation and evaluation of analytical data was performed with help of K. Kulyk. Furthermore, I wrote all versions of the manuscript, as well as the supporting information. UV/vis and cyclic voltammetry measurements were performed by me. DFT and NICS calculations were performed by Dr. Peter Ehlers. Conception, supervision and manuscript revision by Dr. Peter Ehlers and Prof. Dr. Peter Langer.

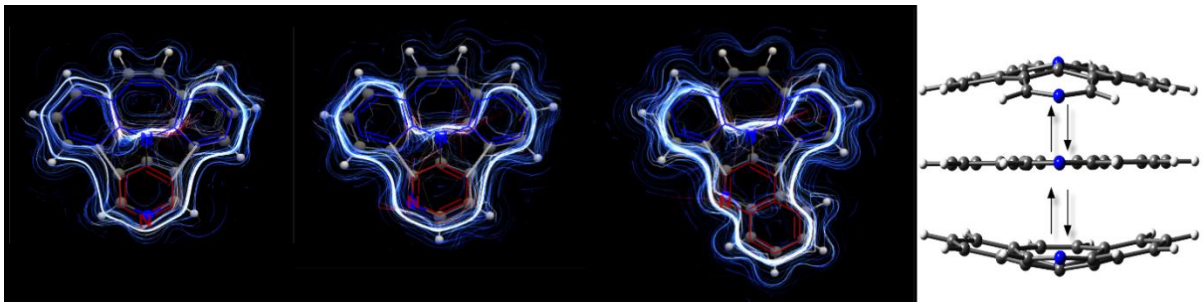
Publication II

N-Doped and Bowl-Shaped Azabenzo[3,4]azulenofluorene: Synthesis and Characterization of Bridged Aza-Triarylamines

Jan Radolko[a], Ha Minh Tuan[a], Ricardo Molenda[a], Alexander Villinger[a], Peter Ehlers[a]*, Peter Langer[a]*

[a] *University of Rostock, Institute of Chemistry, Albert-Einstein-Str. 3a, 18059 Rostock, Germany*

DOI: https://doi.org/10.1002/chem.202403004
Full paper: *Chem. Eur. J.* **2024**, 30, e202403004



Abstract: Triarylamines are frequently employed as electron donor functional groups in a variety of organic electronic materials. We herein report the synthesis and in-depth characterisation of aza-analogues of fully bridged triarylamines, consisting of 5-, 6- and 7-membered rings. The impact of nitrogen doping and π-extension on the structural, electronic and optical-properties of these contorted heteroaromatic PAHs is thoroughly investigated and paves the way for an improved understanding of the structure-property relationships.

Keywords: bowl-shaped compounds, bridged triarylamine, CH-activation, dibenzoazepine, N-doping, N-heterocycles

Contribution to this work: 50%

In this paper, I performed, with the help of T. M. Ha experiments regarding the optimization and substrate scope as well evaluation of analytical data. I performed analytical measurements including UV/Vis and cyclic voltammetry. Furthermore, I undertook crystal structure analysis. In addition, I wrote all versions of the manuscript, as well as the supporting information. DFT and NICS calculations were done by me with the help of R. Molenda. R. Molenda performed additional calculations on the inversion dynamics of the molecules. Dr. Villinger performed single crystal structure measurement and refinement. Conception, supervision, and manuscript revision by Dr. Peter Ehlers and Prof. Dr. Peter Langer.

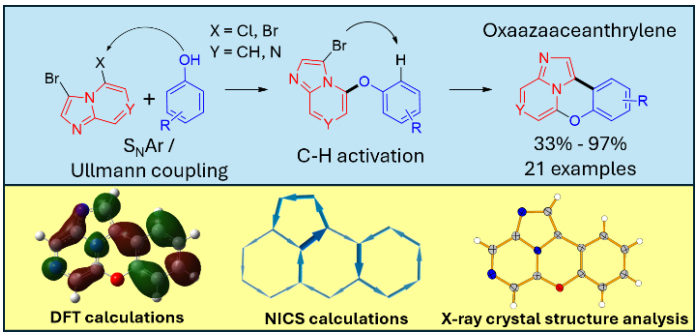
Publication III

Synthesis and Properties of N,O-doped Aceanthrylenes

Jan Radolko[a], Ha Nam Do[a], Peter Ehlers[a], Alexander Villinger[a], Peter Langer[a]*

[a] University of Rostock, Institute of Chemistry, Albert-Einstein Str. 3a, 18059 Rostock, Germany

DOI: doi.org/10.1002/ejoc.202401045
Full paper: *Eur. J. Org. Chem.* **2025**, 28, e202401045



Abstract: N,O-doped aceanthrylenes have been synthesized for the first time via a selective S_NAr reaction or Ullmann-coupling of phenols, followed by an intramolecular direct arylation. The reaction has been carefully optimized and permits the selective synthesis of N,O-doped aceanthrylenes in moderate to excellent yields and tolerate various functional groups. The aromatic behavior of the hitherto unknown heterocyclic scaffold has been further analyzed by NICS and NICS2BC calculations.

Keywords: C-H-activation, Oxaazaaceanthrylenes, Imidazo[1,2-*a*]pyrazine, Imidazo[1,2-*a*]pyridine, N-heterocycles

Contribution to this work: 75%

In this paper, I performed the optimization of 2 steps. With the help of H. N. Do, I synthesized the substrate scope. Furthermore, I did the evaluation of analytical data, performed analytical measurements including UV/Vis and cyclic voltammetry, and undertook crystal structure analysis. In addition, I performed DFT and NICS calculations. I wrote all versions of the manuscript, as well as the supporting information. Dr. Villinger performed single crystal structure measurement and refinement. Conception, supervision and manuscript revision by Dr. Peter Ehlers and Prof. Dr. Peter Langer.

Curriculum vitae

Date and place of birth: 07.10.1991 – Rostock /Germany

Oct. 2021 – Jan. 2025	PhD (Chemistry) University of Rostock • Synthesis of Heterocyclazines by Buchwald-Hartwig reaction and C-H activation
Oct. 2019 –Aug. 2021	Master (Chemistry) • University of Rostock, working group Prof. Dr. Peter Langer Master thesis: Synthesis of indolizine derivatives derived from geminal difluoroalkenes
Oct. 2015 – Juli 2019	Bachelor (Chemistry) • University of Rostock, working group Prof. Dr. Peter Langer Bachelor thesis: Synthesis of Diaryl-*gem*-difluoroethylenes

Publications

- "Synthesis and Properties of N,O-Doped Aceanthrylenes". (*Eur. J. Org. Chem.* **2025**, *28*, e202401045)
- "N-doped and Bowl-Shaped Azabenzo[3,4]azulenofluorene: Synthesis and Characterization of Bridged Aza-Triarylamines". (*Chem. Eur. J.* **2024**, 30, e202403004)
- "Synthesis of 2,2a[1],6-Triazaaceanthrylenes". (*Tetrahedron Lett.,* **2024**, *134*, 154834)
- "Synthesis of chromeno[2,3-*c*]pyrrol-9(2*H*)-ones by domino Michael-Claisen-S_NAr reactions of amino acid esters with 2-chlorophenylpropynones". (*Tetrahedron* **2022**, *104*, 132608)
- "Recent Advances in Transition-Metal-Catalyzed Reactions of *N*-Tosylhydrazones". (*Adv. Synth. Catal.* **2021**, *363*, 3616-3654)

Appendix

I. Publication

II. Publication

III. Publication

I. Publication

Tetrahedron Letters 134 (2024) 154834



Contents lists available at ScienceDirect

Tetrahedron Letters

journal homepage: www.elsevier.com/locate/tetlet





Synthesis of 2,2a1,6-Triazaaceanthrylenes

Jan Radolko [a], Karyna Kulyk [a,b], Peter Ehlers [a], Peter Langer [a,c,*]

[a] Institut für Chemie, Universität Rostock, Albert-Einstein-Str. 3a, Rostock 18059, Germany
[b] Department of Organic and Bioorganic Chemistry, State Scientific Institution "Institute for Single Crystals" NAS of Ukraine, 60 Nauky Ave., Kharkiv 61072, Ukraine
[c] Leibniz-Institute of Catalysis e. V. at the University of Rostock, Albert-Einstein-Str. 29a, Rostock 18059, Germany

ARTICLE INFO

Keywords:
Catalysis
Cyclizations
Heterocycles
Palladium
Regioselectivity

ABSTRACT

Hitherto unknown 6-aryl-6H-2,2a1,6-triazaaceanthrylenes were prepared from readily available 5-bromo-3-iodoimidazo[1,2–*a*]pyridine by chemoselective Suzuki-Miyaura reaction with 2-bromophenylboronic acid and subsequent two-fold Buchwald-Hartwig reaction. 2009 Elsevier Ltd. All rights reserved.

Introduction

Aceanthrylene (**1**) is a polycyclic aromatic hydrocarbon containing an unsaturated five-membered ring *ortho*- and *peri*-fused to positions 1 and 9 of anthracene (Scheme 1). It can also be regarded as a benzoannulated acenaphthylene 2.[1] 6*H*-2,2a1,6-Triazaaceanthrylene **3** represents an heteroanalogue of **1** containing an imidazo[1,2–*a*]pyridine moiety.[2] The latter is a useful building block for the synthesis of complex heteroaromatic systems with a variety of biological[3] and photophysical[4] properties. For example, the imidazo[1,2–*a*]pyridine moiety is present in the drug telacebec which is active against multi-resistant tuberculosis (MDR-TB).[5] Furthermore, DS-1 represents a selective modulator of δ containing GABA type A receptors (GABAA) which results in anxiolytic and anticonvulsant effects.[6]. Scheme 1a.

The Buchwald-Hartwig reaction is of great importance in organic chemistry[7] and has been widely used for the synthesis of alkaloids[8] and pharmaceuticals.[9] In recent years, we have studied the combination of regioselective Pd-catalyzed cross-coupling reactions with twofold Buchwald-Hartwig reactions which allow a convenient synthesis of complex heterocyclic systems.[10] Herein, we report the synthesis of 6*H*-2,2a1,6-triazaaceanthrylenes based on the combination of regioselective Suzuki-Miyaura reactions of dihalogenated imidazopyridines and subsequent cyclization by twofold Buchwald–Hartwig reaction. The heterocyclic core structure of the products has, to the best of our knowledge, not been previously reported.

Results and discussion

Suzuki-Miyaura reaction of known 5-bromo-3-iodoimidazo[1,2–*a*]pyridine (**4**)[11] with 2-bromophenylboronic acid provided 5-bromo-3-(2-bromophenyl)imidazo[1,2–*a*]pyridine (**5**) (Scheme 2).[12] As expected, the reaction took place at the more reactive iodinated carbon atom.

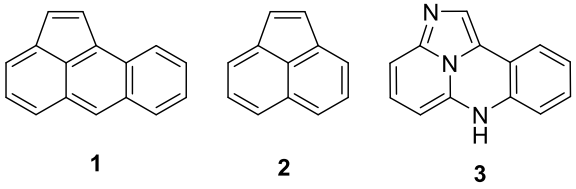
The cyclization by twofold Buchwald-Hartwig reaction was studied next and optimized for the cyclization of **5** with aniline to form 6*H*-2,2a1,6-triazaaceanthrylene **6a** (Table 1).[13] The best yield of **6a** (66 %) was obtained when the reaction was carried out using palladium(II) acetate as the precatalyst, Dicyclohexyl[2′,4′,6′-tris(propan-2-yl)[1,1′-biphenyl]-2-yl]phosphane (**Xphos**)[14] as the ligand, potassium *tert*-butoxide as the base and toluene as the solvent with a reaction time of 48 h (entry 1). The use of Pd_2dba_3 as the catalyst in combination with XPhos, BINAP, Xantphos and Dppf resulted in a decrease of the yield (entries 2–5). However, testing Dppf with $Pd(OAc)_2$ as pre-catalyst afforded a yield of 61 % (entry 6). The yield slightly dropped when dioxane (entry 7) or xylene (entry 8) along with higher temperature was tested. Interestingly, the base played an important role. Employment of sodium *tert*-butoxide or potassium phosphate (entries 9 and 10) resulted in a dramatic decrease of the yield. Finally, shortening the reaction time to 24 h had a negative effect on the yield (entry 11).

Conditions: **5** (1 equiv.), aniline (3 equiv.), catalyst, ligand, base (3 equiv.), solvent, 48 h. [a] Isolated yields, [b] 130 °C instead of 100 °C, [c] 24 h instead 48 h.

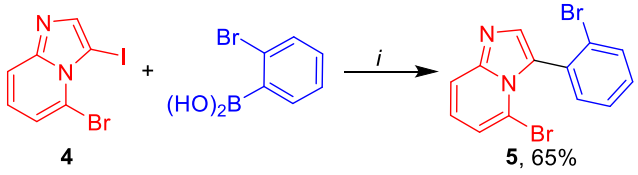
The preparative scope was studied next (Scheme 1). The cyclization

* Corresponding author.
E-mail address: peter.langer@uni-rostock.de (P. Langer).

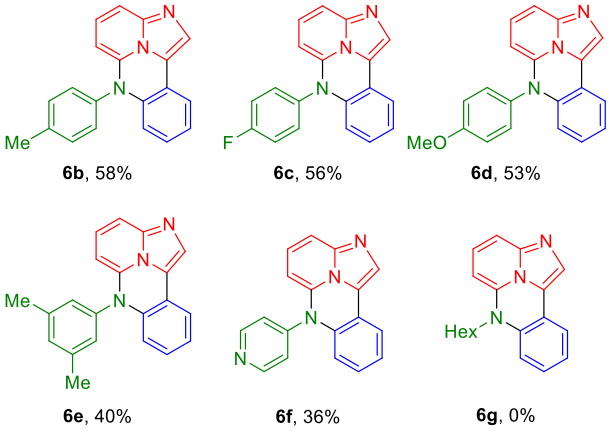
https://doi.org/10.1016/j.tetlet.2023.154834
Received 14 September 2023; Received in revised form 9 November 2023; Accepted 13 November 2023
Available online 15 November 2023
0040-4039/© 2023 Elsevier Ltd. All rights reserved.



Scheme 1. Structures of **1**, **2** and **3**.



Scheme 1. Synthesis of **6a-f.** Reaction conditions: **5** (1 equiv), aniline (3 equiv), $Pd(OAc)_2$ (5 mol%), XPhos (10 mol%), ^tBuOK (3 equiv), toluene, 100 °C, 48 h. [b] Isolated yields.

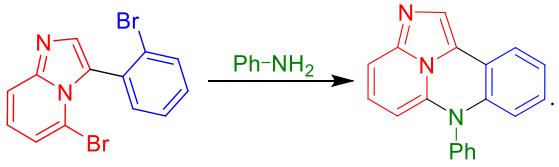


Scheme 2. Synthesis of **5**. *Conditions*: (*i*): **4** (1 equiv.), $Pd(PPh_3)_4$ (0.05 equiv.), K_2CO_3 (2.0 equiv.), dioxane/H_2O (3:1 ratio), 65 °C, 24 h.

of **5** with electron rich and poor anilines afforded products **6b, d, e** and **6c, f**, respectively. No clear trend of the yields was observed. However, a lower yield was observed for **6f**, derived from 4-aminopyidine. Unfortunately, employment of aliphatic amines, such as *n*-hexylamine an cyclohexylamine, or benzylamine proved to be unsuccessful. All products are red-brownish solids.

In order to understand the electronic situation of the products and to compare them with the corresponding hydrocarbon, DFT calculations on the B3LYP/6-311G(d,p) level of theory with polarizable continuum model (PCM) of acetonitrile using the integral equation formalism variant (IEFPCM) were performed for **6a** and its carba-analogue **Ph-A**. [15] The optimized structures of **6a** and **Ph-A** are shown in Fig. 1 displaying the plane polycyclic scaffolds of **6a** and **Ph-A**. The phenyl groups

Table 1
Optimization of the synthesis of **6a**.



Entry	catalyst	ligand	base	solvent	% [a]
1	$Pd(OAc)_2$ (10 mol %)	Xphos (20 mol%)	^tBuOK	toluene	66
2	Pd_2dba_3 (5 mol%)	Xphos (20 mol%)	^tBuOK	toluene	50
3	Pd_2dba_3 (5 mol%)	BINAP (10 mol%)	^tBuOK	toluene	46
4	Pd_2dba_3 (5 mol%)	Xantphos (20 mol %)	^tBuOK	toluene	47
5	Pd_2dba_3 (5 mol%)	Dppf(10 mol%)	^tBuOK	toluene	56
6	$Pd(OAc)_2$ (10 mol %)	Dppf (10 mol%)	^tBuOK	toluene	61
7	$Pd(OAc)_2$ (10 mol %)	Xphos (20 mol%)	^tBuOK	dioxane	56
8[b]	$Pd(OAc)_2$ (10 mol %)	Xphos (20 mol%)	^tBuOK	xylene	51
9	$Pd(OAc)_2$ (10 mol %)	Xphos (20 mol%)	^tBuONa	toluene	6
10	$Pd(OAc)_2$ (10 mol %)	Xphos (20 mol%)	K_3PO_4	toluene	7
11[c]	$Pd(OAc)_2$ (10 mol %)	Xphos (10 mol%)	^tBuOK	toluene	60

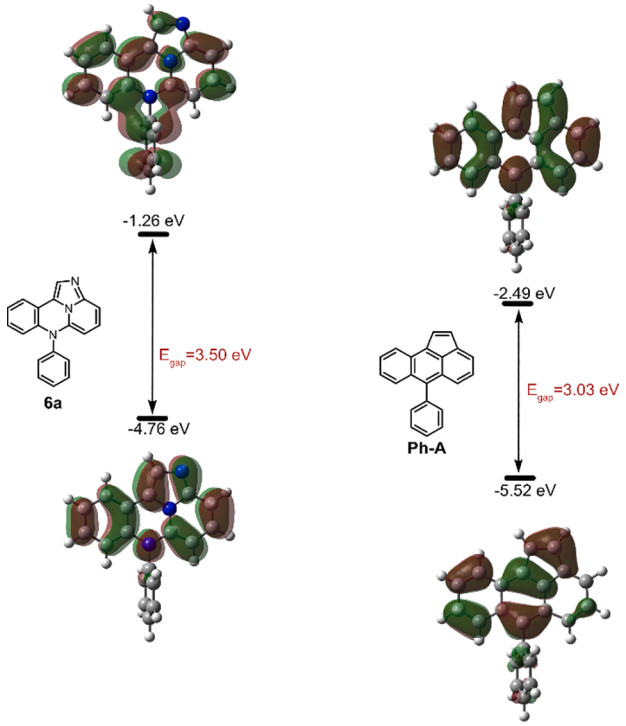


Fig. 1. Calculated frontier molecular orbitals and energy levels at the B3LYP/6-311G(d,p) level of theory for **6a** and **Ph-A.**

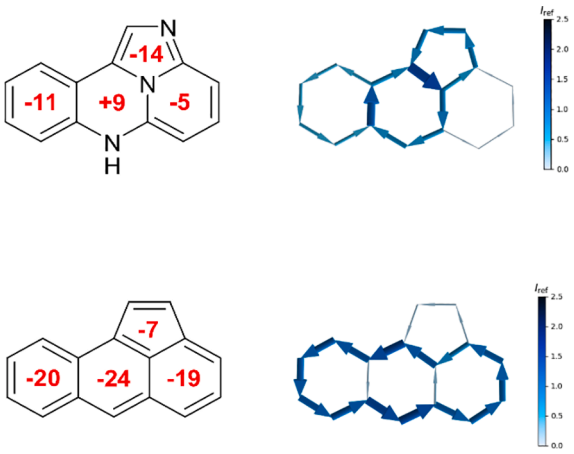


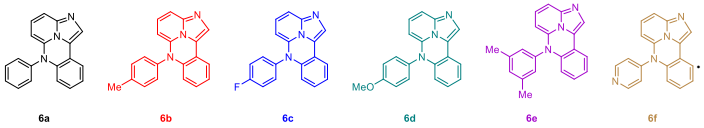
Fig. 2. NICS(1.7) and NICS2BC ring currents (strength reported relative to the ring current of benzene $I_{ref} = 11.5$ nA T^{-1}).

are orthogonally twisted from the heterocyclic core structure. HOMOs and LUMOs are equally distributed over the entire scaffold for both compounds. However, additional contribution by the attached phenyl ring to the LUMO is observed for **6a** despite its orthogonal orientation. HOMO and LUMO of Ph-A are both energetically more stabilized accompanied with a reduced band gap.

To reveal further insights into the aromaticity, NICS(1.7)[16] on the GIOA-B3LYP/6–311 + G(d,p) level of theory with optimized gas-phase structures at the B3LYP/6-311G(d,p) and NICS2BC[17] ring current calculations have been carried out for both compounds. As can been seen from Fig. 2, the fused benzene and imidazole ring of triazaanthrylene show aromaticity which is characterized by their negative NICS(1.7) values while the "pyrimidine" show anti-aromaticity. Consequently, this paratropic ring current impacts the fused "pyridine" ring, which consequently shows only weak to – non-aromaticity. Hence, the NICS2BC ring current maps show local diatropic ring currents for the benzene and imidazole moieties, while the central "pyrimidine" exhibits a strong paratropic ring current which additionally effects the current of the fused "pyridine" ring. These results correlate well with experimentally obtained NMR-spectra, showing characteristic high-field shifts for respective "pyridine-protons". Hence, determined chemical shifts of the "pyridine" are more related to typical enamine or allylamine motifs instead to an aromatic pyridine ring, respectively. In contrast, aceanthrylene show distinct aromaticity for all-six-membered rings of the anthracene moiety. The strong conjugation of these three rings is further approved by the global diatropic ring current of the anthracene component. Hence, the double bound of the five-membered ring behaves more like an isolated double bond what is corroborated by the relatively high NICS value for the five-membered ring. It can be concluded that incorporation of nitrogen atoms into the aceanthrylene scaffold interrupts the electronic conjugation of the overall heterocyclic scaffold leading to drastically altered properties.

Furthermore, photophysical properties of the compounds were investigated by steady-state absorption and photoluminescence spectra (PL). The key optical data are displayed in Table 2 and Fig. 3. The measurements were carried out in dichloromethane at a concentration of 10^{-5} M. All compounds show defined bands with vibrational progression in their absorption spectrum. Two strong and defined bands can be found at ~360 nm and 380 nm accompanied with three weak absorption band at higher wavelength ranging up to ~500 nm. TD-DFT revealed that $S_1 \leftarrow S_0$ is a forbidden transition which explains its low intensity and is mainly described as HOMO → LUMO transition with small contribution from HOMO → LUMO + 2. In general, azaanthrylene

Table 2
Spectroscopic data of azaaceanthrylene derivatives in dichloromethane (10^{-5} M) at 20 °C.



	Ph-A[18]	6a	6b	6c	6d	6e	6f
$\lambda_{1,abs}$ (nm)	349	362	362	362	362	363	362
$\varepsilon_{\lambda 1}$ [$M^{-1}cm^{-1}$]	–	6263	7040	6529	6871	5888	6524
$\lambda_{2,abs}$ (nm)	365	379	380	379	379	380	377
$\varepsilon_{\lambda 2}$ [$M^{-1}cm^{-1}$]	–	7072	7583	7223	7595	6501	6659
$\lambda_{3,abs}$ (nm)	385	426	426	426	428	426	420
$\varepsilon_{\lambda 3}$ [$M^{-1}cm^{-1}$]	–	738	760	1065	986	1180	810
$\lambda_{4,abs}$ (nm)	403	455	455	453	456	453	448
$\varepsilon_{\lambda 4}$ [$M^{-1}cm^{-1}$]	–	457	507	790	679	776	518
$\lambda_{5,abs}$ (nm)	423	486	487	485	488	486	479
$\varepsilon_{\lambda 5}$ [$M^{-1}cm^{-1}$]		170	180	441	282	389	187
$\lambda^{370}_{1,em}$ (nm)	–	409	421	413[b]	407[b]	427	409[b]
$\lambda^{370}_{2\ em}$ (nm)	–	430	432[b]	418	422	431[b]	418
$\lambda^{370}_{3,em}$ (nm)	–	495	497	493	495	493	489
$\lambda^{370}_{4,em}$ (nm)	–	533	536	531	534	535	527
$\lambda^{370}_{5,em}$ (nm)	–	574	575	570	574	571	566
Φ[a]	–	<0.01	<0.01	0.01	<0.01	0.02	<0.01
Optical gap band [eV]	–	3.18	3.20	3.21	3.18	3.20	3.21

[a] Fluorescence standard: Quinine hemisulfate in H_2SO_4 (0.05 M) ($\Phi = 0{,}52$).[19].
[b] shoulder in the spectrum.

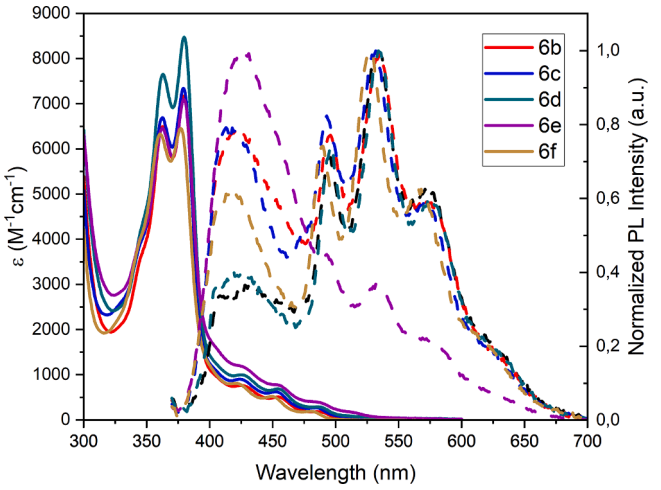


Fig. 3. UV/Vis (solid lines) and emission (dashed lines, $\lambda_{ex} = 370$ nm) spectra of azaaceanthrylene derivatives.

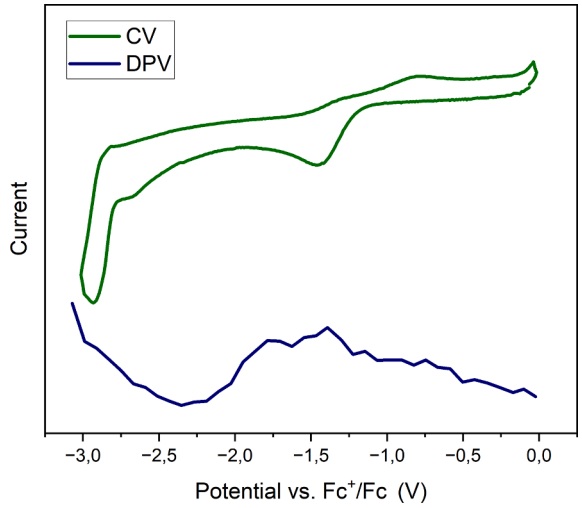


Fig. 4. Cyclic voltammogram of **6a** showing the reduction potential. Measured in acetonitrile with 0.25 M *n*-Bu_4NPF_6 as supporting electrolyte, glassy carbon working electrode, and Pt counter electrode with ferrocene as standard at a scan rate of 200 mV/s.

6a-6f show red-shifted absorption compared to **Ph-A** (Table 2).[18] The change of substituents located at the attached phenyl ring have a negligible effect on the absorption spectra.

All compounds show very weak and complex emission behavior with five distinctive emission bands and quantum yields of 1 % or less, except **6e** with 2 %. Despite its orthogonal orientation, substituents on the phenyl ring have an impact on the intensity of the first emission band, what might be due to certain electron distribution on the aryl rings

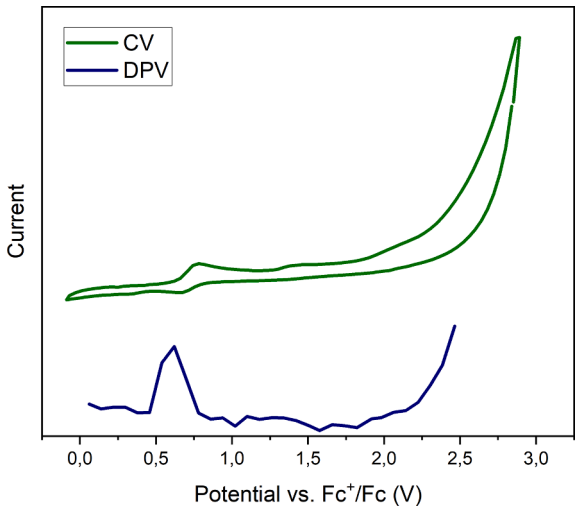


Fig. 5. Cyclic voltammogram of **6a** showing the oxidation potential. Measured in acetonitrile with 0.25 M *n*-Bu_4NPF_6 as supporting electrolyte, glassy carbon working electrode, and Pt counter electrode with ferrocene as standard at a scan rate of 200 mV/s.

found at the LUMO (cf. Fig. 1).

The redox properties of **6a** were additionally determined by cyclic voltammetry and differential pulse voltammetry. The measurements were conducted in acetonitrile with 0.25 M *n*–Bu_4NPF_6 as supporting electrolyte, a working electrode made of glassy carbon, and a platinum counter-electrode. Ferrocene was used as an external standard, and a scan rate of 200 mV/s was selected. To avoid side reactions and side effects, the reduction (Fig. 4) and oxidation (Fig. 5) voltammograms were measured separately. For the reduction, two peaks were found at −1.55 V vs. Fc^+/Fc with an onset potential of −1.31 V and at −2.93 V with an onset potential of −2.80 V vs. Fc^+/Fc. Thus, aceanthrylene is easier reduced compared to **6a** due its lower lying LUMO level. The oxidation took place in a quasi-reversible manner with one peak at 0.78 V vs. Fc^+/Fc and an onset potential of 0.64 V. This is contrast to aceanthrylene which shows no oxidation behaviour in the employed potential range. According to these results, and with the assumption, that the HOMO level of ferrocene locates 4.80 V below the vacuum level, the experimental HOMO and LUMO energy levels were calculated (Table 3).

In summary, hitherto unknown 6*H*–2,2a1,6-triazaaceanthrylenes were prepared from readily available 5-bromo-3-iodoimidazo[1,2–*a*] pyridine by chemoselective Suzuki-Miyaura reaction with 2–bromophenylboronic acid and subsequent two-fold Buchwald-Hartwig reaction. According to DFT calculations, the electronic properties of 6-phenyl-6*H*–2,2a1,6-triazaaceanthrylene greatly differ from those of carbon-analogue 6-phenylaceanthrylene.

Table 3
Optical, electrochemical, and theoretical data for **6a.**

	UV/Vis	Cyclic voltammetry				DFT	
	$E_g^{opt,[a]}$	HOMO[b] (eV)	LUMO[c] (eV)	$\pi_{ox}^{[d]}$ (eV)	$\pi_{red}^{[e]}$ (eV)	HOMO[f] (eV)	LUMO[f] (eV)
6a	3.18	−5.44 eV	−1.75	0.78	−1.55 −2.93	−4.76	−1.26
Ph-A	–	–	–	–	-1.47[20] -2.06[20]	−5.52	−2.49

[a] Taken from the intersection of normalized absorption and emission spectra. [b] Calculated using the equation: $E_{(Homo)}$ = -[E(Ox^{onset} vs. Fc^+/Fc) + 4.80 V]. [c] Estimated using correction factor: E(LUMO) = 1.16 $E_{g,opt}$ – E(HOMO)^{CV}.[21] [d] Oxidation potential taken from CV measurements. [e] Reduction potential taken from CV measurement. [f] Calculated DFT energy levels at the B3LYP/6-31G(p) level of theory.

Declaration of Competing Interest

The authors declare that they have no known competing financial interests or personal relationships that could have appeared to influence the work reported in this paper.

Data availability

Experimental procedures, copies of NMR spectra and details related to the computational studies are found in the Supporting Information.

Acknowledgment

Financial support by the State of Mecklenburg-Vorpommern (scholarship for K. K.) is gratefully acknowledged.

References

[1] *Science of synthesis*, Georg Thieme Verlag KG, Stuttgart, **2010**.
[2] B. van Phuc, Q.H. Dinh, N.L. Chi, Q.T. Nguyen, T.T. Nga Truong, N. van Tuyen, H. Nguyen, P. Langer, T.T. Dang, T.Q. Hung, Tetrahedron 136 (2023), 133360.
[3] 3. a) F. Peytam, Z. Emamgholipour, A. Mousavi, M. Moradi, R. Foroumadi, L. Firoozpour, F. Divsalar, M. Safavi, A. Foroumadi, *Bioorg. Chem.* **2023**, *140*, 106831; b) S. N. Mali, A. Pandey, B. R. Thorat, C.-H. Lai, *Struct. Chem.* **2022**, *33*, 679; c) S. Khatun, A. Singh, G. N. Bader, F. A. Sofi, *J. Biomol. Struct. Dyn.* **2022**, *40*, 14279.
[4] P.A. Chaudhran, A. Sharma, Critical Reviews in Analytical Chemistry (2022) 1–18.
[5] A. Thakur, A. Sharma, Spectrochim. Acta. a, Molecular Biomol Spectrosc. 282 (2022), 121633.
[6] V.R. de Jager, R. Dawson, C. van Niekerk, J. Hutchings, J. Kim, N. Vanker, L. van der Merwe, J. Choi, K. Nam, A.H. Diacon, N. Engl, Journal of Medicine 382 (2020) 1280.
[7] A.C. Humphries, E. Gancia, M.T. Gilligan, S. Goodacre, D. Hallett, K.J. Merchant, S. R. Thomas, Bioorganic & Medicinal Chemistry Letters 16 (2006) 1518.
[8] C.-J. Lu, Q. Xu, J. Feng, R.-R. Liu, Angewandte Chemie (International Ed. in English) 62 (2023) e202216863.
[9] R. Ding, J.-G. Fu, G.-Q. Xu, B.-F. Sun, G.-Q. Lin, The Journal of Organic Chemistry 79 (2014) 240.
[10] a) L. Almirante, A. Mugnaini, P. Rugarli, A. Gamba, E. N. Zefelippo, N. de Toma, W. Murmann, *J. Med. Chem.* **1969**, *12*, 122; b) D. Berthold, A. M. Haydl, J. C. Leung, U. Scholz, Q. Xiao, Z. Zhu, *Methodologies in Amine Synthesis*, John Wiley & Sons, Ltd, **2021**, pp. 377–444.
[11] P. Langer, Synlett 33 (2022) 1215.
[12] **Synthesis of 5-bromo-3-(2-bromophenyl)imidazo [1,2-*a*] pyridine (5):** 200 mg (1.00 equiv., 0.62 mmol) of 5-bromo-3-iodoimidazo[1,2-*a*]pyridine, 149 mg (1.20 equiv., 0.74 mmol) of 2-bromophenylboronic acid, 36 mg (0.05 equiv., 0.03 mmol) of tetrakis(triphenylphosphine)palladium(0) and 171 mg (2.00 equiv., 1.24 mmol) of potassium carbonate were placed under argon in a pressure tube and dissolved in 1,4-dioxane and water (ratio 3:1). The reaction mixture was stirred for 24 hours at a temperature of 65 °C. The product was extracted with ethyl acetate and washed with brine. The collected organic layers were dried over sodium sulfate and filtered over a silica pad. The product was purified by column chromatography on silica gel to give 142 mg of product **5** (65 %) as a brownish solid; mp (119 – 123 °C). R_f = 0.14 (hexane: ethyl acetate, 2:1, v/v). ^{1}H NMR (300 MHz, Chloroform-*d*) δ = 7.70 (dd, $^3J_{H,H}$ = 8.7 Hz, $^4J_{H,H}$ = 1.4 Hz, 1H), 7.66–7.62 (m, 1H), 7.61 (s, 1H), 7.51–7.47 (m, 1H), 7.41–7.31 (m, 2H), 7.14–7.00 (m, 2H). ^{13}C NMR (75 MHz, Chloroform-*d*) δ = 147.3 (C), 135.1 (CH), 133.7 (CH), 132.4 (C), 131.7 (CH), 130.7 (CH), 128.5 (C), 126.5 (C), 126.4 (CH), 124.7 (CH), 118.5 (CH), 117.3 (CH), 113.7 (C). IR (ATR, cm^{-1}): $\tilde{\nu}$ = 1022 (m), 1032 (m), 1044 (m), 1112 (m), 1127 (s), 1149 (s), 1205 (m), 1271 (s), 1298 (w), 1353 (m), 1401 (m). MS (GC-MS, EI, 70 eV): m/z (%) = 355 (7), 354 (49), 353 (15), 352 (100), 350 (52), 193 (14), 192 (96), 191 (11), 182 (7), 180 (7), 165 (6), 164 (11), 101 (11), 96 (17), 75 (7). HRMS (ESI–TOF): calcd. for $C_{13}H_8Br_2N_2$ ([M+H]$^+$) 350.9132, found for $C_{13}H_9Br_2N_2$ ([M+H]$^+$) 350.9137.
[13] **General procedure for the synthesis of 6-aryl-6H-2,2a1,6-triazaaceanthrylenes 6:** 100 mg (1.00 equiv., 0.28 mmol) of 5-bromo-3-(2-bromophenyl)imidazo [1,2-*a*]pyridine, 1.20 equiv. (0.74 mmol) of the aniline, 6 mg (0.10 equiv., 0.03 mmol) of palladium(II) acetate, 27 mg (0.20 equiv.) of Xphos and 191 mg (6.00 equiv., 1.70 mmol) of potassium *tert*-butoxide were placed under argon in a pressure tube and dissolved in 3 mL of toluene. The reaction mixture was stirred for 48 hours at a temperature of 100 °C. The product was extracted with ethyl acetate and washed with brine. The collected organic layers were dried over sodium sulfate and filtered over a silica pad. The product was purified by column chromatography on silica gel (ethyl acetate, 1% acetic acid). After purification, the collected product was concentrated and neutralized with a saturated solution of sodium hydrogen carbonate to remove remaining acetic acid. The compound was extracted with ethyl acetate and the organic phase was evaporated to afford the product. **6-Phenyl-6H-2,2a1,6-triazaaceanthrylene (6a)**. According to general procedure A, product **6** was isolated as a yellow solid (54 mg, 66%); mp (194 – 195 °C). R_f = 0.16 (EtOAc: AcOH, 100:1, v/v). ^{1}H NMR (250 MHz, Chloroform-*d*) δ = 7.66–7.57 (m, 2H), 7.54–7.46 (m, 1H), 7.36–7.29 (m, 2H), 7.14 (s, 1H), 7.00–6.94 (m, 1H), 6.65–6.56 (m, 2H), 6.41–6.28 (m, 2H), 5.69–5.61 (m, 1H), 4.36 (dd, $^3J_{H,H}$ = 6.8 Hz, $^4J_{H,H}$ = 1.3 Hz, 1H). ^{13}C NMR (63 MHz, $CDCl_3$) δ = 143.7 (C), 140.1 (C), 137.0 (C), 131.5 (2C, CH), 130.2 (2C, CH), 129.7 (C), 129.3 (CH), 128.2 (CH), 124.3 (CH), 123.0 (CH), 121.7 (CH), 120.0 (C), 118.5 (C), 114.2 (CH), 107.8 (CH), 88.9 (CH), 77.2 (C). IR (ATR, cm^{-1}): $\tilde{\nu}$ =1625 (m), 1582 (m), 1522 (m), 1502 (s), 1487 (m), 1450 (s), 1372 (m), 1360 (m), 1310 (m), 1269 (m), 1261 (m), 1205 (m), 1151 (m), 1137 (m), 1118 (m), 1073 (m), 1065 (m), 1044 (m), 1034 (m), 1022 (m), 1001 (m). MS (GC-MS, EI, 70 eV): m/z (%) = 284 (23), 283 (87), 207 (20), 206 (100), 142 (6), 77 (6). HRMS(ESI-TOF): calcd. for $C_{19}H_{13}N_3$ ([M+H]$^+$) 284.1188, found for $C_{19}H_{14}N_3$ ([M+H]$^+$) 284.1194.
[14] X. Huang, K.W. Anderson, D. Zim, L. Jiang, A. Klapars, S.L. Buchwald, Journal of the American Chemical Society 125 (2003) 6653–6655.
[15] M. J. Frisch, G. W. Trucks, H. B. Schlegel, G. E. Scuseria, M. A. Robb, J. R. Cheeseman, G. Scalmani, V. Barone, G. A. Petersson, H. Nakatsuji, X. Li, M. Caricato, A. Marenich, J. Bloino, B. G. Janesko, R. Gomperts, B. Mennucci, H. P. Hratchian, J. V. Ortiz, A. F. Izmaylov, J. L. Sonnenberg, D. Williams-Young, F. Ding, F. Lipparini, F. Egidi, J. Goings, B. Peng, A. Petrone, T. Henderson, D. Ranasinghe, V. G. Zakrzewski, J. Gao, N. Rega, G. Zheng, W. Liang, M. Hada, M. Ehara, K. Toyota, R. Fukuda, J. Hasegawa, M. Ishida, T. Nakajima, Y. Honda, O. Kitao, H. Nakai, T. Vreven, K. Throssell, J. A. Montgomery, Jr., J. E. Peralta, F. Ogliaro, M. Bearpark, J. J. Heyd, E. Brothers, K. N. Kudin, V. N. Staroverov, T. Keith, R. Kobayashi, J. Normand, K. Raghavachari, A. Rendell, J. C. Burant, S. S. Iyengar, J. Tomasi, M. Cossi, J. M. Millam, M. Klene, C. Adamo, R. Cammi, J. W. Ochterski, R. L. Martin, K. Morokuma, O. Farkas, J. B. Foresman, and D. J. Fox, Gaussian, Inc., Wallingford CT, **2016**.
[16] a) I. Fernandez (Ed.) *Aromaticity. Modern computational methods and applications*, Elsevier, S.l., **2021**; b) R. Gershoni-Poranne, A. Stanger, *Chem. Eur. J.* **2014**, *20*, 5673-5688; c) A. Stanger *Eur. J. Org. Chem.*, **2020**, 3120–3127; A. Stanger *ChemPhysChem* **2023**, *24*, e202300080.
[17] a) E. Paenurk, R. Gershoni-Poranne, *Phys. Chem. Chem. Phys.* **2022**, *24*, 8631-8644; b) P. v. Ragué Schleyer, C. Maerker, A. Dransfeld, H. Jiao, N. J. R. v. Eikema Hommes *Chem. Rev.* **2005**, 105, 10, 3842–3888.
[18] N.D. Marsh, C.J. Mikolajczak, M.J. Wornat, Spectrochimica Acta. Part A, Molecular and Biomolecular Spectroscopy 56A (2000) 1499.
[19] A.M. Brouwer, Pure and Applied Chemistry 83 (2011) 2213.
[20] C. Koper, M. Sarobe, L.W. Jenneskens, Physical Chemistry Chemical Physics 6 (2004) 319.
[21] J. Sworakowski, Synthetic Metals 235 (2018) 125.

II. Publication

Check for updates

Chemistry–A European Journal
Research Article
doi.org/10.1002/chem.202403004
Chemistry Europe
European Chemical Societies Publishing
www.chemeurj.org

N-doped and Bowl-Shaped Azabenzo[3,4]azulenofluorene: Synthesis and Characterization of Bridged Aza-Triarylamines

Jan Radolko,[a] Ha Minh Tuan,[a] Ricardo Molenda,[a] Alexander Villinger,[a] Peter Ehlers,*[a] and Peter Langer*[a]

Triarylamines are frequently employed as electron donor functional groups in a variety of organic electronic materials. We herein report the synthesis and in-depth characterisation of aza-analogues of fully bridged triarylamines, consisting of 5-, 6- and 7-membered rings. The impact of nitrogen doping and π-extension on the structural, electronic and optical-properties of these contorted heteroaromatic PAHs is thoroughly investigated and paves the way for an improved understanding of the structure-property relationships.

Introduction

Polycyclic aromatic hydrocarbons (PAHs)[1] have been implemented within several electronic devices, such as organic light-emitting diodes (OLEDs),[2] liquid crystals,[3] fluorescence imaging labels,[4] organic solar cells (OSC),[5] organic field-effect transistors (OFETs)[6] or chemical sensors,[7] which experience constant development.

A common strategy to alter the electronic properties of PAHs is the substitution of the scaffold with functional groups which affect the electronic properties as well as the structural alignment in the solid state and consequently its charge transport properties. The triphenylamine (TPA) moiety represents one of the mostly employed functional groups to efficiently influence the electronic properties of PAHs, due to its strong electron donating properties.[8] However, its propeller-shaped geometry opposes an effective electronic communication and, hence, influences the π-conjugation with the respective PAH.[9] To overcome these drawbacks, planarization of the TPA scaffold is a promising approach to tune the optical and electronic properties and transform the TPA group to a novel N-doped PAH. Similarly to inorganic semiconductors,[10] doping of polycyclic aromatic scaffolds by atoms other than carbons is a capable approach to alter the inherent physicochemical properties of the material, such as electronic properties and molecular geometry.[11]

A bridged TPA system **I**, consisting of a doubly pentagon fused TPA, was obtained by Dunlop and Tucker back in 1939 (Scheme 1).[12] Later, Hellwinkel and Melan utilized carbonyl- and methylene bridges to rigidify the TPA scaffold (**IIa** and **IIb**).[13] Such heterotriangulenes have proven to exhibit thermotropic liquid crystallinity, aggregation induced emission (AIE), NIR absorption and generally interesting fluorescence and phosphorescence properties.[14]

Aside from the planarization of TPA, complement studies on the introduction of additional heteroatoms into the heterotriangulene scaffold or the alternation of the ring size is of current interest to modify the electronic properties. For instance, the group of Okada synthesized electron rich and bowl-shaped oxygen analogue **III** and its corresponding radical cation.[15] Interestingly, introduction of oxygen atoms on the periphery of heterotriangulene **III** leads to a bowl-shaped structure in the solid state, while its radical cation is planar. Later, the impact of nitrogen doping on the electronic properties was studied by Kautny (compounds **IV**), leading to donor-acceptor based TPAs which enables the fine-tuning of HOMO and LUMO energy levels.[16]

The groups of Kivala[17] and Lindner[18] independently synthesized a completely fused TPA containing two five- and one seven-membered ring system (compounds **V** and **VI**), which show promising optoelectronic properties for OLED application while a nearly planar scaffold was proposed. Inspired by the recent work of Kivala, Lindner and Kautny and our own interest in the synthesis of nitrogen doped PAHs, we studied the impact of N-doping and its π-extension by incorporation of a pyridine or quinoline ring within the scaffold.

Synthesis

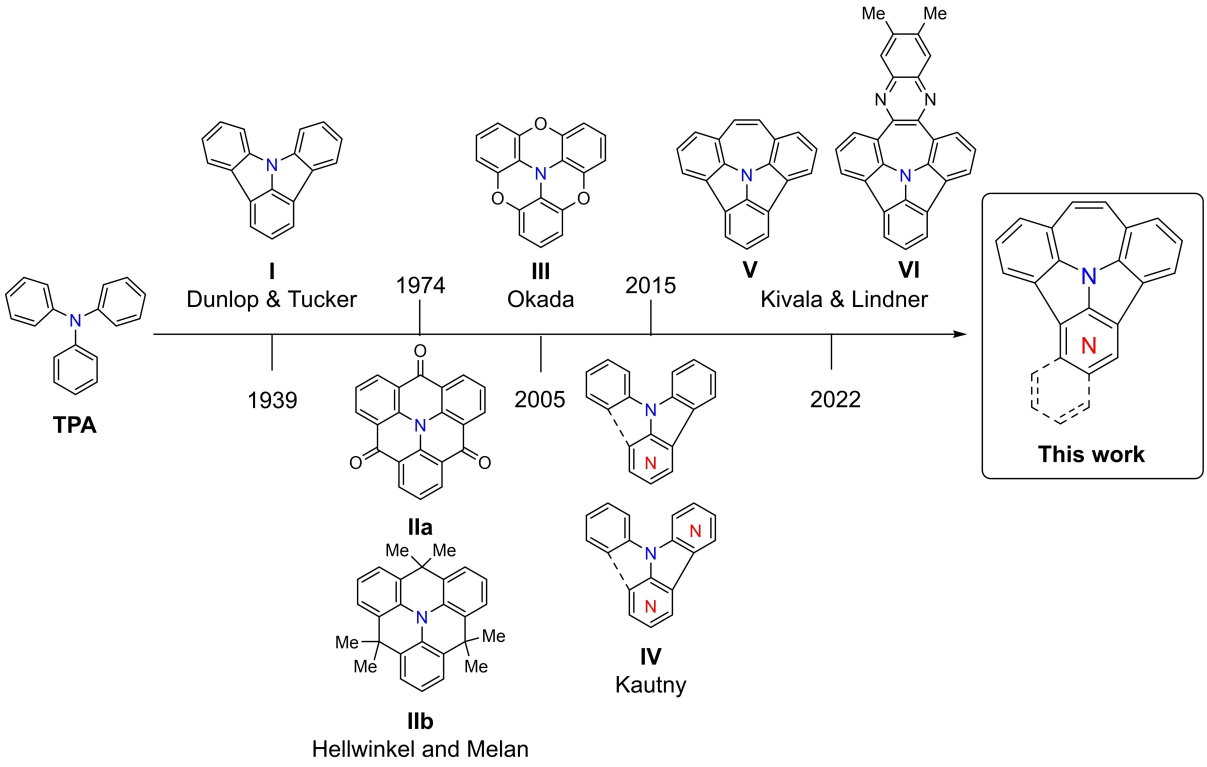
Analogously to the synthetic methodology reported by Kivala and Lindner, we firstly elucidated suitable conditions for the

[a] J. Radolko, H. M. Tuan, R. Molenda, A. Villinger, P. Ehlers, P. Langer
University of Rostock, Institute of Chemistry, Albert-Einstein-Str. 3a, 18059 Rostock, Germany
Phone: +49 381 498 6427
Phone: +49 381 498 6410
E-mail: peter.ehlers@uni-rostock.de
peter.langer@uni-rostock.de
Homepage: www.langer.chemie.uni-rostock.de

Supporting information for this article is available on the WWW under https://doi.org/10.1002/chem.202403004

© 2024 The Author(s). Chemistry - A European Journal published by Wiley-VCH GmbH. This is an open access article under the terms of the Creative Commons Attribution Non-Commercial NoDerivs License, which permits use and distribution in any medium, provided the original work is properly cited, the use is non-commercial and no modifications or adaptations are made.

© 2024 The Author(s). Chemistry - A European Journal published by Wiley-VCH GmbH



Scheme 1. Bridged Triarylamines

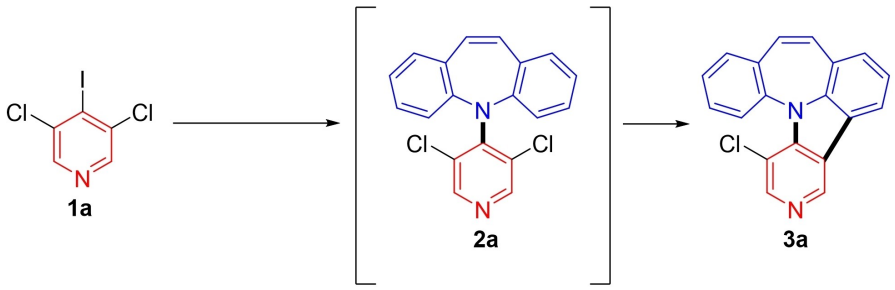
Buchwald-Hartwig reaction of dibenzoazepine with trihalogenated pyridine **1a**.[19] Surprisingly, instead of the expected C–N coupling product **2a**, product **3a**, derived from a Buchwald-Hartwig reaction and subsequent onefold C–H-activation, was isolated in all test reactions (Table S1). Optimization revealed that $Pd(OAc)_2$ and $P(^tBu)_3 \cdot HBF_4$ as catalyst in the presence of sodium *tert*-butoxide in toluene (42%) or dioxane (48%) gave the best product yields of **3a** (Scheme 2).

In contrast, isomeric pyridine **1b**[19] gave exclusively the uncyclized Buchwald-Hartwig product **2b** in moderate yield, while the respective quinoline-derived starting material **1c**[20] afforded a mixture of regioisomeric C–H-activation products **3c** and **3c'** and of Buchwald-Hartwig product **2c** (Scheme S1). Employment of dioxane as solvent led to selective formation of **3c** and, consequently, to an improved isolated yield of 40% (Scheme 3).

The structures of **3a**, **2b** and **3c** were independently confirmed by single crystal structure analysis (Figure 1). The pyridine ring of **2b** occupies a nearly orthogonal orientation in the crystal state. Compounds **3a** and **3c** crystalized in a herringbone type pattern and exhibit a twisted shape, due to the presence of the seven-membered azepine ring within the scaffold.

Next, we turned our attention to the final cyclization step to afford the desired compound **4** (Scheme 4). Employment of the common catalytic system, consisting of $Pd(OAc)_2/P(Cy_3) \cdot HBF_4$,[21] gave the desired fully bridged azatriarylamine derivatives **4a-c** in very good yields. Symmetric compound **4a** was isolated in 90% yield, while non-symmetric products **4b** and **4c** gave a slightly reduced yield of 79 and 77%, respectively.

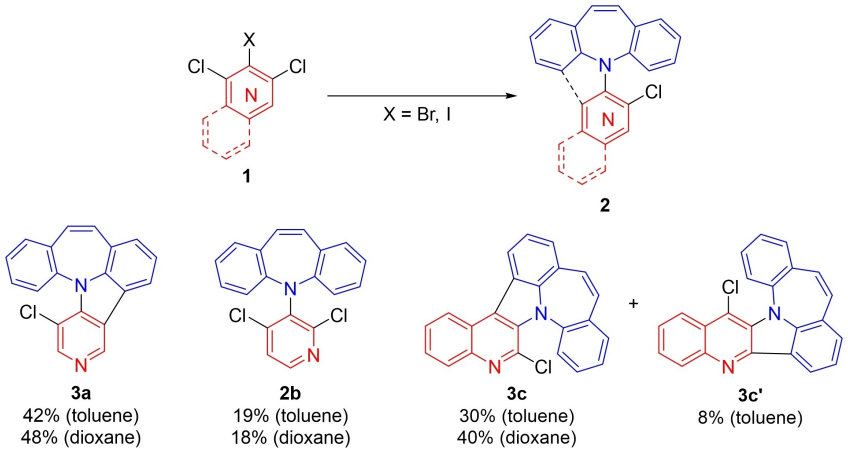
Finally, we developed a one-pot two-step procedure which provided similar or even higher yields for the final products



Scheme 2. Buchwald-Hartwig reaction and subsequent onefold C–H-activation; reaction conditions: **1** (1.2 eq.), 5*H*-dibenzo[*b,f*]azepine (1.0 eq.), $Pd(OAc)_2$ (5 mol%), $P(^tBu_3) \cdot HBF_4$ (10 mol%), ^{t}BuONa (3.0 eq.), toluene or dioxane.

© 2024 The Author(s). Chemistry - A European Journal published by Wiley-VCH GmbH

15213765, 2024, 69, Downloaded from https://chemistry-europe.onlinelibrary.wiley.com/doi/10.1002/chem.202403004 by University Rostock Universitätsbibliothek, Wiley Online Library on [10/08/2025]. See the Terms and Conditions (https://onlinelibrary.wiley.com/terms-and-conditions) on Wiley Online Library for rules of use; OA articles are governed by the applicable Creative Commons License



Scheme 3. Palladium catalyzed reaction of dibenzoazepine with trihalogenated pyridine/quinoline; reaction conditions: **1** (1.2 eq.), 5*H*-dibenzo[*b,f*]azepine (1.0 eq.), $Pd(OAc)_2$ (5 mol%), $P(^tBu_3)\cdot HBF_4$ (10 mol%), ^{t}BuONa (3 eq.), toluene or dioxane, 100 °C, 24 h.

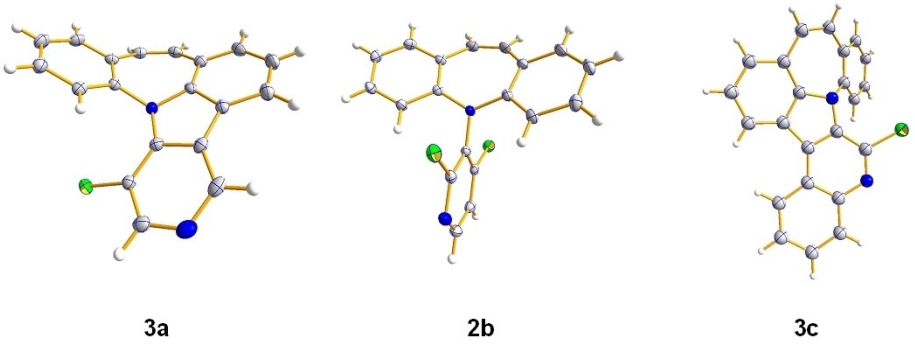
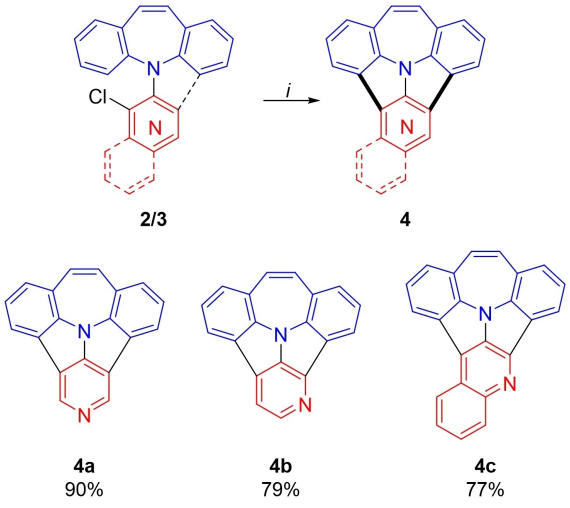


Figure 1. Crystal structures of **3a**, **2b** and **3c**.



Scheme 4. Reaction and scope of the C–H-activation; reaction conditions: *i:* **2**/**3** (1.2 eq.), $Pd(OAc)_2$ (5 mol%), $P(Cy)_3\cdot HBF_4$ (10 mol%), DBU, DMA, 150 °C, 24 h.

without the necessity of isolation and purification of intermediates (Scheme 5).

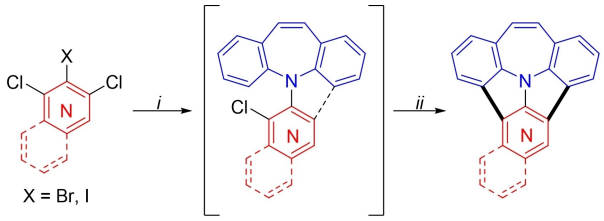
Crystal Structure Analysis

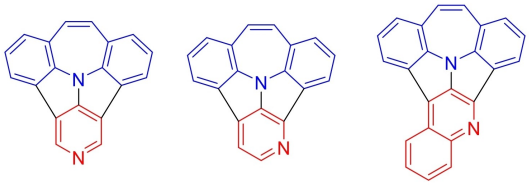
We obtained single crystals of all three final products **4a–c** by slow evaporation of a respective ethyl acetate solution with a superimposed layer of heptane. All three compounds **4a–c** crystalize in bowl-shaped conformations. The depths determined from the distance of the central TPA nitrogen atom and the plane of the three carbon atoms of the peripheral six-membered rings were found to be 0.64 Å and 0.68 Å for **4a** and **4b**, respectively, which are comparable to structurally related compound **VI** synthesized by Lindner. In contrast, quinoline derived product **4c** adopts a more concave structure with a depth of 0.95 Å. This increased pyramidalization is further corroborated by the C–N–C bond angles of 354.5° (**4a**), 352.0° (**4b**) and 348.3° (**4c**) and increasing π-orbital axis vector (POAV) angles of 7.6° (**4a**), 9.0° (**4b**) and 11.2° (**4c**) for the central nitrogen.[22]

All compounds adopt slip-stacking arrangements. In the crystal lattice of **4a**, two molecules of the stacks take up a face-to-face alignment with opposite spatial orientation of their concave and convex faces. In contrast, molecules of **4b** build slipped stacks with face-to-face orientation with the same spatial orientation, while compound **4c** align in alternate stacks

© 2024 The Author(s). Chemistry - A European Journal published by Wiley-VCH GmbH

15213765, 2024, 69, Downloaded from https://chemistry-europe.onlinelibrary.wiley.com/doi/10.1002/chem.202403004 by University Rostock Universitatsbibliothek, Wiley Online Library on [10/08/2025]. See the Terms and Conditions (https://onlinelibrary.wiley.com/terms-and-conditions) on Wiley Online Library for rules of use; OA articles are governed by the applicable Creative Commons License





	4a	4b	4c
two-steps procedure	43%[a]	15%[a]	31%[a]
one-pot two steps procedure	**41%[b]**	**60%[b]**	**38%[b]**

Scheme 5. One-Pot Two-Step Synthesis of Compounds **4**; Reaction conditions: *i*: **1** (1.2 eq.), 5*H*-dibenzo[*b,f*]azepine (1.0 eq.), $Pd(OAc)_2$ (5 mol%), $P(^tBu_3)\cdot HBF_4$ (10 mol%), ^{t}BuONa (3 eq.), toluene, 100 °C, 24 h, *ii:* $Pd(OAc)_2$ (5 mol%), $P(Cy)_3\cdot HBF_4$ (10 mol%), DBU, DMA, 150 °C, 24 h; [a] overall isolated yields over two steps, [b] isolated yields for one-pot two-step reaction without purification of intermediates

in an ABAB arrangement with a distance of around 3.30 Å between each layer (Figure 2).

In contrast to the bowl-like structures in the crystals of compounds **4**, the group of Kivala recently reported a planar structure for carbon analogue **V**, which prompted us to further

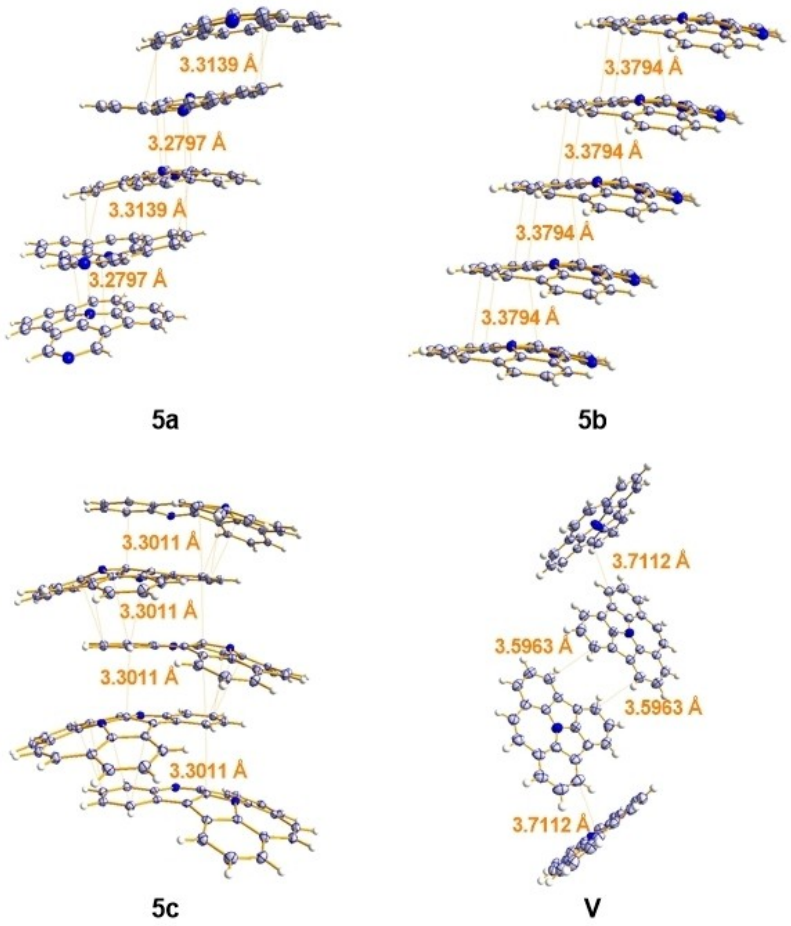


Figure 2. Crystal packing arrangement, π–π contacts (in Ångström) and orientation of compounds **4** and **V**

© 2024 The Author(s). Chemistry - A European Journal published by Wiley-VCH GmbH

15213765, 2024, 69, Downloaded from https://chemistry-europe.onlinelibrary.wiley.com/doi/10.1002/chem.202403004 by University Rostock Universitätsbibliothek, Wiley Online Library on [10/08/2025]. See the Terms and Conditions (https://onlinelibrary.wiley.com/terms-and-conditions) on Wiley Online Library for rules of use; OA articles are governed by the applicable Creative Commons License

elaborate the structures of bridged TPAs **4** and **V** by DFT calculations. Hence, geometry optimization with various functionals and basis set combinations were performed and compared to experimental data (Table S8). All employed methods predict a bowl-shaped structure as energy minimum for all compounds. The best agreement between experimental and calculated bowl-depths was obtained at the B3LYP-D3(BJ)/6-311G(d,p) level (for details see supporting information). Calculations further predict an even more concave structure for compounds **4a**–**c**, with the highest deviation from planarity for **4c**. Interestingly, compounds **V** and **4a** differ only by 0.07 Å (Figure 3), while variation of the position of the pyridinic nitrogen leads to deeper bowl depth by ~0.25 Å for compounds **4b**, despite its location at the edge of the molecule. π-Extension at the pyridine moiety (**4c**) results in a slightly increased bowl-depth compared to **4b**, which has been similarly proven in case of Lindner's compound **VI**, for which calculations predict a shallower bowl depth of 0.72 Å as compared to **V**.

The inversion dynamic of the bridged-TPAs **4** an **V** were further elucidated by DFT calculations and reveal, that for all compounds the inversion proceeds *via* a planar transition state (TS) with inversion activation free energies between 3.7–6.9 KJ mol^{-1} (Figure 4 and Tables S9–S13). Thus, interconversion of the bridged-TPAs occurs rapidly at room temperature. However, the inversion barrier of compounds **4b** and **4c** is roughly twice that of **4a** and **V**, indicating a stronger stabilization of the ground state and destabilization of TS state for **4b** and **4c** thus emphasizing the effect of selective N-doping within the bridged- TPA backbone.

Based on the experimental and theoretical results, the planar TS-like conformation obtained by Kivala resembles the calculated transition state (TS) of the inversion process and might be attributed to crystal packing effects. Thus, we examined the presence and extent of dispersion forces, i.e. π···π- and CH···π contacts in the crystal lattices of the bridged-TPAs (Tables S9–S13). In contrast to **4** and **VI**, which adopt a slipped stacking arrangement, the crystal packing of **V** follows a herringbone motif, which is solely dominated by strong C–H···π interactions. In fact, π···π contacts shorter than the sum of the van der Waals radii are not observed. Conversely, several close CH···π and π···π contacts are present in the packing structures of compounds **4a**–**c** with the latter predominant for compounds **4a** and **4c**. Similar features are shown in the crystal structure of Lindner's quinoxaline fused compound **VI**, which likewise possesses several short contacts with dominating π···π interactions. Hence, we propose a correlation between the pyramid-

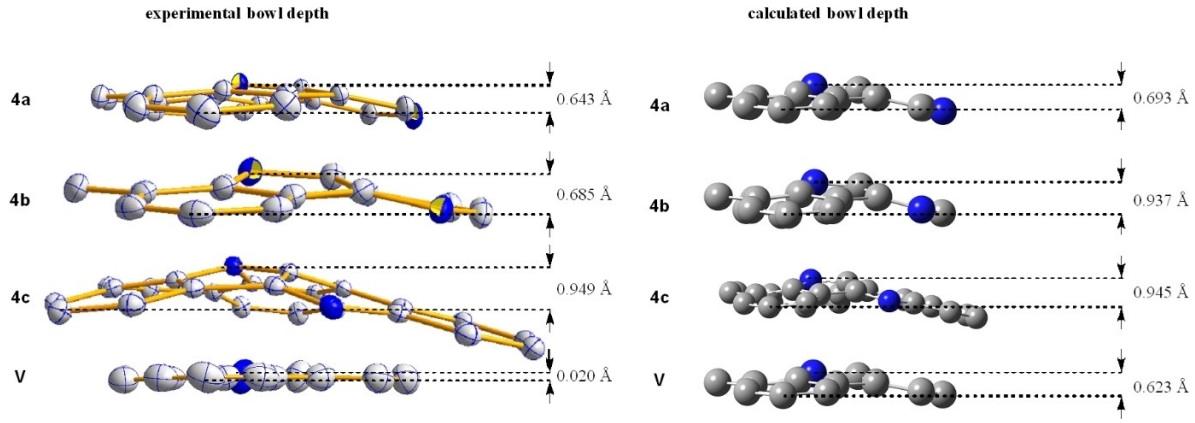
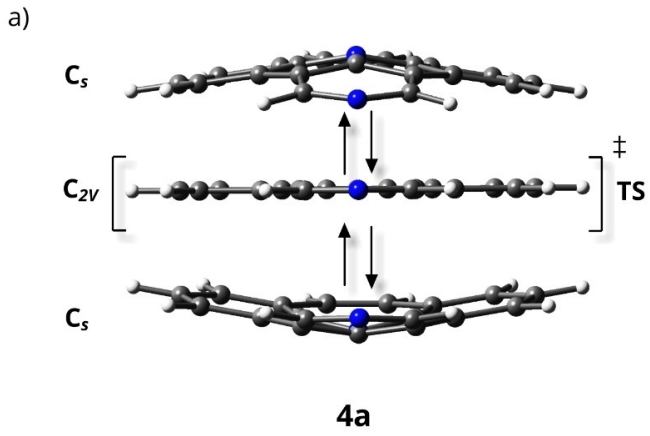


Figure 3. Bowl depths of **4** and **V**, left: experimental, right: DFT-optimized gas phase structures at the B3LYP-D3(BJ)/6-311G(d,p) level. Thermal ellipsoids are drawn at the 50% probability level.



b)

Inversion barrier

	$\Delta E^{\ddagger}_{inv.}$ (kJ mol^{-1})	$\Delta G^{\ddagger}_{inv.}$ (298 K) (kJ mol^{-1})
V	0.4	3.7
4a	0.8	3.8
4b	4.6	6.6
4c	4.6	6.9

Figure 4. (a) Inversion dynamic of bridged-TPAs illustrated for **4a**. (b) Inversion barriers calculated at the PW6B95-D3/6-311G(d,p)//B3LYP-D3(BJ)/6-311G(d,p) level in the gas-phase.

© 2024 The Author(s). Chemistry - A European Journal published by Wiley-VCH GmbH

15213765, 2024, 69, Downloaded from https://chemistry-europe.onlinelibrary.wiley.com/doi/10.1002/chem.202403004 by University Rostock Universitatsbibliothek, Wiley Online Library on [10/08/2025]. See the Terms and Conditions (https://onlinelibrary.wiley.com/terms-and-conditions) on Wiley Online Library for rules of use; OA articles are governed by the applicable Creative Commons License

alization of bridged-TPAs and the presence of close CH···π and π···π interactions within the crystal lattice. Thus, predominance of CH···π interactions enable the stabilization of a planar TS-like structure, while strong π···π interactions or the simultaneous occurrence of both types of dispersion forces stabilize a bowl-like conformation in the crystal state. The extent and ratio of the respective dispersion interactions therefore determines the degree of curvature.

Aromaticity

To receive further insight into the conjugation and aromaticity[23] of compounds **4**, we calculated nucleus-independent chemical shifts (NICS) as a magnetic criterion of aromaticity and visualized the respective ring currents of **4a–c**. Finally, the results were compared with compound **V**.

As shown in Figure 5, all six- and five-membered rings of the analyzed molecules possess negative NICS values and hence indicate aromaticity. Positive NICS values are obtained for the 7-membered azepine ring indicating its anti-aromatic character. Incorporation of nitrogen leads to less negative NICS values for the pyridine and its fused pyrrole rings, while the benzene rings of the dibenzoazepine moiety remain virtually unaffected (Figure 6). Meanwhile, incorporation of nitrogen reduces the anti-aromatic character of the azepine ring in compounds **4a–c**. This effect is more pronounced for the non-symmetrical compounds **4b** and **4c**.

The corresponding ring currents have been visualized by anisotropy of the induced current density (ACID)[24] (Figure 6), NICS2BC bond current[25] (Figure S6) and gauge-including magnetically induced current[26] (GIMIC) methods (Figure S7). Visualization of the ring currents reflects the experimental crystal data and calculated NICS values very well.

All methods reveal a paratropic (counterclockwise) ring current for the 7-membered ring and a diatropic (clockwise) current mapping for the respective (aza)indolocarboline moieties of **4a–c**, which correlates well with the bond lengths obtained from the crystal structures. Typical double bond length for the ethylene bridge of the azepine ring and characteristic single bond length of its connecting bonds are observed, hinting to an isolated double bond character within the azepine ring (Figure S5). Local diatropic ring currents are observed for the central benzene and pyridine rings, while a semi-global diatropic current encircle the quinoline ring. The two benzene rings of the dibenzoazepine component and the two pyrrole rings, on the other hand, do not form local currents, instead contributing to the formation of the diatropic current that shapes the (aza)indolocaboline fragment. Additional investigations of the ethylene bridge were performed with ^{1}H-NMR spectroscopy for **4** in chloroform for a comparison with compound **V**, synthesized by the group Lindner and in dichloromethane for comparison of compound **V** synthesized by the Kivala group. With support of measured ^{1}H-^{1}H-COSY-Spectra (Figures S28, S32 and S36, Table S19, S20 and S21), assignments for the signal of the ethylene bridge were

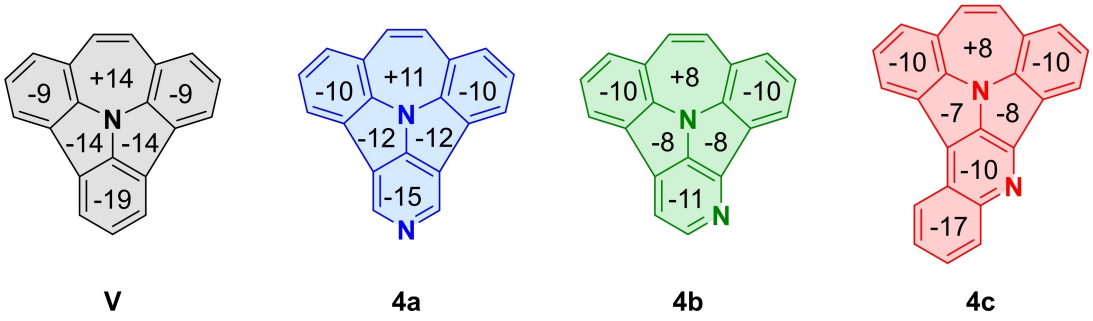


Figure 5. Scheme of molecule with respective NICS(1.7)$_{\pi ZZ}$ values in the geometric center of each ring

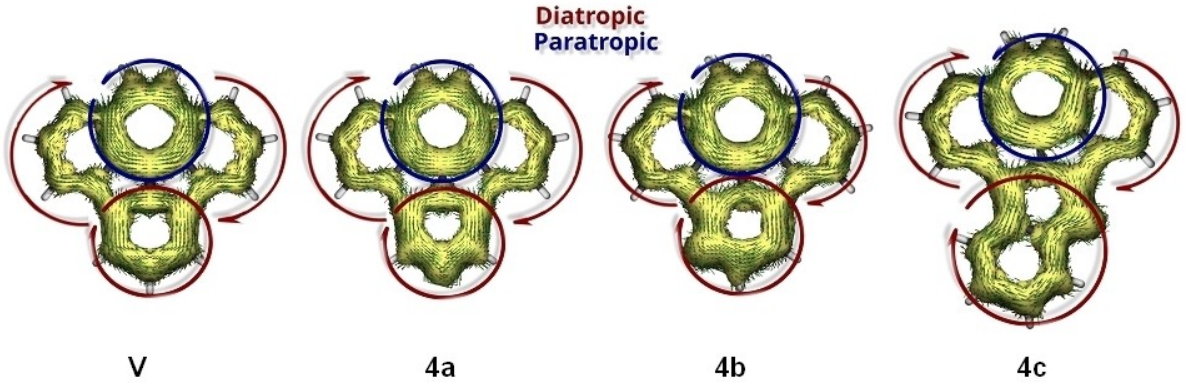


Figure 6. ACID plots of compounds **4** and **V** with contribution from π-orbitals only (isosurface value = 0.035 a.u). Red arrows indicate diatropic (clockwise) current, blue arrows indicate paratropic (counterclockwise) current.

© 2024 The Author(s). Chemistry - A European Journal published by Wiley-VCH GmbH

15213765, 2024, 69, Downloaded from https://chemistry-europe.onlinelibrary.wiley.com/doi/10.1002/chem.202403004 by University Rostock Universitatsbibliothek, Wiley Online Library on [10/08/2025]. See the Terms and Conditions (https://onlinelibrary.wiley.com/terms-and-conditions) on Wiley Online Library for rules of use; OA articles are governed by the applicable Creative Commons License

allocated and compared in their chemical shifts (Figure 7). A paratropic ring current in the seven membered ring would assume a shielding effect on the protons attached to the ethylene bridge and, therefore, a high field shift for the signals in ^{1}H-NMR is expected. This was observed for compounds **4a–c** in chloroform and dichloromethane. The trend of their corresponding chemical shifts could be affirmed by calculated NICS(1.7) $_{\pi ZZ}$ values for dichloromethane (Table 1). Unfortunately, for measurements in chloroform, this trend could not be observed. Closer inspection of the signal revealed a splitting pattern for unsymmetric examples, along with a strong roof effect of the two duplets for compound **4b** and **4c** in chloroform and **4c** in dichloromethane. The coupling constant of the observed duplets were in the range of 12 Hz and can be considered as evidence for a non-aromatic or an olefinic character of the double bond with protons in *cis*-position according to the Karplus equation.[27] For **4c** a mean value of 6.11 ppm was determined for both duplet signals.

Optical Properties

To gain insights into the impact of nitrogen doping on the optical properties, steady-state absorption, and photoluminescence spectra (PL) for the compounds **4a–c** were studied in dichloromethane. Spectra are depicted in Figure 7 and the key optical data is summarized in Table 2.

Derivative **4a** possesses very similar spectral features as compared to **V**, including fine structure of its absorption and emission spectra as well as its extinction coefficients. However, incorporation of nitrogen leads to a slight bathochromic shift of the absorption spectrum. The bathochromic shift of the absorption spectra is more pronounced for non-symmetric compounds **4b** and **4c**, accompanied by a loss of fine structure. As expected, the mostly pronounced redshift is found for benzo-annulated derivative **4c**. The location of the emission bands is less affected by the position of nitrogen within the compound, but rather than their emission intensity. Particularly, **4b** possess less intense $\lambda_{em,2}$ and $\lambda_{em,3}$ bands as compared to **4a**, while benzannulation leads to a less intense $\lambda_{em,1}$, but stronger $\lambda_{em,3}$ band which appears as shoulder for **4c**. Moreover, **4c** possesses a much higher quantum yield of 9% as compared to **4a** (2%) and **4b** (3%).

The redox properties of **4a–c** were determined by cyclic voltammetry (CV) and differential pulse voltammetry (DPV) measurements and are exemplarily shown for **4a** in Figures 8 and S8(**4b**, **4c**).

Two quasi-reversible reduction and three irreversible oxidation peaks were detected for all three compounds. All compounds show somewhat higher oxidation potentials as compared to its carbon analogue **V** which might be due to the presence of the electron-deficient pyridine ring. Interestingly, compound **4a** with pyridinic nitrogen in *para*-orientation to the "TPA"-nitrogen is oxidized at slightly increased potential as compared to non-symmetric compounds **4b** and **4c**.

We further performed DFT calculations to analyze the impact of N-doping on the frontier molecular orbitals (FMOs). Visualization of the electron density distribution in the HOMO und LUMO of compounds **4a–c**, in comparison to **V**, is shown in Figure 9. Compounds **4a–b** display similar HOMO and LUMO

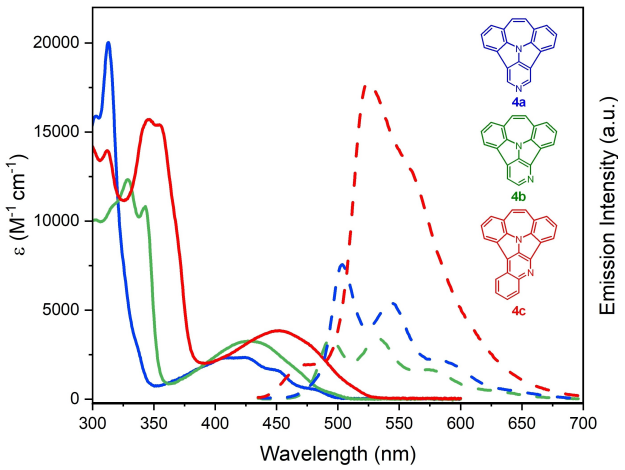


Figure 7. UV-vis absorption (solid line) and emission (dashed line, λ_{ex} = 420 nm) spectra in CH_2Cl_2 ($c = 10^{-5}$ M) at 20 °C.

Table 1. Comparison of signals for protons on the ethylene bridge with calculated NICS(1.7)$_{\pi ZZ}$ values.

Compound	Chemical Shift [ppm] for ethylene bridge protons		Calculated NICS(1.7)$_{\pi ZZ}$ value of the seven membered ring
	in $CDCl_3$	in CD_2Cl_2	
4a	5.76	5.97	+11
4b	5.92	6.12	+8
4c	5.80	6.11	+8
V	5.86	5.89	+14

Table 2. UV-vis and photoluminescence data of compounds **4** and **V** in CH_2Cl_2.

	V	4a	4b	4c
$\lambda_{1,abs}$ (nm)	–	303	329[c]	345[c]
$\varepsilon_{\lambda,1}$ (M^{-1}cm^{-1})	–	15893	12308	15702
$\lambda_{2,abs}$ (nm)	–	313	343	347[c]
$\varepsilon_{\lambda,2}$ (M^{-1}cm^{-1})	–	20037	10830	15685
$\lambda_{3,abs}$ (nm)	414[a]	424	426	452
$\varepsilon_{\lambda,3}$ (M^{-1}cm^{-1})	3100	2348	3247	3849
$\lambda_{1,em}^{420}$ (nm)	514[b]	494	504	525
$\lambda_{2,em}^{420}$ (nm)	556[b]	532	543	562
$\lambda_{2,em}^{420}$ (nm)	602[b]	573	592	–
Φ[d]	<0.02	0.02	0.03	0.09
$E_g^{(opt)}$ Optical band gap [eV][e]	2.39	2.68	2.66	2.63

[a] maximum absorption wavelength. [b] excitation wavelength not known. [c] shoulder in the spectrum. [d] fluorescence standard: coumarine 153 in ethanol (Φ = 0.38).[28] [e] determined from the intersection of the normalized absorption and emission spectrum.

© 2024 The Author(s). Chemistry - A European Journal published by Wiley-VCH GmbH

15213765, 2024, 69, Downloaded from https://chemistry-europe.onlinelibrary.wiley.com/doi/10.1002/chem.202403004 by University Rostock Universitatsbibliothek, Wiley Online Library on [10/08/2025]. See the Terms and Conditions (https://onlinelibrary.wiley.com/terms-and-conditions) on Wiley Online Library for rules of use; OA articles are governed by the applicable Creative Commons License

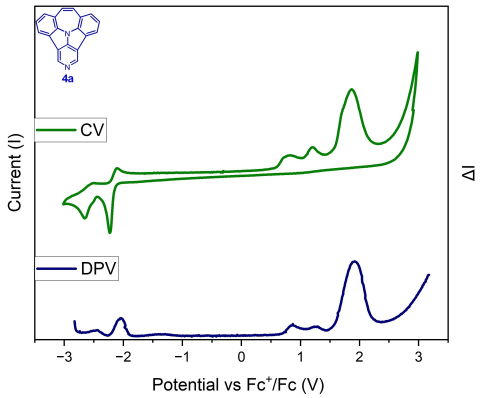


Figure 8. Cyclic voltammogram (CV) showing in green and differential pulse voltammetry (DPV) measurement in blue of **4a**. Measured in acetonitrile with 0.25 M *n*-Bu_4NPF_6 as supporting electrolyte, glassy carbon working electrode, and Pt counter electrode with ferrocene as standard at a scan rate of 200 mV/s.

distribution to **V** with nodes at the α-positions of the pyridine rings in the HOMO and a nodal plane bisecting the long molecular axis in the LUMO. Compared to **V** and **4a**, slightly increased electron density distribution and larger orbital coefficients are seen in the HOMO and LUMO for non-symmetric compound **4b**, while the HOMO and LUMO of **4c** is nearly fully distributed across the entire molecule. Incorporation of the pyridine ring into the scaffold leads to a stabilization of both the HOMO and LUMO energy levels with a slightly stronger effect on the HOMO. This results in a slightly larger HOMO-LUMO gap of about 0.1 eV for **4a** and **4b**. Upon π-extension, the HOMO energy remains unchanged relative to **4a**–**b**, while the LUMO is further slightly stabilized, which lowers the band gap by 0.1 eV as compared to reference compound **V**.

Conclusions

Hitherto unknown diazabenzoazulenofluorenes have been prepared by a newly developed one-pot two step synthetic procedure consisting of a Pd-catalyzed Buchwald-Hartwig reaction of dibenzoazepine and trihalogenated pyridines and quinoline followed by intramolecular CH-arylation. Three different isomers were synthesized with good overall yield. The optical-, electrochemical and structural properties of these bridged, N-doped and π-expanded TPAs have been studied. It has been disclosed that N-doping leads to bowl shaped structural alignment in the crystal state, stabilized FMO energies and higher oxidation potentials as well as improved fluorescence quantum yields as compared to its carbon analog **V**. Moreover, non-symmetric, N-doped compounds **4b** and **4c** possess increased bowl depths in the crystal state despite its doping at the edge of the molecular scaffold. The obtained results highlight the importance of selective N-doping to fine-tune the optoelectronic properties of PAHs.

Experimental Data

3,5-Dichloro-4-iodopyridine (1a)

According to general procedure as described in SI, product **1a** was isolated as yellow solid (1.42 g, 5.18 mmol, 77%); mp (147–148 °C), R_f = 0.24 (heptane: ethyl acetate, 20:1, v/v). **^{1}H NMR** (300 MHz, $CDCl_3$) δ = 8.38 (s, 2H). **^{13}C NMR** (75 MHz, $CDCl_3$) δ = 145.6 (CH), 138.3, 114.6 (C). **IR** (ATR, cm^{-1}): $\tilde{\nu}$ = 3083 (w), 3042 (w), 2957 (w), 2926 (w), 2862 (w), 1801 (w), 1535 (m), 1515 (m), 1506 (m), 1395 (m), 1383 (s), 1193 (s), 1175 (m), 1115 (m). **MS** (GC-MS, EI, 70 eV): m/z (%) = 273 (100, M^+), 148 (26), 146 (40), 127 (21), 121 (16), 119 (25), 112 (7), 110 (21), 86 (15), 84 (42), 75 (7). **HRMS** (ESI-TOF): calcd. for $C_5H_3Cl_2IN$ ($[M+H]^+$) 273.8687, found for $C_5H_3Cl_2IN$ ($[M+H]^+$) 273.8687.

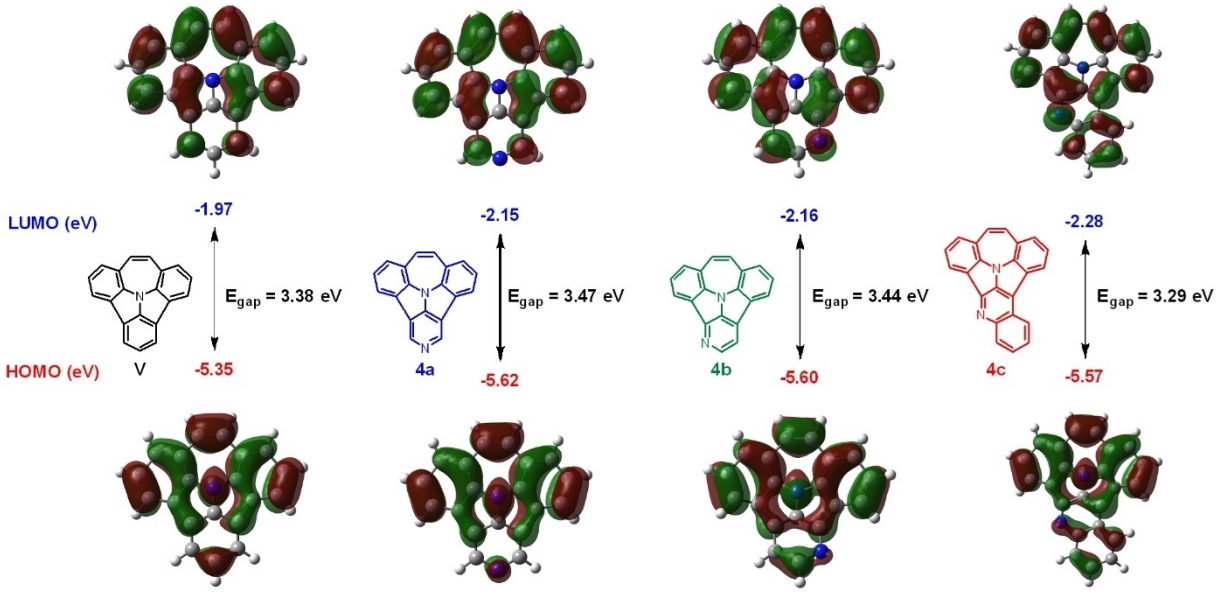


Figure 9. Frontier molecular orbitals and energy levels calculated at the B3LYP–D3(BJ)/6-311G(d,p) level of theory (isovalue = 0.02 au).

© 2024 The Author(s). Chemistry - A European Journal published by Wiley-VCH GmbH

15213765, 2024, 69, Downloaded from https://chemistry-europe.onlinelibrary.wiley.com/doi/10.1002/chem.202403004 by University Rostock Universitatsbibliothek, Wiley Online Library on [10/08/2025]. See the Terms and Conditions (https://onlinelibrary.wiley.com/terms-and-conditions) on Wiley Online Library for rules of use; OA articles are governed by the applicable Creative Commons License

15213765, 2024, 69, Downloaded from https://chemistry-europe.onlinelibrary.wiley.com/doi/10.1002/chem.202403004 by University Rostock Universitatsbibliothek, Wiley Online Library on [10/08/2025]. See the Terms and Conditions (https://onlinelibrary.wiley.com/terms-and-conditions) on Wiley Online Library for rules of use; OA articles are governed by the applicable Creative Commons License

2,4-Dichloro-3-iodopyridine (1 b)

According to general procedure as described in SI, product **1 b** was isolated as yellow solid (1.64 g, 5.99 mmol, 88%); mp (90–91 °C), R_f = 0.22 (heptane: ethyl acetate, 20:1, v/v). **^{1}H NMR** (300 MHz, $CDCl_3$) δ = 8.21 (d, $^3J_{H,H}$ = 5.1 Hz, 1H), 7.28 (d, $^3J_{H,H}$ = 5.1 Hz, 1H). **^{13}C NMR** (75 MHz, $CDCl_3$) δ = 156.9, 151.2 (C), 148.6, 122.9 (CH), 100.7 (C). **IR** (ATR, cm^{-1}): $\tilde{\nu}$ = 3095 (m), 3089 (m), 3060 (m), 3025 (m), 1543 (s), 1523 (m), 1418 (s), 1337 (vs), 1197 (s), 1006 (s). **MS** (GC-MS, EI, 70 eV): m/z (%) = 273 (100, M^+), 238 (10), 148 (27), 146 (41), 127 (57), 119 (7), 112 (10), 111 (10), 110 (30), 86 (11), 85 (18), 84 (27), 76 (15), 75 (21), 50 (12), 49 (17). **HRMS** (ESI-TOF): calcd. for $C_5H_3Cl_2IN$ ($[M+H]^+$) 273.8609, found for $C_5H_3Cl_2IN$ ($[M+H]^+$) 273.8691.

3-Bromo-2,4-dichloroquinolin (1 c)

According to general procedure as described in SI, product **1 c** was isolated as colorless solid (1.52 g, 5.9 mmol, 88%); mp (95–97 °C). **^{1}H NMR** (250 MHz, $CDCl_3$) δ = 8.20 (dd, $^3J_{H,H}$ = 8.4 Hz, $^4J_{H,H}$ = 2.0 Hz, 1H), 8.02 (dd, $^3J_{H,H}$ = 8.4 Hz, $^4J_{H,H}$ = 1.9 Hz, 1H), 7.80 (ddd, $^3J_{H,H}$ = 8.4 Hz, $^3J_{H,H}$ = 7.0 Hz, $^4J_{H,H}$ = 1.4 Hz, 1H), 7.67 (ddd, $^3J_{H,H}$ = 8.4 Hz, $^3J_{H,H}$ = 7.0 Hz, $^4J_{H,H}$ = 1.2 Hz, 1H). **^{13}C NMR** (126 MHz, $CDCl_3$) δ = 149.9, 145.8 (C), 131.4, 129.0 (CH), 129.0 (C), 128.7 (CH), 126.2 (C), 124.8 (CH), 118.3 (C). **IR** (ATR, cm^{-1}): $\tilde{\nu}$ = 1541 (m),1480 (m), 1352 (m), 1282 (m), 1183 (s), 884 (m), 841 (m), 760 (vs), 744 (s), 608 (m), 441 (m). **MS** (GC-MS, EI, 70 eV): m/z (%) = 277 (100, M^+), 275 (65), 242 (22), 240 (17), 163 (11), 161 (32), 99 (13). **HRMS** (EI): calcd. for $C_9H_4BrCl_2N$ (M^+) 274.8899, found for 274.8898; $C_9H_4BrCl^{37}ClN$ (M+) 276.8869, found for 276.8865; $C_9H_4Br^{37}Cl_2N$ (M^+) 278.8840, found for 278.8841; $C_9H_4{}^{81}BrCl^{37}ClN$ (M^+) 278.8849, found for 278.8841.

General Procedure for the Synthesis of pyridinyl-*H*-dibenzo[*b,f*]azepines (2 and 3): In an argon flushed pressure tube was placed 200 mg (0.73 mmol) **1**, 6.8 mg (0.03 mmol) $Pd(OAc)_2$, 17.6 mg (0.06 mmol) $P(^tBu)_3 \cdot HBF_4$, 118 mg (0.61 mmol) 5*H*-Dibenzo[*b,f*]azepine and 175 mg (1.83 mmol) ^{t}BuONa. To this mixture were added 4 ml of dry toluene or dioxane. The reaction was warmed to 100 °C in a stainless-steel heating block and stirred for 24 h. Afterwards, the reaction mixture was quenched with water and extracted with ethyl acetate (3×30 ml). The collected organic phases were washed with brine and dried over sodium sulfate. The product was purified by flash column chromatography on silica gel.

11-Chlorobenzo[6,7]azepino[3,2,1-*hi*]pyrido[4,3-*b*]indole (3 a)

According to the general procedure, product **3 a** was isolated as yellow solid (92.9 mg, 0.307 mmol, 42% with toluene as solvent and 106.1 mg, 0.350 mmol, 48% with dioxane as solvent); mp (176–177 °C), R_f = 0.20 (heptane: ethyl acetate, 5:1, v/v). **^{1}H NMR** (300 MHz, $CDCl_3$) δ = 9.12 (s, 1H), 8.55 (s, 1H), 7.79 (dd, $^3J_{H,H}$ = 7.8 Hz, $^4J_{H,H}$ = 1.1 Hz, 1H), 7.29–7.05 (m, 5H), 6.67–6.48 (m, 3H). **^{13}C NMR** (75 MHz, $CDCl_3$) δ = 150.1 (C), 146.2 (CH), 143.6 (C), 141.0 (CH), 137.7 (C), 132.1, 131.2 (CH), 131.2 (C), 130.7, 129.3, 128.0 (CH), 126.8 (C), 126.0 (CH), 125.9 (C), 124.6, 124.5 (CH), 124.1 (C), 119.3 (CH), 118.3 (C). **IR** (ATR, cm^{-1}): $\tilde{\nu}$ = 3066 (w), 2961 (w), 2922 (w), 2856 (w), 1482 (m), 1368 (s), 1243 (m), 1201 (s). **MS** (GC-MS, EI, 70 eV): m/z (%) = 302 (100, M^+), 267 (16), 266 (24), 265 (12), 240 (10), 239 (15), 238 (13), 133 (10), 119 (27), 106 (8). **HRMS** (ESI-TOF): calcd. for $C_{19}H_{12}ClN_2$ ($[M+H]^+$) 303.0684, found for $C_{19}H_{12}ClN_2$ ($[M+H]^+$) 303.0687.

5-(2,4-Dichloropyridin-3-yl)-5*H*-dibenzo[*b,f*]azepine (2 b)

According to the general procedure, product **2 b** was isolated as yellow solid (23.5 mg, 0.069 mmol, 19% with toluene as solvent and 22.3 mg, 0.066 mmol, 18% with dioxane as solvent); mp (127–128 °C), R_f = 0.19 (heptane: ethyl acetate, 5:1, v/v). **^{1}H NMR** (300 MHz, $CDCl_3$) δ = 8.25 (d, $^3J_{H,H}$ = 5.2 Hz, 1H), 7.46 (d, $^3J_{H,H}$ = 5.2 Hz, 1H), 7.10 (dt, $^3J_{H,H}$ = 8.2 Hz, $^3J_{H,H}$ = 0.9 Hz, 2H), 7.00 (ddd, $^3J_{H,H}$ = 8.2 Hz, $^4J_{H,H}$ = 5.1 Hz, $^5J_{H,H}$ = 3.8 Hz, 2H), 6.95–6.88 (m, 4H). **^{13}C NMR** (75 MHz, $CDCl_3$) δ 157.0, 150.0, 147.6 (C), 147.3 (CH), 141.3, 133.5 (C), 132.5, 131.6, 129.0, 125.3, 124.7, 123.5 (CH). **IR** (ATR, cm^{-1}): $\tilde{\nu}$ = 3052 (w), 3027 (w), 2953 (w), 2922 (m), 2852 (w), 1543 (m), 1488 (m), 1366 (s), 1183 (s), 1109 (s). **MS** (GC-MS, EI, 70 eV): m/z (%) = 338 (100, M^+), 305 (10), 304 (10), 303 (31), 302 (14), 301 (8), 268 (19), 267 (16), 266 (17), 193 (10), 192 (64), 191 (30), 190 (20), 178 (30), 165 (25), 152 (10), 151 (11), 133 (12), 120 (10). **HRMS** (ESI-TOF): calcd. for $C_{19}H_{13}Cl_2N_2$ ($[M+H]^+$) 339.0456, found for $C_{19}H_{13}Cl_2N_2$ ($[M+H]^+$) 339.0452.

5-(2,4-Dichloroquinolin-3-yl)-5*H*-dibenzo[*b,f*]azepine (2 c)

According to general procedure, product **2 c** was isolated as yellow solid (14.1 mg, 0.036 mmol, 5% with dioxane as solvent); mp (236–238 °C), R_f = 0.11 (heptane: ethyl acetate, 15:1, v/v). **^{1}H NMR** (300 MHz, $CDCl_3$) δ = 8.29 (ddd, $^3J_{H,H}$ = 8.4 Hz, $^4J_{H,H}$ = 1.5 Hz, $^5J_{H,H}$ = 0.6 Hz, 1H), 8.07 (ddd, $^3J_{H,H}$ = 8.4 Hz, $^4J_{H,H}$ = 1.3 Hz, $^5J_{H,H}$ = 0.6 Hz, 1H), 7.80 (ddd, $^3J_{H,H}$ = 8.4 Hz, $^3J_{H,H}$ = 6.9 Hz, $^4J_{H,H}$ = 1.4 Hz, 1H), 7.68 (ddd, $^3J_{H,H}$ = 8.3 Hz, $^4J_{H,H}$ = 7.0 Hz, $^4J_{H,H}$ = 1.3 Hz, 1H), 7.08 (dt, $^3J_{H,H}$ = 8.0 Hz, $^4J_{H,H}$ = 1.0 Hz, 2H), 6.98–6.85 (m, 6H), 6.31 (s, 2H). **^{13}C NMR** (75 MHz, $CDCl_3$) δ = 154.6, 148.3, 148.0, 145.8, 138.0, 133.4 (C), 132.7 (2 C), 131.9 (2 C), 131.7, 129.1 (2 C), 128.9, 128.4 (CH), 126.8 (C), 125.5, 124.6 (2 C), 123.6 (2 C). **IR** (ATR, cm^{-1}): $\tilde{\nu}$ = 1484 (m), 1473 (m), 1339 (m), 1282 (m). **MS** (EI, 70 eV): m/z = 388 (100, M^+), 353 (50), 318 (43), 317 (44), 316 (37), 315 (13), 192 (47), 191 (38), 178 (23), 177 (14), 176 (16), 165 (32), 164 (12), 163 (14), 161 (15), 158 (17), 145 (13). **HRMS** (ESI-TOF) m/z: [M^+] calcd. for $C_{23}H_{14}Cl_2N_2$ ($[M+H]^+$) 389.05286, found for $C_{23}H_{14}Cl_2N_2$ ($[M+H]^+$) 389.05258, calcd. for $C_{23}H_{14}Cl^{37}ClN_2$ ($[M+H]^+$) 391.0499, found for $C_{23}H_{14}Cl^{37}ClN_2$ ($[M+H]^+$) 391.0497, calcd. for $C_{23}H_{15}{}^{37}Cl_2N_2$ ($[M+H]^+$) 393.0470, found for $C_{23}H_{15}{}^{37}Cl_2N_2$ ($[M+H]^+$) 393.0482.

15-Chlorobenzo[6′,7′]azepino[3′,2′,1′:7,1]indolo[2,3-*c*]quinoline (3 c)

According to general procedure, product **3 c** was isolated as yellow solid (76.4 mg, 0.217 mmol, 30% with toluene as solvent, 101.9 mg, 0.289 mmol, 40% with dioxane as solvent); mp (220–221 °C), R_f = 0.16 (heptane: ethyl acetate, 15:1, v/v). **^{1}H NMR** (300 MHz, $CDCl_3$) δ = 8.64–8.57 (m, 1H), 8.25–8.18 (m, 2H), 7.78–7.71 (m, 2H), 7.35 (dd, $^3J_{H,H}$ = 8.0 Hz, $^3J_{H,H}$ = 7.4 Hz, 1H), 7.26–7.10 (m, 4H), 6.76–6.70 (m, 1H), 6.66–6.57 (m, 2H). **^{13}C NMR** (75 MHz, $CDCl_3$) δ = 151.6, 144.3, 140.0, 139.1, 132.6 (C), 132.4, 131.6 (CH), 131.2, 131.0 (C), 130.7, 129.7, 129.5 (CH), 128.2 (C), 128.1, 127.7, 127.6, 125.9 (CH), 125.6 (C), 125.3, 124.7 (CH), 123.7 (C), 123.3, 121.8 (CH). **IR** (ATR, cm^{-1}): $\tilde{\nu}$ = 1504 (m), 1492 (m), 1352 (s), 1317 (m), 1280 (m), 1135 (s), 1080 (s). **MS** (GC-MS, EI, 70 eV): m/z (%) = 352 (100, M^+), 317 (16), 316 (36), 315 (27), 314 (12), 288 (12), 176 (10), 158 (17), 132 (11). **HRMS** (EI): calcd. for $C_{23}H_{13}ClN_2$ [M^+] 352.0762, found for $C_{23}H_{13}ClN_2$ [M^+] 352.0757.

15-Chlorobenzo[6′,7′]azepino[3′,2′,1′:7,1]indolo[3,2-*b*]quinoline (3 c′)

According to general procedure, product **3 c′** was isolated as yellow solid (20.4 mg, 0.058 mmol, 8% with dioxane as solvent); mp (222–225 °C), R_f = 0.15 (heptane: ethyl acetate, 15:1, v/v). **^{1}H NMR** (300 MHz, $CDCl_3$) δ = 8.37 (dd, $^3J_{H,H}$ = 8.4 Hz, $^4J_{H,H}$ = 1.5 Hz, 1H), 8.30 (d, $^3J_{H,H}$ = 8.5 Hz, 1H), 8.17 (dd, $^3J_{H,H}$ = 7.7 Hz, $^4J_{H,H}$ = 1.3 Hz, 1H), 7.78 (ddd, $^3J_{H,H}$ = 8.4 Hz, $^3J_{H,H}$ = 6.8 Hz, $^4J_{H,H}$ = 1.5 Hz, 1H), 7.67 (ddd, $^3J_{H,H}$ = 8.3 Hz, $^3J_{H,H}$ = 6.8 Hz, $^4J_{H,H}$ = 1.3 Hz, 1H), 7.30 (pt, $^3J_{H,H}$ = 7.5 Hz, 1H), 7.23–7.06 (m, 4H), 6.75–6.69 (m, 1H), 6.65–6.56 (m, 2H).**^{13}C NMR** (75 MHz, $CDCl_3$) δ = 154.2, 150.4, 146.4, 139.6 (C), 132.7 (CH), 132.5,

© 2024 The Author(s). Chemistry - A European Journal published by Wiley-VCH GmbH

131.2 (C), 130.9, 130.7, 130.4, 129.5, 129.2, 128.5 (CH), 127.1 (C), 126.8 (CH), 126.2, 126.1 (C), 125.3 (CH), 125.1 (C), 124.6, 123.5, 123.2, 120.9 (CH). **IR** (ATR, cm^{-1}): $\tilde{\nu}$ = 1492 (m), 1374 (m), 1323 (m), 1201 (m), 1189 (m), 1137 (m). **MS** (GC-MS, EI, 70 eV): m/z (%) = 352 (100, M^+), 317 (20), 316 (34), 315 (14), 314 (11), 176 (12), 158 (11). **HRMS** (EI): calcd. for $C_{23}H_{13}ClN_2$ [M^+] 352.0762, found for $C_{23}H_{13}ClN_2$ [M^+] 352.0763.

General Procedure for the Synthesis of Diazabenzoazulenofluorenes (4)

In an argon filled pressure tube was placed 100 mg (0.376 mmol) **2** or **3**, 4.2 mg (0.0187 mmol) $Pd(OAc)_2$, 13.8 mg (0.0375 mmol) $P(Cy)_3 \cdot HBF_4$, and 1 ml of 1,8-Diazabicyclo(5.4.0)undec-7-ene (DBU) solved in 4 ml of DMA. The reaction was stirred in a stainless-steel heating block at 150 °C for 24 h. After cooling to room temperature, the reaction was quenched with water and extracted with ethyl acetate (3×30 ml). The collected organic phase was washed with brine and dried over sodium sulfate. The product was purified by flash column chromatography on silica gel.

General Procedure for the Two-Step Synthesis of Diazabenzoazulenofluorenes (4)

1 (200.0 mg, 0.722 mmol, 1.0 eq), 5*H*-dibenzoazepine (153.5 mg, 0.794 mmol, 1.1 eq), ^{t}BuONa (208.2 mg, 2.167 mmol, 3 eq), $Pd(OAc)_2$ (8.1 mg, 0.036 mmol, 0.05 eq), $P^tBu \cdot HBF_4$ (21 mg, 0.072 mmol, 0.1 eq) were added to an oven-dried and argon flushed pressure tube equipped with magnetic stir bar, following by dry dioxane (6 ml). The mixture was purged with argon and stirred in a stainless-steel heating block at 100 °C for 24 h. After the mixture was cooled to room temperature, the solvent was removed under vacuum, and the crude was dissolved in 4 ml DMA. $Pd(OAc)_2$ (16.1 mg, 0.072 mmol, 0.1 eq) and $PCy_3 \cdot HBF_4$ (53.1 mg, 0.144 mmol, 0.2 eq) were added to the argon flushed pressure tube, followed by DBU (2 ml). The reaction mixture was again purged with argon and stirred in a stainless-steel heating block at 150 °C for 24 h. After the mixture was cooled to room temperature, the reaction was quenched with distilled water and extracted with DCM (3 times). The organic phase was dried over Na_2SO_4, concentrated in vacuum, and purified by silica gel column chromatography (heptane/ethyl acetate v/v 3:1).

3a2,5-Diazabenzo[3,4]azuleno[2,1,8,7-*jklm*]fluorene (4a)

According to general procedure, product **4a** was isolated as yellow solid (79.2 mg, 0.297 mmol, 90%); mp (187–189 °C), R_f = 0.31 (ethyl acetate). **^{1}H NMR** (300 MHz, $CDCl_3$) δ = 8.92 (s, 2H), 7.46 (dd, $^3J_{H,H}$ = 7.9 Hz, $^4J_{H,H}$ = 0.8 Hz, 2H), 6.81 (pt, $^3J_{H,H}$ = 7.7 Hz, 2H), 6.62 (dd, $^3J_{H,H}$ = 7.5 Hz, $^4J_{H,H}$ = 0.8 Hz, 2H), 5.76 (s, 2H). **^{13}C NMR** (75 MHz, $CDCl_3$) δ = 146.5, 141.1 (C), 139.9, 129.1, 127.2 (CH), 127.0, 125.5 (C), 124.7, 124.2 (CH), 117.5 (C). **IR** (ATR, cm^{-1}): $\tilde{\nu}$ = 3033 (w), 2922 (w), 2852 (w), 1599 (w), 1562 (m), 1482 (m), 1459 (m), 1216 (m), 1170 (m). **MS** (GC-MS, EI, 70 eV): m/z (%) = 266 (100, M^+), 265 (9), 264 (18), 133 (8), 119 (12). **HRMS** (ESI-TOF): calcd. for $C_{19}H_{11}N_2$ ([M + H]$^+$) 267.0922, found for $C_{19}H_{11}N_2$ ([M + H]$^+$) 267.0926.

3a2,4-Diazabenzo[3,4]azuleno[2,1,8,7-*jklm*]fluorene (4b)

According to general procedure, product **4b** was isolated as yellow solid (62.0 mg, 0.233 mmol, 79%); mp (153–154 °C), R_f = 0.43 (ethyl acetate). **^{1}H NMR** (300 MHz, $CDCl_3$) δ = 8.68 (s, 1H), 7.71 (dd, $^3J_{H,H}$ = 8.0 Hz, $^4J_{H,H}$ = 0.9 Hz, 1H), 7.54–7.42 (m, 2H), 6.89 (pt, $^3J_{H,H}$ = 7.7 Hz, 1H), 6.81 (pt, $^3J_{H,H}$ = 7.7 Hz, 1H), 6.70 (ddd, $^3J_{H,H}$ = 7.5 Hz, $^4J_{H,H}$ = 2.0 Hz, $^5J_{H,H}$ = 0.8 Hz, 2H), 5.92 (dd, $^3J_{H,H}$ = 12.0 Hz, $^4J_{H,H}$ = 1.0 Hz, 2H). **^{13}C NMR** (75 MHz, $CDCl_3$) δ = 146.0 (CH), 143.9, 143.8, 143.7, 129.6 (C), 129.2 (CH), 129.1, 128.5, 128.2 (C), 128.0 (CH), 127.7, 126.2, 125.7 (C), 125.2, 124.4, 124.1, 123.9, 114.2 (CH). **IR** (ATR, cm^{-1}): $\tilde{\nu}$ = 3054 (w), 3021 (w), 2924 (w), 2852 (w), 1630 (m), 1480 (m), 1436 (m), 1403 (m), 1315 (m), 1164, (m). **MS** (GC-MS, EI, 70 eV): m/z (%) = 266 (100, M^+), 265 (9), 264 (19), 133 (13), 119 (19). **HRMS** (ESI-TOF): calcd. for $C_{19}H_{11}N_2$ ([M + H]$^+$) 267.0922, found for $C_{19}H_{11}N_2$ ([M + H]$^+$) 267.0923.

3a2,8-Diazabenzo[*b*]benzo[3,4]azuleno[7,8,1,2-*jklm*]fluorene (4c)

According to general procedure, product **4c** was isolated as yellow solid (62.6 mg, 0.198 mmol, 77%); mp (168–170 °C), R_f = 0.31 (heptane: ethyl acetate, 3:1, v/v). **^{1}H NMR** (300 MHz, $CDCl_3$) δ = 8.46–8.37 (m, 1H), 8.18 (dd, $^3J_{H,H}$ = 7.8 Hz, $^4J_{H,H}$ = 1.8 Hz, 1H), 7.76 (dd, $^3J_{H,H}$ = 7.9 Hz, $^4J_{H,H}$ = 0.9 Hz, 1H), 7.69 (ddd, $^3J_{H,H}$ = 8.5 Hz, $^3J_{H,H}$ = 6.9 Hz, $^4J_{H,H}$ = 1.8 Hz, 1H), 7.63 (ddd, $^3J_{H,H}$ = 8.3 Hz, $^3J_{H,H}$ = 6.9 Hz, $^4J_{H,H}$ = 1.5 Hz, 1H), 7.55 (d, $^3J_{H,H}$ = 8.0 Hz, 1H), 6.86 (pt, $^3J_{H,H}$ = 7.7 Hz, 1H), 6.79–6.67 (m, 2H), 6.53 (d, $^3J_{H,H}$ = 7.4 Hz, 1H), 5.80 (pt, $^3J_{H,H}$ = 12.6 Hz, 2H). **^{13}C NMR** (75 MHz, $CDCl_3$) δ = 149.2, 146.8, 145.7, 143.1, 137.9 (C), 131.4, 129.8, 129.0 (CH), 129.0, 128.9 (C), 127.0, 126.5, 126.4, 126.3 (CH), 125.8 (C), 125.2, 124.9 (CH), 124.7 (C), 124.6, 124.5 (CH), 124.2, 121.5 (C). **IR** (ATR, cm^{-1}): $\tilde{\nu}$ = 1465 (w), 1449 (m), 1434 (m), 1385 (m), 1366 (m), 1352 (w), 1339 (m). **MS** (GC-MS, EI, 70 eV): m/z (%) = 316 (100, M^+), 314 (14), 289 (4), 288 (4), 158 (13), 144 (11). **HRMS** (ESI-TOF): calcd. for $C_{23}H_{13}N_2$ ([M + H]$^+$) 317.1078, found for $C_{23}H_{13}N_2$ ([M + H]$^+$) 317.1075.

Accession Codes

CCDCs 2364941(**3a**), 2367226 (**2b**) 2364943 (**3c**), 2145722 (**V**), 2364918 (**4a**), 2364919 (**4b**), 2364942 (**4c**), 2128847 (**VI**), contain the supplementary crystallographic data for this paper. These data can be obtained free of charge from the Cambridge Crystallographic Data Centre via. http://www.ccdc.cam.ac.uk/data_request/cif

Acknowledgements

This work has been supported by the RoHan Project funded by the German Academic Exchange Service (DAAD, No. 57315854 and 57560571) and the Federal Ministry for Economic Cooperation and Development (BMZ) inside the framework "SDG Bilateral Graduate school programme. Additional financial support by the federal state of Mecklenburg-Western Pomerania is gratefully acknowledged. Open Access funding enabled and organized by Projekt DEAL.

Conflict of Interests

The authors declare no conflict of interest.

© 2024 The Author(s). Chemistry - A European Journal published by Wiley-VCH GmbH

15213765, 2024, 69, Downloaded from https://chemistry-europe.onlinelibrary.wiley.com/doi/10.1002/chem.202403004 by University Rostock Universitatsbibliothek, Wiley Online Library on [10/08/2025]. See the Terms and Conditions (https://onlinelibrary.wiley.com/terms-and-conditions) on Wiley Online Library for rules of use; OA articles are governed by the applicable Creative Commons License

Data Availability Statement

The data which support the findings of this study are available in the supplementary material of this article.

Keywords: Bowl-shaped compounds · Bridged triarylamine · CH-activation · Dibenzoazepine · N-doping · N-heterocycles

[1] a) M. Stępień, E. Gońka, M. Żyła, N. Sprutta, *Chem. Rev.* **2017**, *117*, 3479; b) A. Borissov, Y. K. Maurya, L. Moshniaha, W.-S. Wong, M. Żyła-Karwowska, M. Stępień, *Chem. Rev.* **2022**, *122*, 565; c) X.-Y. Wang, X. Yao, A. Narita, K. Müllen, *Acc. Chem. Res.* **2019**, *52*, 2491.
[2] a) O. Nuyken, S. Jungermann, V. Wiederhirn, E. Bacher, K. Meerholz, *Monatsh. Chem.* **2006**, *137*, 811; b) C.-S. Hsu, *Angew. Chem. Int. Ed.* **2006**, *45*, 7115.
[3] A. Kumar, G. Singh, *J. Mol. Liq.* **2023**, *386*, 122607.
[4] G. Hong, S. Diao, A. L. Antaris, H. Dai, *Chem. Rev.* **2015**, *115*, 10816.
[5] a) J. Xin, W. Li, Y. Zhang, Q. Liang, C. Song, Y. Zhao, Z. He, J. Liu, W. Ma, *Battery Energy* **2023**, *2*, 20220040; b) H. Gao, Y. Sun, L. Meng, C. Han, X. Wan, Y. Chen, *Small* **2023**, *19*, e2205594.
[6] Y. Zhao, W. Wang, Z. He, B. Peng, C.-A. Di, H. Li, *Chin. Chem. Lett.* **2023**, *34*, 108094.
[7] R. Ionescu, Y. Broza, H. Shaltieli, D. Sadeh, Y. Zilberman, X. Feng, L. Glass-Marmor, I. Lejbkowicz, K. Müllen, A. Miller, et al., *ACS Chem. Neurosci.* **2011**, *2*, 687.
[8] a) A. Iwan, D. Sek, *Prog. Polym. Sci.* **2011**, *36*, 1277; b) S. Jhulki, J. N. Moorthy, *J. Mater. Chem. C* **2018**, *6*, 8280; c) S. Shahnawaz, S. Sudheendran Swayamprabha, M. R. Nagar, R. A. K. Yadav, S. Gull, D. K. Dubey, J.-H. Jou, *J. Mater. Chem. C* **2019**, *7*, 7144; d) Y. Tao, C. Yang, J. Qin, *Chem. Soc. Rev.* **2011**, *40*, 2943; e) J. Urieta-Mora, I. García-Benito, A. Molina-Ontoria, N. Martín, *Chem. Soc. Rev.* **2018**, *47*, 8541.
[9] A. N. Sobolev, V. K. Belsky, I. P. Romm, N. Y. Chernikova, E. N. Guryanova, *Acta. Cryst. C* **1985**, *41*, 967.
[10] S. Wang, F. Wang, *J. Mol. Graphics Modell.* **2023**, *125*, 108604.
[11] K. Mainali, S. H. Mood, M. R. Pelaez-Samaniego, V. Sierra-Jimenez, M. Garcia-Perez, *Catal. Today* **2023**, *423*, 114248.
[12] H. G. Dunlop, S. H. Tucker, *J. Chem. Soc.* **1939**, 1945.
[13] D. Hellwinkel, M. Melan, *Chem. Ber.* **1974**, *107*, 616.
[14] a) E. Hamzehpoor, D. F. Perepichka, *Angew. Chem. Int. Ed.* **2020**, *59*, 9977; b) N. Hammer, T. A. Schaub, U. Meinhardt, M. Kivala, *Chem. Rec.* **2015**, *15*, 1119.
[15] M. Kuratsu, M. Kozaki, K. Okada, *Angew. Chem. Int. Ed.* **2005**, *44*, 4056.
[16] T. Kader, B. Stöger, J. Fröhlich, P. Kautny, *Chem. – Eur. J.* **2019**, *25*, 4412.
[17] I. Michalsky, V. Gensch, C. Walla, M. Hoffmann, F. Rominger, T. Oeser, P. Tegeder, A. Dreuw, M. Kivala, *Chem. – Eur. J.* **2022**, *28*, e202200326.
[18] J. Wagner, P. Zimmermann Crocomo, M. A. Kochman, A. Kubas, P. Data, M. Lindner, *Angew. Chem. Int. Ed.* **2022**, *61*, e202202232.
[19] E. Marzi, A. Bigi, M. Schlosser, *Eur. J. Org. Chem.* **2001**, *2001*, 1371.
[20] a) R. Hardman, M. W. Partridge, *J. Chem. Soc.* **1955**, 510–513; b) R. Hardman, M. W. Partridge, *J. Chem. Soc.* **1958**, 614–619.
[21] I. A. Stepek, K. Itami, *ACS Mater. Lett.* **2020**, *2*, 951.
[22] R. C. Haddon, *J. Am. Chem. Soc.* **1986**, *108*, 2837–2842.
[23] I. Fernandez, *Aromaticity*, Elsevier Amsterdam **2021**.
[24] D. Geuenich, K. Hess, F. Köhler, R. Herges, *Chem. Rev.* **2005**, *105*, 3758.
[25] E. Paenurk, R. Gershoni-Poranne, *Phys. Chem. Chem. Phys.* **2022**, *24*, 8631.
[26] a) J. Juselius, D. Sundholm, J. Gauss, *J. Chem. Phys.* **2004**, *121*, 3952–3963; b) H. Fliegl, S. Taubert, O. Lehtonen, D. Sundholm, *Phys. Chem. Chem. Phys.* **2011**, *13*, 20500–20518.
[27] a) M. Karplus, *J. Chem. Phys.* **1959**, *30*(1), 11–15; b) M. Karplus, *J. Am. Chem. Soc.* **1963**, *85*(18), 2870–2871.
[28] A. M. Brouwer, *Pure Appl. Chem.* **2011**, *83*, 2213.

Manuscript received: August 9, 2024
Accepted manuscript online: September 30, 2024
Version of record online: November 5, 2024

© 2024 The Author(s). Chemistry - A European Journal published by Wiley-VCH GmbH

15213765, 2024, 69, Downloaded from https://chemistry-europe.onlinelibrary.wiley.com/doi/10.1002/chem.202403004 by University Rostock Universitätsbibliothek, Wiley Online Library on [10/08/2025]. See the Terms and Conditions (https://onlinelibrary.wiley.com/terms-and-conditions) on Wiley Online Library for rules of use; OA articles are governed by the applicable Creative Commons License

III. Publication

Check for updates

EurJOC
European Journal of Organic Chemistry

Research Article
doi.org/10.1002/ejoc.202401045

Chemistry Europe
European Chemical Societies Publishing

www.eurjoc.org

Synthesis and Properties of N,O-Doped Aceanthrylenes

Jan Radolko,[a] Ha Nam Do,[a] Peter Ehlers,[a] Alexander Villinger,[a] and Peter Langer*[a]

N,O-doped aceanthrylenes have been synthesized for the first time via a selective S_NAr reaction or Ullmann-coupling of phenols, followed by an intramolecular direct arylation. The reaction has been carefully optimized and permits the selective synthesis of N,O-doped aceanthrylenes in moderate to excellent yields and tolerate various functional groups. The aromatic behavior of the hitherto unknown heterocyclic scaffold has been further analyzed by NICS and NICS2BC calculations.

Introduction

Imidazo[1,2-*a*]pyridines[1] and imidazo[1,2-*a*]pyrazines[2] both have been proven to be versatile building blocks[3] and to encompass various applications[4] in the field of medicinal chemistry, due to their versatile biological activities and of natural product chemistry.[5] Especially imidazo[1,2–*a*]pyridines are known for a wide range of biological activities including antiviral,[6] antifungal,[7] anticancer,[8] antibacterial,[9] anti-inflammatory,[10] analgesic,[11] antituberculosis,[12] anti-epileptic,[13] anti-proliferative[14] and antitumor activities.[15] Imidazo[1,2–*a*]pyrazines[16] are particularly known for their bioluminescence properties, e.g. as new luciferin derivatives, and, hence, have potential in optoelectronic applications.[17] Likewise, they are also known for numerous biological activities, such as inhibitors of spleen tyrosine kinase,[18] aurora kinase[19] and act as an acid pump antagonist.[20] Benzannulated derivatives show strong DNA intercalating effects with potential antiproliferative and cytostatic properties.[21] Moreover, π-extended imidazopyridines and -pyrazines have shown promising optoelectronic properties such as strong photoluminescence[22] and electron mobility[23] (Figure 1).

Nowadays, direct arylation reactions have emerged as convenient synthetic strategy to adjust the biological or optoelectronic properties of polycyclic heteroaromatic compounds.[24] For example, the group of Gryko reported the functionalization of imidazopyridine by an intramolecular direct arylation in position 3, what led to fluorescent naphthyl functionalized imidazopyridines, which have been later planarized by a reductive intramolecular cyclization using elemental potassium.[25] Herein, we report a straightforward and efficient strategy for the selective functionalization of imidazopyridines and –pyrazines by an intramolecular direct arylation leading to novel hitherto unexplored heteroaceanthrylenes which can be also regarded as π-extended and N,O-doped [3.3.2]cyclazines (Scheme 2). Aceanthrylenes are known for their efficient electron affinity[26] and as strong DNA intercalators[27] and find applications in various electronic devices.[28] However, heteroatom doped aceanthrylene are rarely found in literature.[29] Our synthesis reported herein consists of a chemoselective C–O bond forming step by either nucleophilic substitution reaction (S_NAr) or copper catalyzed Ullmann coupling of phenols. A final intramolecular direct arylation reaction leads to the desired N,O-doped aceanthrylenes.

Results and Discussion

We started our investigations with the synthesis of heterocyclic biaryl ethers by S_NAr reaction[30] of phenol with 3-bromo-5-chloro-imidazopyrazine (Scheme 1, **1a**). The nucleophilic substitution of **1a** with phenol, carried out in the presence of potassium carbonate in DMA (100 °C), selectively afforded product **3a** in very good yield (87%). Noteworthy, the reaction took place exclusively at the pyrazine moiety, while the imidazole ring remained unattacked. Next, we turned our attention to 3,5–dibromo-imidazopyridine (**2a**)[31]. Unfortunately, the conditions mentioned above could not be applied for this reaction, which might be explained by the presence of bromine instead of chlorine located in the pyridine moiety and/or by the fact that the pyridine ring is less electron-deficient compared to pyrazine. Hence, we turned our attention to catalytic Ullmann coupling reactions.[32] The use of 10 mol% of copper powder under otherwise similar reaction conditions gave the desired product **4a** in good yield (80%). The reaction proceeded regioselectively at position 5 of the imidazopyridine and no reaction was observed at the imidazole moiety.

With efficient and selective reaction conditions in hand, we started to analyze the preparative scope of the reaction (Table 1). The utilized conditions tolerate various functional groups located at the phenol, such as alkyl, CF_3, CN, Br, Cl, F or OMe substituents. No clear trend of the reaction yield with regard to electronic or steric effects was observed. However, for both substrates, the use of *p*-methylphenol (products **3b**, **4b**) gave slightly lower yield compared to *meta*- (products **3f**, **4f**) or

[a] J. Radolko, H. Nam Do, P. Ehlers, A. Villinger, P. Langer
University of Rostock, Institute of Chemistry, Albert-Einstein-Str. 3a, 18059 Rostock, Germany
Phone: +49 381 498 6410
E-mail: peter.langer@uni-rostock.de
Homepage: www.langer.chemie.uni-rostock.de

Supporting information for this article is available on the WWW under https://doi.org/10.1002/ejoc.202401045

© 2024 The Author(s). European Journal of Organic Chemistry published by Wiley-VCH GmbH. This is an open access article under the terms of the Creative Commons Attribution Non-Commercial NoDerivs License, which permits use and distribution in any medium, provided the original work is properly cited, the use is non-commercial and no modifications or adaptations are made.

© 2024 The Author(s). European Journal of Organic Chemistry published by Wiley-VCH GmbH

Research Article
doi.org/10.1002/ejoc.202401045

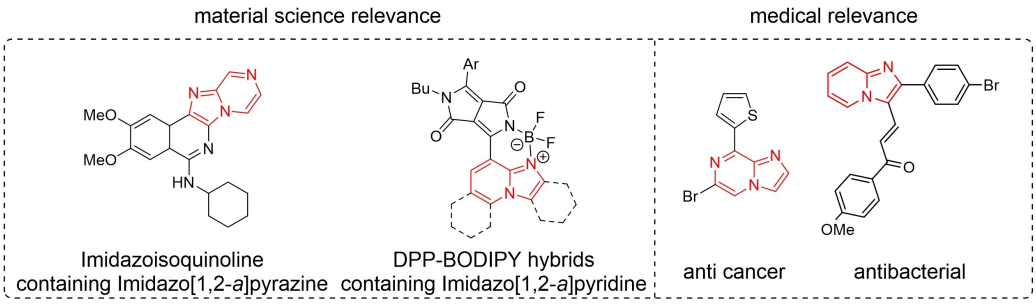
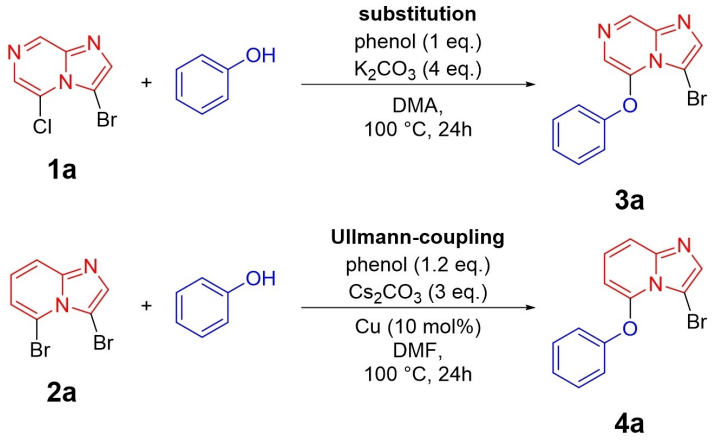
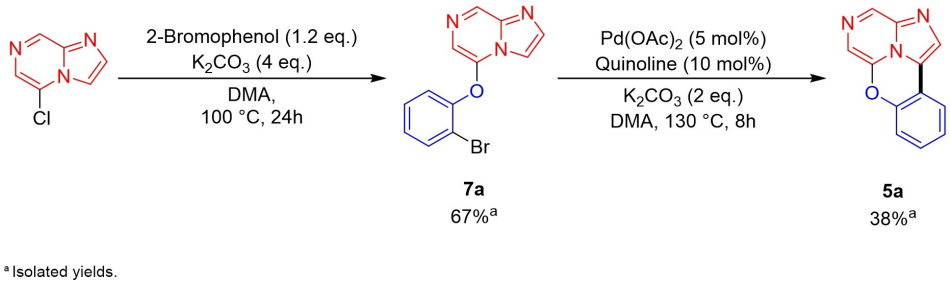


Figure 1. Imidazo[1,2*a*]pyridine/-pyrazine derivatives with interesting photoelectronic and bioactive properties.



Scheme 1. Reaction conditions for the selective substitution reaction and Ullmann-coupling with phenol.



Scheme 2. Alternative synthesis of **5a**. [a]Isolated yields.

ortho-substituted methylphenols (products **3e**, **4e**). In general, Ullmann coupling using **2a** gave lower yields compared to the S_NAr reaction of **1a**.

With various starting materials in hand, we probed the intramolecular direct arylation. As a starting point, we tested conditions which we previously used for a related transformation forming oxepine rings (Table 2, entry 1). However, these conditions led only to traces of the desired product. Reducing the temperature or changing the base did not improve the yield. Thus, we studied the impact of different phosphine ligands on the reaction (entries 4–7). To our delight, more electron-rich and bulky ligands, such as Buchwald's biaryl ligands and $PCy_3 \cdot HBF_4$ improved the yield drastically. Especially, the use of $PCy_3 \cdot HBF_4$ resulted in a high yield of 87% for the ring-closing reaction. However, employing this ligand for the reaction of alkylphenols led to inseparable mixtures which were caused by cleavage of the bromine of the five-membered ring as the main side reaction. Hence, instead of typically employed phosphine ligands, the use of nitrogen-containing ligands was examined.[33] Employment of 2,2′–bipyridine provided a promising yield of 74%. Finally, the use of quinoline led to very good yields of up to 98% (Table 2, entry 8 and 9). These conditions were used for exploring the scope of the cyclization reaction.

The optimized conditions were employed to phenol ethers **3a–k** and **4a–k** (Table 3). The respective final cyclization products were obtained in moderate to excellent yield. The only exceptions are precursors **3k** and **4k** containing a cyano group which were not converted to the respective cyclization products. As expected, substituents on position 2 of the phenol moiety led to slightly diminished yields. Electron donating

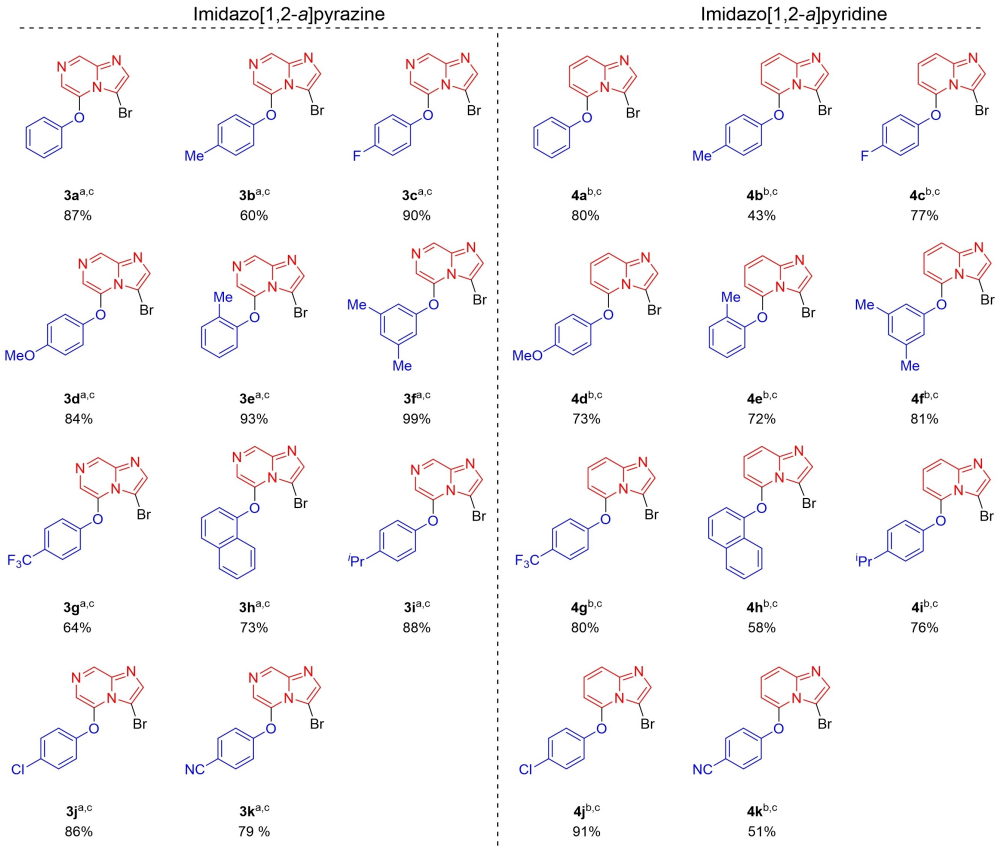
© 2024 The Author(s). European Journal of Organic Chemistry published by Wiley-VCH GmbH

10990690, 2025, 2, Downloaded from https://chemistry-europe.onlinelibrary.wiley.com/doi/10.1002/ejoc.202401045 by University Rostock Universitatsbibliothek, Wiley Online Library on [10/08/2025]. See the Terms and Conditions (https://onlinelibrary.wiley.com/terms-and-conditions) on Wiley Online Library for rules of use; OA articles are governed by the applicable Creative Commons License

Research Article
doi.org/10.1002/ejoc.202401045

Chemistry Europe
European Chemical Societies Publishing

Table 1. Scope of a nucleophilic aromatic substitution-reaction of imidazo[1,2-*a*]pyrazine **1 a** and Ullmann-coupling of imidazo[1,2-*a*]pyridine **2 a**.



[a] reaction conditions for nucleophilic substitution reaction: **1 a** (1.0 eq.), phenol derivative (1.0 eq), K_2CO_3 (4.0 eq.), DMA; [b] reaction conditions for the Ullmann-coupling: **2 a** (1.0 eq.), phenol derivative (1.2 eq.), Cs_2CO_3 (3.0 eq.), Cu (10 mol%), DMF; [c] isolated yields.

groups on the phenol seem generally to be beneficial for both starting materials and products derived from imidazopyrazine **1 a** and gave mostly higher yields compared to the corresponding imidazopyridine derivatives.

Finally, we were interested in an alternative reaction set-up. Starting from 5-chloro-imidazopyrazine, a S_NAr reaction with 2-bromophenol was examined (Scheme 2). The respective phenol ether **7 a** was obtained in acceptable 67% yield. The following CH-activation reaction, using our optimized conditions, led to final product **5 a** in 38% yield. Hence, this synthetic strategy resulted in a reduced yield in the final intramolecular direct arylation, although the conditions are not optimized for this specific reaction. On the other hand, bromination of the imidazopyrazine is not required during the synthesis of the starting material, which also has to be considered with regard to overall yield. Ullmann coupling of 2–bromophenol to imidazopyridine was not successful, potentially due to selectivity issues caused by the presence of an additional bromine atom.

The structure of **5 a** was independently confirmed by X-Ray crystallography (Figure 2). The polycyclic compound adopts a planar alignment across all four fused rings. Molecules align in a herringbone arrangement with close intermolecular π-π-interactions (3.28 Å and 3.36 Å) found between the pyran and the pyrazine rings within the individual stacks. Adjacent columns are nearly orthogonally twisted (~81°) and stabilized by close OH-hydrogen bonds between the stacks. Additional close NH-hydrogen bonds are found via the pyrazine rings of adjacent molecules (~2.6 Å).

UV-Vis-Spectra for **5 a** and **6 a** were measured to shortly assess optical properties, yet the low quantity of fluorescence made further evaluation of these compounds ineffectual and eventual calculated quantum yields remained under 1 percent, which falls within the error margin of utilized method (Figure S2).

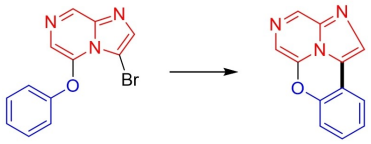
Additional DFT calculations were performed to obtain further information on the electronic structure of the as-prepared heterocyclic aceanthrylene analogs **5 a** and **6 a**. Structural optimization by DFT on B3LYP 6-311G(d,p)-optimized gas phase structures with D3 dispersion correction in the gas-phase reproduced the crystallographic data of **5 a** very well (for depiction of HOMO-LUMO levels see SI).[34] Additional $NICS(1.7)_{\pi ZZ}$[35] values were calculated at the GIAO–B3LYP/6-311 + G(p) level of theory using the σ-only model[36] by means of a "local aromaticity"[37] approach. NICS2BC graphs were obtained by using BC-Wizard program, developed by Paenurk and Gershoni-Poranne et al.[38] and gave further insights into the

© 2024 The Author(s). European Journal of Organic Chemistry published by Wiley-VCH GmbH

10990690, 2025, 2, Downloaded from https://chemistry-europe.onlinelibrary.wiley.com/doi/10.1002/ejoc.202401045 by University Rostock Universitatsbibliothek, Wiley Online Library on [10/08/2025]. See the Terms and Conditions (https://onlinelibrary.wiley.com/terms-and-conditions) on Wiley Online Library for rules of use; OA articles are governed by the applicable Creative Commons License

Research Article
doi.org/10.1002/ejoc.202401045

Table 2. Optimization of the cyclization.



3a **5a**

Entry	Co-catalyst/ catalyst	Ligand	Base	Solvent	Time [h]	T [°C]	Yield[a] [%]
1	$Pd(PPh_3)_4$	-	K_3PO_4	DMA	24	150	2
2	$Pd(PPh_3)_4$	-	K_3PO_4	DMA	24	130	4
3	$Pd(PPh_3)_4$	-	K_2CO_3	DMA	24	130	-
4	$Pd(OAc)_2$	DavePhos	K_2CO_3	DMA	24	130	52
5	$Pd(OAc)_2$	Xphos	K_2CO_3	DMA	24	130	62
6	$Pd(OAc)_2$	PCy_3	K_2CO_3	DMA	24	130	34
7	$Pd(OAc)_2$	$PCy_3 \cdot HBF_4$	K_2CO_3	DMA	24	130	87
8	$Pd(OAc)_2$	2,2′-Bipyridine	K_2CO_3	DMA	24	130	74
9	**$Pd(OAc)_2$**	**Quinoline**	**K_2CO_3**	**DMA**	**24**	**130**	**98**
10	$Pd(OAc)_2$	Quinoline	KOAc	DMA	24	130	45
11	$Pd(OAc)_2$	Quinoline	K_2CO_3	NMP	24	130	61
12	$Pd(OAc)_2$	Quinoline	K_2CO_3	NMP	24	100	33
13	**$Pd(OAc)_2$**	**Quinoline**	**K_2CO_3**	**DMA**	**8**	**130**	**97**

[a] Isolated yields.

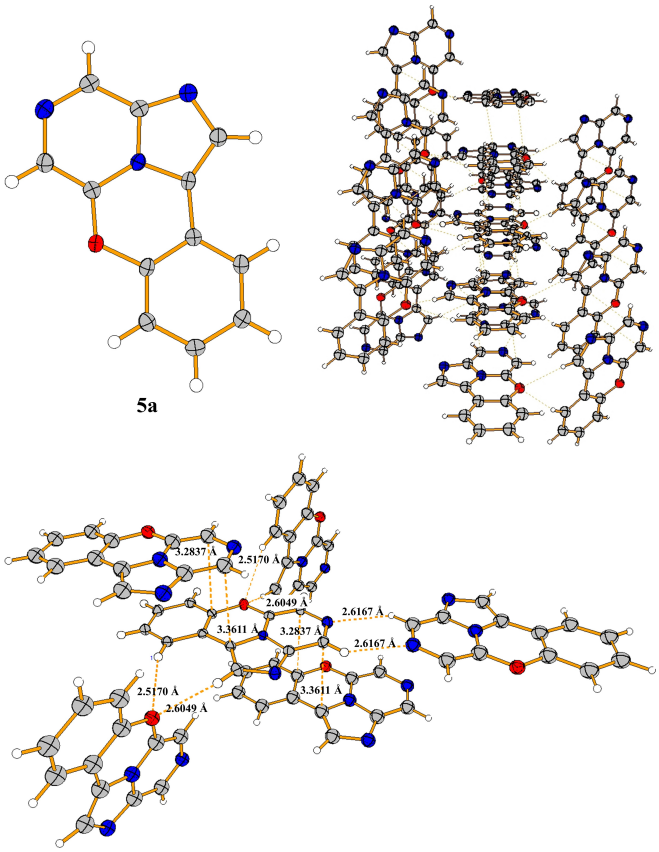


Figure 2. Left: confirmation of the structure **5a** via X-Ray; right: staggered stacking of crystal, bottom measured distance of π–π-interactions and hydrogen bonds of the compound.

aromaticity and conjugation within both molecular scaffolds **5a** and **6a** (Figure 3).

NICS calculations reveal different magnetic properties for individual rings of the scaffold. As expected, the benzene and imidazole moieties are strongly aromatic, while the pyrazine ring reflects non-aromatic behavior. The central pyran ring is strongly anti-aromatic. Similar values are calculated for the respective imidazopyridine analog **6a**. Hence, the additional nitrogen atom of **5a** does not impact the aromatic properties of the entire molecule. NICS2BC calculations of both structures corroborates these findings. Strong, diatropic and local ring currents are found for the imidazole and benzene ring, while a paratropic ring current is observed for the pyran ring. However, a weak semi-global ring current is found for the fused imidazopyrazine and -pyridine moieties, respectively.

Steady-state absorption measurements have been exploited to gain further insights into the optical properties of compounds **5a** and **6a**. Both compounds show strong absorption features in UV area with weak vibrational progression into the visible spectral range which corroborates weak conjugation between the imidazpyridine – or pyrazine moiety with the fused phenyl ring.

Conclusions

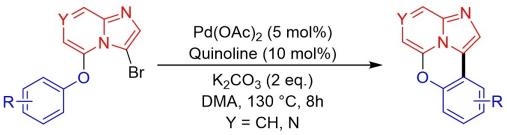
In conclusion, we developed a convenient methodology to hitherto unknown 6–oxa–2,2a[1]–diazaaceanthrylenes and 6-oxa-2,2a[1],4-triazaaceanthrylenes by combining an Ullmann-coupling

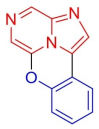
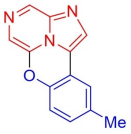
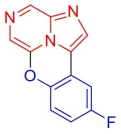
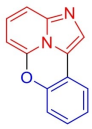
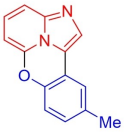
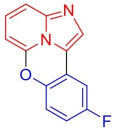
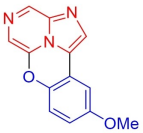
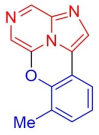
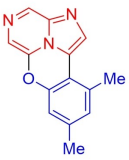
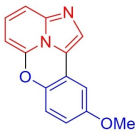
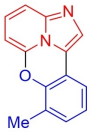
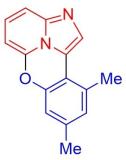
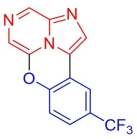
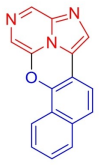
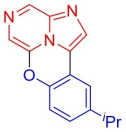
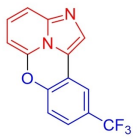
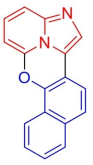
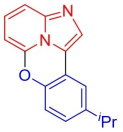
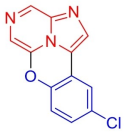
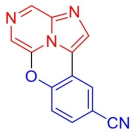
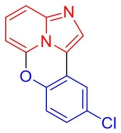
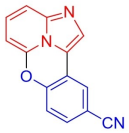
© 2024 The Author(s). European Journal of Organic Chemistry published by Wiley-VCH GmbH

10990690, 2025, 2, Downloaded from https://chemistry-europe.onlinelibrary.wiley.com/doi/10.1002/ejoc.202401045 by University Rostock Universitatsbibliothek, Wiley Online Library on [10/08/2025]. See the Terms and Conditions (https://onlinelibrary.wiley.com/terms-and-conditions) on Wiley Online Library for rules of use; OA articles are governed by the applicable Creative Commons License

Research Article
doi.org/10.1002/ejoc.202401045

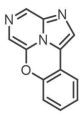
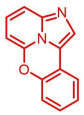
Table 3. Scope of 6-oxa-2,2a[1]-diazaaceanthrylenes and 6-oxa-2,2a[1],4-triazaaceanthrylenes.[a]



Imidazo[1,2-*a*]pyrazine			Imidazo[1,2-*a*]pyridine		
					
5a 97%[b]	**5b** 85%[b]	**5c** 70%[b]	**6a** 78%[b]	**6b** 84%[b]	**6c** 68%[b]
					
5d 82%[b]	**5e** 78%[b]	**5f** 71%[b]	**6d** 77%[b]	**6e** 51%[b]	**6f** 80%[b]
					
5g 48%[b]	**5h** 54%[b]	**5i** 77%[b]	**6g** 53%[b]	**6h** 60%[b]	**6i** 87%[b]
					
5j 33%[b]	**5k** 0%[b]		**6j** 56%[b]	**6k** 0%[b]	

[a] Isolated yields.

Table 4. UV-vis and photoluminescence data of compounds **5a** and **6a** in CH_2Cl_2.

	 5a	 6a
$\lambda_{1,abs}$ (nm)	314	319[c]
$\varepsilon_{\lambda,1}$ (M^{-1} cm^{-1})	2537	2458
$\lambda_{2,abs}$ (nm)	328	332
$\varepsilon_{\lambda,2}$ (M^{-1} cm^{-1})	4399	4207
$\lambda_{3,abs}$ (nm)	343	348
$\varepsilon_{\lambda,3}$ (M^{-1} cm^{-1})	5247	4846

[a] maximum absorption wavelength [b] shoulder in the spectrum

or S_NAr reaction followed by an intramolecular direct arylation. The developed reaction conditions tolerate various functional groups and show good to high yields accompanied with excellent selectivity. Theoretical calculations revealed low conjugation between the fused rings, due to the anti-aromatic behavior of the central pyran ring, despite the overall planar conformation. Further research will be devoted to the synthesis of novel polycyclic heteroaromatic compounds consisting of the imidazopyridine or -pyrazine scaffold with alternating ring sizes or heteroatoms.

© 2024 The Author(s). European Journal of Organic Chemistry published by Wiley-VCH GmbH

10990690, 2025, 2, Downloaded from https://chemistry-europe.onlinelibrary.wiley.com/doi/10.1002/ejoc.202401045 by University Rostock Universitatsbibliothek, Wiley Online Library on [10/08/2025]. See the Terms and Conditions (https://onlinelibrary.wiley.com/terms-and-conditions) on Wiley Online Library for rules of use; OA articles are governed by the applicable Creative Commons License

Research Article
doi.org/10.1002/ejoc.202401045

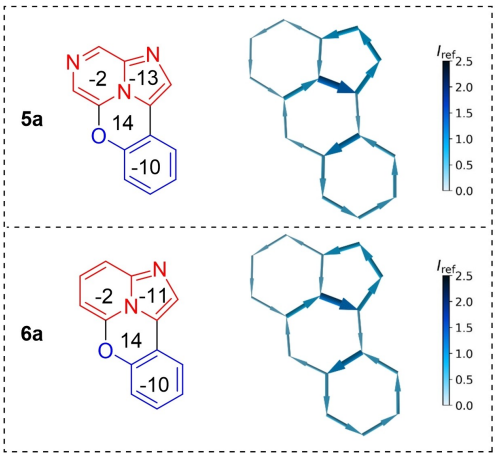


Figure 3. NICS calculations for **5a** and **6a**. Left part: scheme of molecule with respective NICS(1.7)$_{\pi ZZ}$ values in the geometric center of each ring. Right part: NICS2BC graphs (current was calculated from NICS(1.25)$_{ZZ}$; strength relative to I_{ref} (ring current of benzene, 11.5 nAT^{-1}).[35]

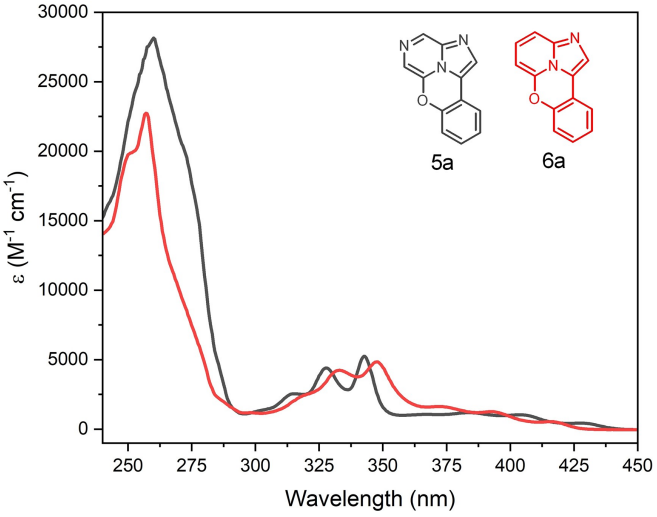


Figure 4. UV-vis absorption, λ_{ex} = 420 nm) spectra in CH_2Cl_2 (c = 10^{-4} M) at 20 °C.

Accession Codes

CCDC 2381186 (**5a**) contains the supplementary crystallographic data for this paper. These data can be obtained free of charge from the Cambridge Crystallographic Data Centre via. http://www.ccdc.cam.ac.uk/data_request/cif

Acknowledgements

This work has been supported by the RoHan Project funded by the German Academic Exchange Service (DAAD, No. 57315854 and 57560571) and the Federal Ministry for Economic Cooperation and Development (BMZ) inside the framework "SDG Bilateral Graduate school programme. Additional financial support by the federal state of Mecklenburg-Western Pomerania is gratefully acknowledged. Open Access funding enabled and organized by Projekt DEAL.

Conflict of Interests

The authors declare no conflict of interest.

Data Availability Statement

The data that support the findings of this study are available in the supplementary material of this article.

Keywords: C–H-activation · Oxaazaaceanthrylenes · Imidazo[1,2-*a*]pyrazine · Imidazo[1,2-*a*]pyridine · N–heterocycles

[1] J. Panda, B. P. Raiguru, M. Mishra, S. Mohapatra, S. Nayak, *ChemistrySelect* **2022**, *7*, e202103987.
[2] a) V. A Basiuk, *Russ. Chem. Rev.* **1997**, *1997*, 187; b) R. Goel, V. Luxami, K. Paul, *Org. Biomol. Chem.* **2015**, *13*, 3525.
[3] J. Y. Lee, J. Y. Shim, H. K. Kim, D. Ko, M.-H. Baik, E. J. Yoo, *J. Org. Chem.* **2017**, *82*, 4352–4361.
[4] L. Valla, D. Pitrat, J.-C. Mulatier, T. Le Bahers, E. Jeanneau, L. M. A. Ali, C. Nguyen, M. Gary-Bobo, C. Andraud, Y. Bretonnière, *J. Org. Chem.* **2024**, *89*, 8407.
[5] R. Rawat, S. M. Verma, *Synth. Commun.* **2020**, *50*, 3507.
[6] K. S. Gudmundsson, B. A. Johns, *Bioorg. Med. Chem. Lett.* **2007**, *17*, 2735.
[7] Z. A. Kaplancikli, G. Turan-Zitouni, A. Ozdemir, G. Revial, *J. Enzyme Inhibit. Med. Chem.* **2008**, *23*, 866.
[8] a) A. M. H. Altaher, M. A. Adris, S. H. Aliwaini, *System. Rev. Pharm.* **2021**, *12*, 3330; b) M. Firouzi, Z. Haghighijoo, M. Eskandari, M. Mohabbati, R. Miri, M. H. Jamei, A. Poustforoosh, S. Nazari, O. Firuzi, M. Khoshneviszadeh, *BMC Chem.* **2024**, *18*, 6.
[9] N. P. Mishra, S. Mohapatra, T. Das, S. Nayak, *J. Heterocycl. Chem.* **2022**, *59*, 2051.
[10] L. Almirante, L. Polo, A. Mugnaini, E. Provinciali, P. Ruggarli, A. Biancotti, A. Gamba, W. Murmann, *J. Med. Chem.* **1965**, *8*, 305.
[11] T. L. S. Kishbaugh, *Curr. Top. Med. Chem.* **2016**, *16*, 3274–3302.
[12] S. Samanta, S. Kumar, E. K. Aratikatla, S. R. Ghorpade, V. Singh, *RSC Med. Chem.* **2023**, *14*, 644.
[13] A. Deep, R. K. Bhatia, R. Kaur, S. Kumar, U. K. Jain, H. Singh, S. Batra, D. Kaushik, P. K. Deb, *Curr. Top. Med. Chem.* **2017**, *17*, 238.
[14] K. Zurbonsen, A. Michel, P. A. Bonnet, M. N. Mathieu, C. Chevillard, *Gen. Pharmacol.: Vasc. Syst.* **1999**, *32*, 135.
[15] R. Goel, V. Luxami, K. Paul, *Curr. Top. Med. Chem.* **2016**, *16*, 3590.
[16] R. H. Martin, Z. Tarasiejska, *Bull. Soc. Chim. Belg.* **1957**, *66*, 136.
[17] E. P. Coutant, Y. L. Janin, *Chem. Eur. J.* **2015**, *21*, 17158.
[18] K. S. Currie, J. E. Kropf, T. Lee, P. Blomgren, J. Xu, Z. Zhao, S. Gallion, J. A. Whitney, D. Maclin, E. B. Lansdon, *J. Med. Chem.* **2014**, *57*, 3856.
[19] T. Yu, J. R. Tagat, A. D. Kerekes, R. J. Doll, Y. Zhang, Y. Xiao, S. Esposite, D. B. Belanger, P. J. Curran, A. K. Mandal, *ACS Med. Chem. Lett.* **2010**, *1*, 214.
[20] N. Agarwal, A. Bajpai, S. P. Gupta, *Biochem. Res. Intern.* **2013**, *2013*, 141469.
[21] R. Goel, V. Luxami, K. Paul, *RSC Adv.* **2014**, *4*, 9885.
[22] D. C. Young, M. Tasior, A. D. Laurent, Dobrzycki, M. K. Cyrański, N. Tkachenko, D. Jacquemin, D. T. Gryko, *J. Mater. Chem. C* **2020**, *8*, 7708–7717.
[23] a) K. R. J. Anupriya, Thomas, M. R. Nagar, Shahnawaz, J.-H. Jou, *J. Mater. Sci.: Mater. Electron.* **2021**, *32*, 26838; b) M. Stahlberger, O. Steinlein, C. R. Adam, M. Rotter, J. Hohmann, M. Nieger, B. Köberle, S. Bräse, *Org. Biomol. Chem.* **2022**, *20*, 3598–3604.
[24] a) W. Hagui, H. Doucet, J.-F. Soulé, *Chem* **2019**, *5*, 2006–2078; b) A. H. Romero, *Top. Curr. Chem.* **2019**, *377*, 21; c) L. Théveau, C. Schneider, C. Fruit, C. Hoarau, *ChemCatChem* **2016**, *8*, 3183; d) R. Rossi, M. Lessi, C. Manzini, G. Marianetti, F. Bellina, *Adv. Synth. Catal.* **2015**, *357*, 3777–3814.

© 2024 The Author(s). European Journal of Organic Chemistry published by Wiley-VCH GmbH

10990690, 2025, 2, Downloaded from https://chemistry-europe.onlinelibrary.wiley.com/doi/10.1002/ejoc.202401045 by University Rostock Universitatsbibliothek, Wiley Online Library on [10/08/2025]. See the Terms and Conditions (https://onlinelibrary.wiley.com/terms-and-conditions) on Wiley Online Library for rules of use; OA articles are governed by the applicable Creative Commons License

[25] a) D. Firmansyah, M. Banasiewicz, I. Deperasińska, A. Makarewicz, B. Kozankiewicz, D. T. Gryko, *Chem. Asian J.* **2014**, *9*, 2483; b) D. Firmansyah, M. Banasiewicz, D. T. Gryko, *Org. Biomol. Chem.* **2015**, *13*, 1367.
[26] a) X. Zhu, B. Yuan, K. N. Plunkett, *Tetrahedron Lett.* **2015**, *56*, 7105; b) A. Modelli, L. Mussoni, D. Fabbri, *J. Phys. Chem. A* **2006**, *110*, 6482.
[27] R. G. Harvey, N. E. Geacintov, *Acc. Chem. Res.* **1988**, *21*, 66.
[28] a) P. Wang, L. Ye, M. Wu, *Opt. Quant. Electron.* **2018**, *50*, 732; b) D. Zhang, P. Xu, T. Wu, Y. Ou, X. Yang, A. Sun, B. Cui, H. Sun, Y. Hua, *J. Mater. Chem. A* **2019**, *7*, 5221; c) J.-W. Jang, H. Park, M.-K. Shin, H. H. Kang, D.-H. Oh, S. O. Jung, S.-K. Kwon, Y.-H. Kim, *Dyes Pigm.* **2011**, *88*, 44; d) T.-H. Huang, J. T. Lin, Y.-T. Tao, C.-H. Chuen, *Chem. Mater.* **2003**, *15*, 4854.
[29] a) H. D. Becker, L. Hansen, *J. Org. Chem.* **1985**, *50*, 277; b) D. Firmansyah, I. Deperasińska, O. Vakuliuk, M. Banasiewicz, M. Tasior, A. Makarewicz, M. K. Cyrański, B. Kozankiewicz, D. T. Gryko, *Chem. Comm.* **2016**, *52*, 1262; c) L. Havlíček, D. Moravcová, V. Kryštof, M. Strnad, *J. Heterocycl. Chem.* **2015**, *52*, 669.
[30] A. R. Harris, D. M. Nason, E. M. Collantes, W. Xu, Y. Chi, Z. Wang, B. Zhang, Q. Zhang, D. L. Gray, J. E. Davoren, *Tetrahedron* **2011**, *67*, 9063.
[31] C. W. Rees, D. I. Smith, *J. Chem. Soc., Perkin Trans. 1* **1987**, 1159.
[32] a) N. D. D'Angelo, J. J. Peterson, S. K. Booker, I. Fellows, C. Dominguez, R. Hungate, P. J. Reider, T.-S. Kim, *Tetrahedron Lett.* **2006**, *47*, 5045; b) M. S. Kuska, M. Majdi Yazdi, A. A. Witham, H. A. Dahlmann, S. J. Sturla, S. D. Wetmore, R. A. Manderville, *J. Org. Chem.* **2013**, *78*, 7176.
[33] K. Mackey, D. J. Jones, L. M. Pardo, G. P. McGlacken, *Eur. J. Org. Chem.* **2021**, *2021*, 495.
[34] a) Gaussian 09, Revision E.01, M. J. Frisch, G. W. Trucks, H. B. Schlegel, G. E. Scuseria, M. A. Robb, J. R. Cheeseman, G. Scalmani, V. Barone, B. Mennucci, G. A. Petersson, H. Nakatsuji, M. Caricato, X. Li, H. P. Hratchian, A. F. Izmaylov, J. Bloino, G. Zheng, J. L. Sonnenberg, M. Hada, M. Ehara, K. Toyota, R. Fukuda, J. Hasegawa, M. Ishida, T. Nakajima, Y. Honda, O. Kitao, H. Nakai, T. Vreven, J. A. Montgomery Jr., J. E. Peralta, F. Ogliaro, M. Bearpark, J. J. Heyd, E. Brothers, K. N. Kudin, V. N. Staroverov, T. Keith, R. Kobayashi, J. Normand, K. Raghavachari, A. Rendell, J. C. S169 Burant, S. S. Iyengar, J. Tomasi, M. Cossi, N. Rega, J. M. Millam, M. Klene, J. E. Knox, J. B. Cross, V. Bakken, C. Adamo, J. Jaramillo, R. Gomperts, R. E. Stratmann, O. Yazyev, A. J. Austin, R. Cammi, C. Pomelli, J. W. Ochterski, R. L. Martin, K. Morokuma, V. G. Zakrzewski, G. A. Voth, P. Salvador, J. J. Dannenberg, S. Dapprich, A. D. Daniels, O. Farkas, J. B. Foresman, J. V. Ortiz, J. Cioslowski, D. J. Fox, Gaussian, Inc., Wallingford CT, **2013**; b) Gaussian 16, Revision A.03, M. J. Frisch, G. W. Trucks, H. B. Schlegel, G. E. Scuseria, M. A. Robb, J. R. Cheeseman, G. Scalmani, V. Barone, G. A. Petersson, H. Nakatsuji, X. Li, M. Caricato, A. V. Marenich, J. Bloino, B. G. Janesko, R. Gomperts, B. Mennucci, H. P. Hratchian, J. V. Ortiz, A. F. Izmaylov, J. L. Sonnenberg, D. Williams-Young, F. Ding, F. Lipparini, F. Egidi, J. Goings, B. Peng, A. Petrone, T. Henderson, D. Ranasinghe, V. G. Zakrzewski, J. Gao, N. Rega, G. Zheng, W. Liang, M. Hada, M. Ehara, K. Toyota, R. Fukuda, J. Hasegawa, M. Ishida, T. Nakajima, Y. Honda, O. Kitao, H. Nakai, T. Vreven, K. Throssell, J. A. Montgomery Jr., J. E. Peralta, F. Ogliaro, M. J. Bearpark, J. J. Heyd, E. N. Brothers, K. N. Kudin, V. N. Staroverov, T. A. Keith, R. Kobayashi, J. Normand, K. Raghavachari, A. P. Rendell, J. C. Burant, S. S. Iyengar, J. Tomasi, M. Cossi, J. M. Millam, M. Klene, C. Adamo, R. Cammi, J. W. Ochterski, R. L. Martin, K. Morokuma, O. Farkas, J. B. Foresman, D. J. Fox, Gaussian, Inc., Wallingford CT, **2016**.
[35] a) A. Stanger, *Eur. J. Org. Chem.* **2020**, *2020*, 3120; b) R. Gershoni-Poranne, A. Stanger, *Chem. Eur. J.* **2014**, *20*, 5673; c) P. v. R. Schleyer, C. Maerker, A. Dransfeld, H. Jiao, N. J. R. van Eikema Hommes, *J. Am. Chem. Soc.* **1996**, *118*, 6317.
[36] A. Stanger, *J. Org. Chem.* **2010**, *75*, 2281.
[37] I. Fernandez, *Modern Computational Methods and Applications*, Elsevier, Amsterdam, **2021**.
[38] E. Paenurk, R. Gershoni-Poranne, *Phys. Chem. Chem. Phys.* **2022**, *24*, 8631.

Manuscript received: September 10, 2024
Revised manuscript received: October 29, 2024
Accepted manuscript online: November 1, 2024
Version of record online: November 16, 2024

© 2024 The Author(s). European Journal of Organic Chemistry published by Wiley-VCH GmbH

10990690, 2025, 2, Downloaded from https://chemistry-europe.onlinelibrary.wiley.com/doi/10.1002/ejoc.202401045 by University Rostock Universitatsbibliothek, Wiley Online Library on [10/08/2025]. See the Terms and Conditions (https://onlinelibrary.wiley.com/terms-and-conditions) on Wiley Online Library for rules of use; OA articles are governed by the applicable Creative Commons License